Resources, Conservation & Recycling 168 (2021) 105273

Contents lists available at ScienceDirect

Resources, Conservation & Recycling

journal homepage: www.elsevier.com/locate/resconrec

Review

A review of membrane crystallization, forward osmosis and membrane capacitive deionization for liquid mining

Aamer Ali [a,*], Cejna Anna Quist-Jensen [a], Mads Koustrup Jørgensen [a], Anna Siekierka [b,c], Morten Lykkegaard Christensen [a], Marek Bryjak [b], Claus Hélix-Nielsen [d,*], Enrico Drioli [e,f]

[a] Center for Membrane Technology, Department of Chemistry and Bioscience, Aalborg University, Fredrik Bajers Vej 7H, 9220 Aalborg, Denmark
[b] Wroclaw University of Science and Technology, Department of Process Engineering and Technology of Polymer and Carbon Materials, Wyb. Wyspianskiego 27, 50-370 Wroclaw, Poland
[c] Deakin University, Institute for Frontier Materials, Waurn Ponds 3216, Australia
[d] Department of Environmental Engineering, Technical University of Denmark, Bygningstorvet Building 115, 2800 Kgs, Lyngby, Denmark
[e] Institute on Membrane Technology (ITM-CNR), National Research Council, c/o the University of Calabria, Cubo 17 C, Via Pietro Bucci, 87036, Rende CS, Italy
[f] Nanjing Tech University, College of Engineering, Nanjing, China

ARTICLE INFO

Keywords:
Forward osmosis
Membrane crystallization
Membrane capacitive deionization
Metal recovery
Green technologies

ABSTRACT

Socio-economic development and new technological advancements have greatly increased the demand for metals, minerals and nutrients. Thus, substantial interest in developing technologies to recover these commodities from seawater, various brines and wastewater streams (industrial and domestic) has emerged. Less explored and innovative membrane processes including membrane crystallization (MCr), forward osmosis (FO) and membrane capacitive deionization (MCDI) are gaining interest in this regard. The current study provides a critical review of the current trends in applying MCr, FO and MCDI for recovery of metals, minerals and nutrients from various streams. The processes are compared in terms of types of fouling, energy consumption, overall composition of suitable feed solutions, feasible concentration ranges and potential to recover the targeted metal from a multi-component solution. The ultimate objective is to establish future research directions for further improvement of each process and to identify which of the processes is more suitable under a given scenario.

1. Introduction

Modern lifestyle is undisputedly associated with the intensive consumption of metals, minerals and nutrients (Krohns et al., 2017) (Elshkaki et al., 2018). Major metals, including Cu and Zn, are of fundamental importance in modern transport, communication and several other industries. Production and further development of many modern technological products, such as smart phones, computer chips and renewable energy devices, rely upon the deeply embedded metals and their properties within these products (Elements in short supply 2011) (National Research Council 2008). In terms of employment, in Europe alone, over 30 million jobs in automotive, aerospace and renewable energy are dependent upon adequate supply of raw materials (European Commission 2018). With developing countries surging ahead, the demand of metals is expected to increase multifold in near future (Harvey, 2013) (Ali et al., 2017) (Mogollón et al., 2018). Thus, further technological and socioeconomic developments are strongly dependent upon sustainable and sufficient supply of metals and minerals (Backman, 2008). At present, the increased demand is fulfilled mainly by mining more metals and minerals – some of these being rare earth metals in limited supply– consequently the easily accessible reservoirs of raw materials are depleting at increasingly rapid rate. Furthermore, the quality of remaining ores is inferior, extraction cost is high, and mining techniques often cause adverse environmental effects such as air, water, soil pollution, and deforestation (Dudka and Adriano, 2010). Metal recycling-another potential route of fulfilling the metals demand- will contribute only a small fraction of future metals demands in next few decades (Elshkaki et al., 2018). Thus, sustainable supply of metals in future is entirely dependent upon availability of alternative sustainable sources of metals and development of relevant recovery technologies (Graedel et al., 2013).

A significant amount of metals and minerals, in form of dissolved solids, is present in liquid sources such as seawater, brines (geothermal, desalination etc.) and wastewater streams from various production

* Corresponding author.
E-mail addresses: aa@bio.aau.dk (A. Ali), clhe@env.dtu.dk (C. Hélix-Nielsen), e.drioli@itm.cnr.it (E. Drioli).

https://doi.org/10.1016/j.resconrec.2020.105273
Received 28 August 2020; Received in revised form 3 November 2020; Accepted 9 November 2020

processes as shown in Table 1. For instance, seawater and desalination brine have substantial amount of different elements (more than 60 including 17 rare earth metals) (Quist-Jensen et al., 2019) (Bardi, 2010) (Shahmansouri et al., 2015). Municipal wastewater is a source of nutrients such as phosphorus and ammonia (De-Bashan and Bashan, 2004). Produced water, a waste byproduct of oil and gas industry, contains several precious metals including Li and Ba in quantities much higher than seawater (Fakhru'l-Razi et al., 2009; A. Ali et al., 2015). Recovery of metals from these liquid sources, commonly known as ″water mining″, does not only contribute in strengthening their sustainable supply but also makes the primary process more green and economical by reducing its environmental footprint and by converting ″waste″ into product (Westerhoff et al., 2015). Brine from desalination capacities is a typical example where disposal of untreated brine poses a serious threat to environment and marine ecosystems (Dawoud and Al Mulla, 2012). Recovery of dissolved solids does not only alleviate these concerns but also contribute in significantly decreasing the freshwater cost, thus making it affordable for developing countries (C.A. Quist-Jensen et al., 2016). Additionally, liquid sources such as seawater, are more uniformly distributed across the globe than traditional reservoir which are concentrated in certain geographical regions. Thus, the development of appropriate technologies for recovery of metals from liquid streams is crucial to fulfill the demand of strategic metals in a sustainable way.

Membrane technology is emerging as a promising route to recover metals from liquid streams. Compared to chemical based recovery processes (chemical precipitation, adsorption, ion exchange), membrane processes are based on principles of physical separation and, therefore, are inherently green in nature. Aside addressing some of the issues faced by the conventional recovery techniques, membrane technology also offers additional advantages such as better product quality and production of freshwater as byproduct (Baker, 2020) (Drioli et al., 2017) (Visvanathan et al., 2000) (Sohn et al., 2011). Traditional membrane processes (nanofiltration and reverse osmosis) can concentrate the dissolved metals to certain extent but are not designed to achieve precipitation or direct capture of the desired metals and minerals from the solution. However, due to new separation requirements and scientific developments, novel or less explored membrane processes with improved separation capabilities have emerged (Ali et al., 2018), thus expanding the use of the technology beyond the production of freshwater only. The new processes can achieve metal recovery either by concentrating the solutions to their saturation level, thus inducing precipitation of the desired component or by selectively adsorbing targeted ions from the solution. Among these processes, membrane crystallization (MCr), forwards osmosis (FO) and membrane capacitive deionization (MCDI) have shown promising potential for recovery of dissolved metals and minerals from liquid streams. These processes offer green route for recovery of metals/minerals and clean water from liquid streams, such as desalination brine and wastewater, normally declared as waste, thus represent important tools to achieve the green transition.

MCr, FO and MCDI are governed by different driving forces as shown in Fig. 1. MCr is driven by a vapor pressure gradient induced through a temperature difference across a microporous hydrophobic membrane (Drioli et al., 2012) (Drioli et al., 2012). The vapor pass through the membrane pores, leaving all the dissolved and suspended nonvolatile components into the retentate stream. Depending upon the configuration applied, the vapor can be condensed on the other side of the membrane by using a cold water stream, a condensing surface or external cooling media such as liquid nitrogen. In FO, the driving force is induced by applying a high-osmotic solution commonly known as draw solution (Klaysom et al., 2013). Under the influence of a trans-membrane osmotic pressure gradient, the water from the feed solution passes through the membrane into the draw solution, leaving the dissolves solids behind in the solution (Klaysom et al., 2013). Both MCr and FO have the potential to concentrate the solutions to saturation, thus inducing crystallization of dissolved components. MCDI is driven by an electric potential applied across the solution flowing between two oppositely charged porous electrodes. Ion exchange membranes (IEMs) are placed in front of the electrodes and ions from the solution are adsorbed within the electrodes and an outlet stream with low ionic concentration is obtained. IEMs block the exit of counterions from the electrodes which increases the ion separation efficiency of the system. Additionally, the applied membranes improve the flushing efficiency of the counterions from the electrodes during the ion release cycle (Biesheuvel and van der Wal, 2010).

Application of MCr, FO and MCDI for minerals recovery from different liquid sources (brines, wastewaters, seawater etc.) has been demonstrated in the recent literature (Qiu et al., 2015) (Luo et al., 2016) (Kim et al., 2018) (Sakar et al., 2017) (Ge et al., 2018) (Lee et al., 2017) (Ali et al., 2015). However, the current literature lacks of comparative critical analysis of these processes for metals recovery from liquid streams of different natures and compositions. Here we review the important developments in MCr, FO and MCDI for recovery of dissolved metals and minerals from liquid streams. Relative differences and the suitable case scenarios for the processes are identified and future research directions and perspectives for each of the processes are discussed.

Table 1
Concentration of various metals and nutrients in wastewaters originating from different processes.

Elements	Stream	Concentration range (ppm)
Na	SB, PW, AW	17,800–72,100 (Brika et al., 2016) (Jeppesen et al., 2009), 520–120,000 (Fakhru'l-Razi et al., 2009), 202, 000 (Lisbona et al., 2012)
Mg	SB, PW, L	580–800 (Brika et al., 2016), 0.9–6000 (Fakhru'l-Razi et al., 2009), 12–722 (Iskander et al., 2017) (S. Wu et al., 2018)
Li	PW, GB	3–235 (Fakhru'l-Razi et al., 2009), 10–1400 (Munk et al., 2016)
Sr	SB, PW	26 (Macedonio et al., 2013), 0–6200 (Fakhru'l-Razi et al., 2009)
Ni	PW, AW,L	0–9.2 (Fakhru'l-Razi et al., 2009), 3.2–5.3 (Ates and Uzal, 2018), 0.2 (S. Wu et al., 2018; Li et al., 2012) (Qin et al., 2016)
Cu	SB, PW, AMW, L	0.45 (Brika et al., 2016), 0–5 (Fakhru'l-Razi et al., 2009), 50–6294 (Bi Cai et al., 2015), 0.03–0.8 (S. Wu et al., 2018; Qin et al., 2016)
Al	PW, AW	0–410 (Fakhru'l-Razi et al., 2009), 67–167,000 (Ates and Uzal, 2018) (Lisbona et al., 2012) (Magalhães et al., 2005)
Ba	PW	0–1740 (Fakhru'l-Razi et al., 2009)
Cr	SB, PW, AW	0.21 (Brika et al., 2016), 0–1.1 (Fakhru'l-Razi et al., 2009), 0.2–1.3 (Ates and Uzal, 2018)
Mn	SB, PW	0.45 (Brika et al., 2016), 0.004–175 (Fakhru'l-Razi et al., 2009)
Zn	PW, AW, AMW, L	0–35 (Fakhru'l-Razi et al., 2009), 0.18–1, 23–133 (Bi Cai et al., 2015), 0.7–7.6 (S. Wu et al., 2018; Qin et al., 2016)
Ag	PW	0.001–7 (Fakhru'l-Razi et al., 2009)
K	SB, PW, AW, L	610[21], 24–4300 (Fakhru'l-Razi et al., 2009), 422 (Lisbona et al., 2012), 1299–2000 (Iskander et al., 2017; S. Wu et al., 2018; Qin et al., 2016)
Fe	SB, PW, AW, AMW, L	0.009 (Brika et al., 2016), 0–680 (Fakhru'l-Razi et al., 2009), 72.2 (Lisbona et al., 2012), 720–26,858 (Bi Cai et al., 2015), 23.8–882 (S. Wu et al., 2018; Qin et al., 2016)
S	SB, PW, AW, AMW	870, 0–1650 (Fakhru'l-Razi et al., 2009), 1530 (Lisbona et al., 2012), 2148–8341 (Bi Cai et al., 2015)
Nutrients		
P	MWW, AW, L	5–300, 40 (Lisbona et al., 2012), 3.9–16.4 (S. Wu et al., 2018; Qin et al., 2016)
NH_3	WW, L	100–8449 (Duong et al., 2013; Y. Zhang et al., 2014)

SB Seawater brine PW Produced water GB Geological brines AW Anodizing waste AMW Acid mine waste L Leachate.

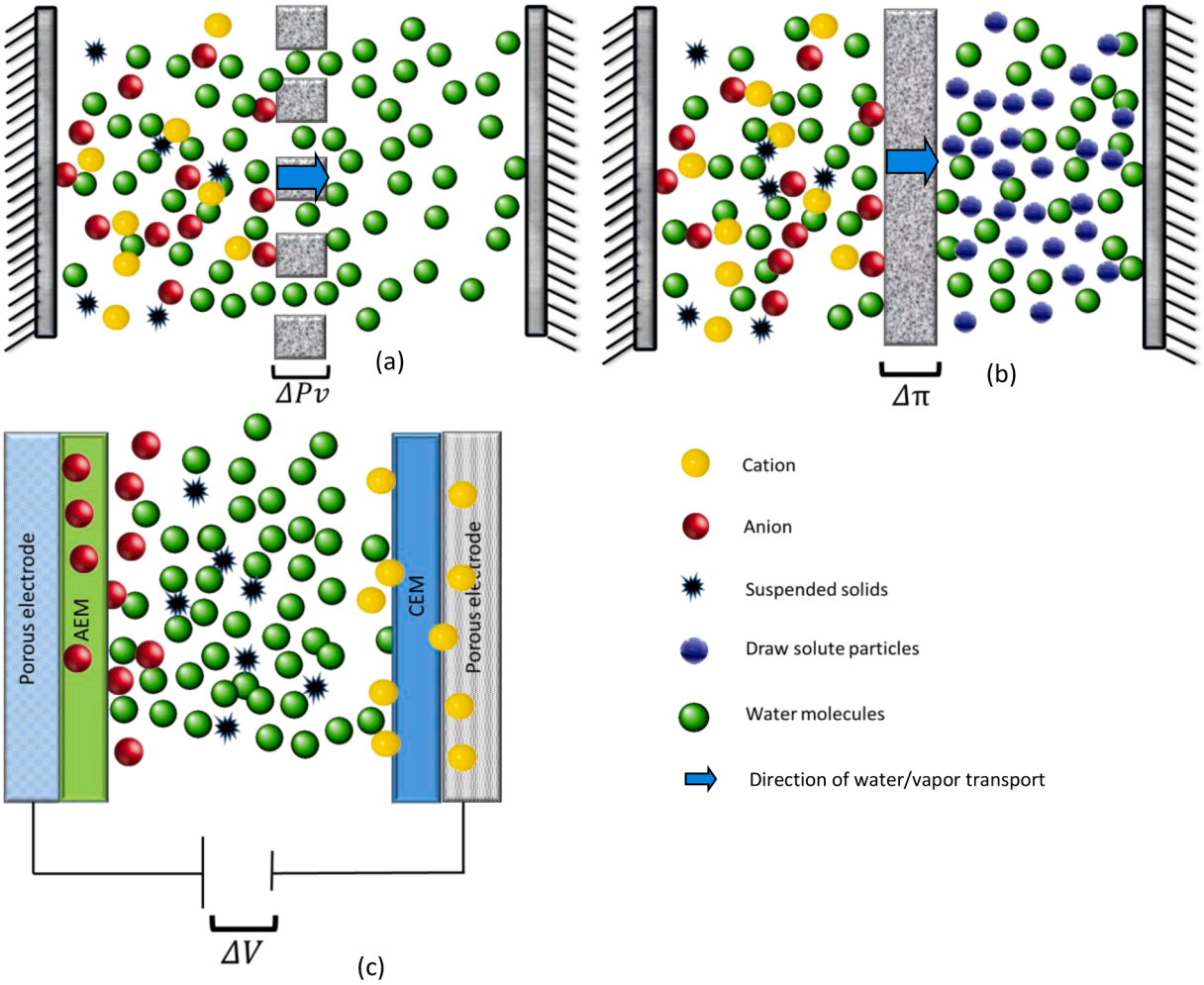

Fig. 1. Schematic diagrams of (a) MCr, (b) FO and (c) MCDI processes. In MCr (a), volatiles pass through the membrane pores while liquid water and non-volatile are retained by a hydrophobic membrane. In FO, water diffuses through a hydrophilic membrane, leaving solutes and suspended solid behind. In MCDI, the applied voltage moves cations and anions towards their respective electrodes.

2. Membrane crystallization

2.1. Introduction and background

In MCr, the crystallization occurs because of the saturation induced by the transport of solvent (in form of vapors) through the membrane pores. Evaporation and crystallization, two main steps of a traditional crystallization process occurring within the same equipment, are separated in MCr (Fig. 2) resulting into a well-controlled pathway of crystallization and uniform crystal product. Evaporation occurs inside the membrane module while crystal growth takes place in a crystallization tank. Mouth of each micro-size pore of the hydrophobic membrane acts as evaporation point leading to a uniform saturation gradient and a uniform crystallization driving force throughout the membrane module. Due to easy operative control of solvent transport, crystals with high purity, narrow size distribution and tunable polymorphic structure can be obtained (Chabanon et al., 2016).

Overall advantages of MCr is the possibility to operate at extremely high concentrations to precipitate minerals, and at the same time, to produce fresh water. Another advantage of MCr, is the use of relatively low temperatures. In field of desalination and wastewater treatment, MCr is generally used at temperatures ranging from 30 to 85 °C, which is below conventional distillation; see Table 2. The low temperatures offers the possibility to use low-grade heat (e.g. solar and geothermal) or waste heat (e.g. surplus heat from industrial processes) for operation, which can reduce the cost of the process significantly and also offers a 'green route' for processing different streams.

A timeline of important milestones in MCr technology is illustrated in Fig. 3. As the timeline indicates main interest in applying MCr as a crystallization technique gained momentum in the early 2000s (Curcio et al., 2001) based on earlier work dating back to 1986 where the first study on crystallization using a membrane was published (Azoury et al., 1986). Compared to the current form of MCr, where microporous hydrophobic membranes are applied, RO was applied in the first study. Application of MD as MCr was suggested in 1987 for crystallization of taurine (Wu et al., 1991). In 1996 Sluys et al. (Sluys et al., 1996) used microfiltration (MF) for the crystallization of $CaCO_3$ by using seeding crystallization to obtain supersaturation. One of the disadvantages of using pressure driven membrane processes as membrane crystallizers is the limitations of applied pressure for reaching saturation and thus the overall cost of the process. In 2001, Curcio et al. (Curcio et al., 2001) reported MCr using direct contact MD (DCMD) or osmotic MD (OMD). Since then, thermally driven processes applying microporous hydrophobic membrane have collectively been referred to as MCr. Integration of MCr with pressure driven processes, such as nanofiltration and RO, was for treatment of desalination brine was suggested in 2002–04. Two main application areas within this technology have appeared (i) Crystallization of macromolecular mainly for the food and pharmaceutical industry (Curcio et al., 2001; Di Profio et al., 2007; Drioli et al., 2005), (ii) mineral recovery from desalination brines and industrial waste

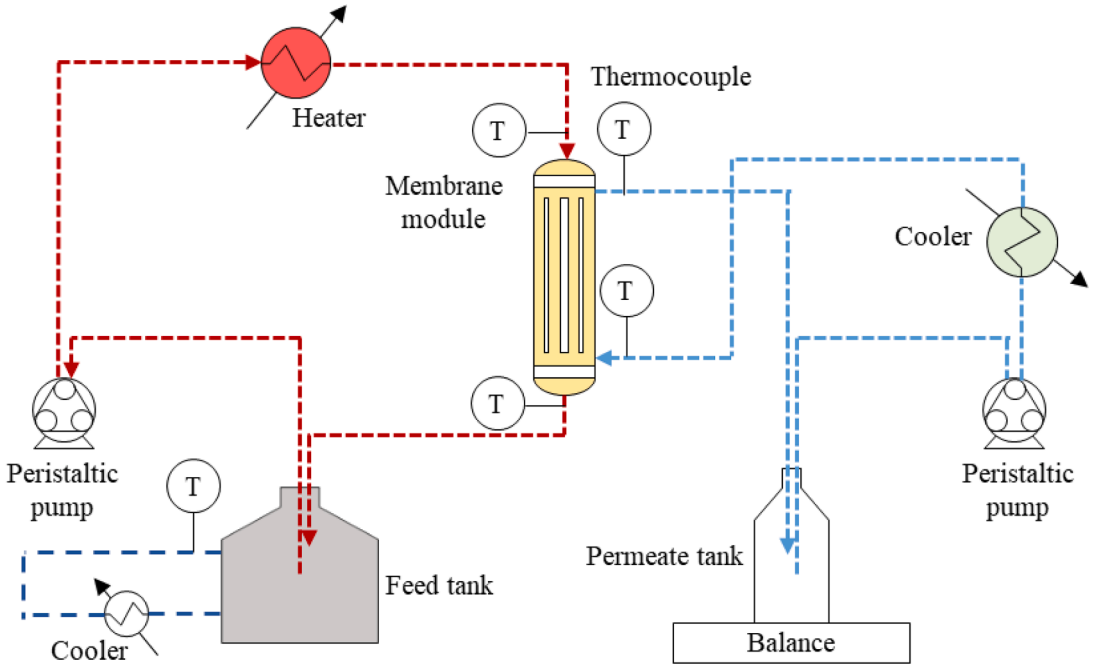

Fig. 2. A schematic illustration of typical direct contact MCr process. Membrane module serves the purpose of evaporator whereas main crystal growth takes place in feed tank where temperature is generally controlled to facilitate the crystal growth.

solutions (Drioli et al., 2012) which is also the main focus of this review. It is also evident from the timeline that the recent research focus on MCr has shifted mainly to develop alternative configurations and to recover more valuable components such as Li and Rb. An advanced and emerging topic in MCr is tuning the crystallization process and crystalline form of the product by using specific surfaces such as patterned membranes (Perrotta et al., 2020) (Pina and Mallada, 2020).

2.1.1. New variants

Today, new and alternative membrane crystallizers are emerging as shown in Fig. 4. Examples of the new variants include submerged membrane distillation crystallizers (Choi et al., 2018; Julian et al., 2018; T. Zou et al., 2019), where the membrane separation and crystallization occurs in the same tank, thus eliminating the need of feed circulation, MD integrated with cooling crystallization through controlled cooling by solid hollow fibers (L. Luo et al., 2018; K.J. Lu et al., 2019) and bubble membrane crystallization, where hydrophobic hollow fibers are used to aerate the feed solution which in turn accelerates evaporation (Liu et al., 2018). Another example is Percrystallization (Motuzas et al., 2018). In this process, water and salt are transported together through the membrane, but due to an applied vacuum the water evaporates on the permeate side of the membrane, thus semi dried crystalline product and freshwater are produced in a single step. A recent study (A. Ali et al., 2018) has conceptualized another operating variant of MCr for simultaneous production of minerals, freshwater and electricity. In this design, the vapor passing through the hydrophobic membrane is condensed as freshwater at a constant volume, thus yielding a high pressure that can be used to drive a hydro-turbine. The feed solution, meanwhile, gets concentrated and yields crystals upon reaching saturation. Another variation of MCr is to use the membrane for dosing antisolvent into feed solution and hereby inducing crystallization. However, this method is mainly used for crystallization of macromolecules and not for minerals recovery (Tuo et al., 2019; Zarkadas and Sirkar, 2006; Profio et al., 2009).

2.2. Current developments in MCr for treatment of brine and industrial wastewater

Global desalination installations are producing more than 95 million m^3 of freshwater each day (Jones et al., 2019). The corresponding brine production has exceeded 141 million m^3 per day, which has led to an increasing demand for innovative brine management and treatment solutions. MCr is suggested as a productive alternative of brine disposal (Pérez-González et al., 2012). In the desalination industry, MD/MCr can add a positive effect on the entire process by increasing the overall water production and recovery of valuable salts from the brine thus approaching a zero-liquid-discharge scenario. Due to the high (~35, 000 ppm) concentration of NaCl in seawater, it is the main recoverable component from brine (Table 2).

Today, NaCl is recovered from seawater by evaporation ponds, which occupies a large footprint and is very much weather dependent. Despite NaCl not being a high-value product, there is huge perspectives in removing NaCl from desalinated brine by MCr. Since desalination plants have relative low (~50%) water recovery factors, MCr can help to increase this to above 90%. Moreover, the negative environmental impact of discharging the concentrated stream is avoided. Lastly, removal of major fraction of NaCl is required to achieve the precipitation of more valuable minerals from desalination brine (Quist-Jensen et al., 2019). This aspect is becoming of particular importance due to increasing interest of applying MCr for recovery of high-value products such as Li and Rb from brines.

As evident from *Table 2*, MCr is normally operated in the range of 30–85 °C, thus potentially waste heat or low-grade energy can drive the process. Together with its lower footprint as compared with other technologies, MCr can easily be integrated into existing processes. Literature (see *Table 2*) also indicates that direct contact configuration is the main applied configuration of MCr due to its simplicity and low cost. Other configurations include the osmotic configuration which is needed when heat-sensitive solutions are processed, and vacuum configuration for crystallization of highly soluble salts. One example in which VMD is required, is for LiCl crystallization, which is saturated around 14 M. The driving force possible to achieve through DCMD is not large enough and therefore VMD was used instead (Quist-Jensen et al., 2016). In principle,

Table 2
An overview of different studied on minerals recovery from seawater brine and produced water through MCr.

Mineral	Solution	Configuration	Membrane	Driving force	Reference
NaCl	synthetic RO brine	DCMD	Microdyn (MD020CP-2 N)	Tf = 35±1.5 °C Tp = 15±1 °C	(Drioli et al., 2004; C.A. Quist-Jensen et al., 2016)
NaCl	natural and synthetic RO brines	DCMD	Accurel PP polypropylene	Tf = 40 °C ΔT ≈ 20 °C	(Ji et al., 2010)
NaCl	4.5 M NaCl solution	DCMD	PVDF Millipore, GVHP	Tf = 50 and 60 °C Tp = 20 and 30 °C	(Tun et al., 2005)
NaCl	28.30 g of NaCl/100 g of H2O	DCMD	Microdyn (MD020CP-2 N)	Tf = 29 Tp = 9 °C	(Curcio et al., 2001)
NaCl	Na, 15,300 ppm; Mg, 29 ppm; Ca, 820 ppm; and K, 970 ppm. The concentration of chloride ions, equal to 25,400 ppm	DCMD	Accurel PP S6/2 membrane, Akzo Nobel	Tf = 358 Tp = 293K	(Gryta, 2002; Gryta et al., 2001)
NaCl	Synthetic RO brine	DCMD	Microdyn (MD020CP-2 N)	Tf =38.4 ± 0.4 Tp = 21.0 ± 0.5	(Macedonio et al., 2013)
NaCl	Real RO brine (TDS: 78.9, 90, 142 g/L) RO + WAIV + MCr	DCMD	Microdyn (MD020CP-2 N)	Tf = 33–38 °C ΔT = 13–15 °C	(Macedonio et al., 2011)
NaCl	Real produced water (248 g/L of TDS)	DCMD	Lab-made PVDF membranes	Tf = 35 °C, 45 °C and 55 °C Tp = 10 °C	(A. Ali et al., 2015)
NaCl	26.4 wt% NaCl	DCMD	Modified PVDF HSV 900	Tf = 40±0.1 °C and 70±0.1 °C Tp = 17±0.1 °C	(Edwie and Chung, 2013)
NaCl	NaCl 26.7%	DCMD	Polyvinylidene fluoride (PVDF) hollow fiber	Tf = 333, 338, 341 K Tp = 288, 293, 303 K	(G. Chen et al., 2014)
$CaCO_3$, NaCl	Real shale gas produced water	DCMD	polypropylene - Accurel PP S6/2, Membrana GmbH	Tf = 60 °C Tp = 20 °C	(J. Kim et al., 2018)
$BaCO_3$, $CaCO_3$, NaCl	Synthetic shale gas produced water	DCMD	polytetrafluoroethylene (PTFE) polymer and supported by a polyethylene (PE) net FGLP14250, Millipore	Tf = 60 ± 0.5 °C Tp = 20 ± 0.5 °C	(J. Kim et al., 2017)
$MgSO_4•7H_2O$	Synthetic NF brine	DCMD	Microdyn (MD020CP-2 N)	Tf = 35±1.5 °C Tp = 15±1 °C	(Drioli et al., 2004)
	651 g/L $MgSO_4•7H_2O$ solution	DCMD	Lab made PVDF	Tf = 36.1 ± 1.4 Tp = 24.7 ± 2.0 °C	(C.A. Quist-Jensen et al., 2016)
LiCl (orthorhombic or cubic depending operative conditions)	6 M LiCl (DCMD) 7 M LiCl (OMD) 8 M LiCl (VMD)	DCMD Osmotic MD VMD	DCMD/OMD: Microdyn-Nadir (MD020CP2N) VMD: Membrana (Accurel® S6/2)	DCMD: Tf = 52 Tp = 20 °C OMD: Tf = 52 Tp = 20 °C + 4.5 M CaCl2•2H2O VMD: Tf = 40, 50, 60 °C	(C.A. Quist-Jensen et al., 2016)
NaCl LiCl	Single salt solutions NaCl: 5.5 M LiCl: 13M	VMD	Coating of hydrophobic polymethylsilsesquioxane aerogels on alumina membrane supports Coating of Fluoroalkylsilanes hydrophobic agent at alumina hollow fibers.	NaCl: T_f = 37–48 °C, Vacuum pressure: 3 kPa LiCl: T_f = 62–70 °C, Vacuum pressure: 3kPa	(Ko et al., 2018)
Rb	Synthetic SWRO brine	MD coupled with adsorption	PTFE flat sheet membrane (General Electric, US Adsorption material: Polymer encapsulated potassium copper hexacyanoferrate	Tf = 55 ± 0.5 °C Tp = 25 ± 0.5 °C	(Naidu et al., 2017)
Rb	Synthetic SWRO brine	Submerged MD coupled with adsorption	granular potassium copper hexacyanoferrate	Tf = 55 ± 0.5 °C	(Y. Choi et al., 2019)
Na_2SO_4	2 M Na_2SO_4 solution	DCMD	PVDF Millipore, GVHP	Tf = 50 and 60 °C Tp = 20 and 30 °C	(Tun et al., 2005)
Na_2SO_4 anhydrous	60 g/L NF pretreated (50% recovery) ~120 g/l Na_2SO_4	DCMD	Accurel PP Elements	Tf = 40 °C ΔT = 12 °C	(Curcio et al., 2010)
Na_2SO_4 anhydrous	Real industrial waste water (4.5–5.5 wt.%)	DCMD	Polypropylene Microdyn-Nadir (MD020CP2N)	Tf = 31 to 51 °C Tp = 19 to 38 °C	(C.A. Quist-Jensen et al., 2017)
Na_2SO_4 anhydrous	284 g/L Na_2SO_4	DCMD	Flatsheet polyvinylidene fluoride polymer made by Millipore	Tf = 40, 50, 60, 70 °C Tp = 25 °C	(Bouchrit et al., 2017)
Na_2SO_4	Real wastewater from anodizing industry	DCMD	Accurel PP	Tf = 38, 47, 56 °C	(A. Ali et al., 2019)
$Na_2SO_4•10H_2O$	60 g/L to 180 g/L Na_2SO_4	Osmotic MD	Liqui-cel, MiniModule membrane contactor, Germany	100 g/L to 300 g/L NaCl	(Li et al., 2014)
Na_2CO_3 and Na_2SO_4	160 g/L to 200 g/L Na_2CO_3 60 g/L Na_2SO_4	Osmotic MD	Liqui-cel, MiniModule membrane contactor, Germany	300 g/L NaCl	(Li et al., 2016)
Individual solutions of $Na_2SO_4•10H_2O$, $Na_2CO_3•10H_2O$, KNO_3	100 g/L	Osmotic MD	Extra flow, Liqui-cel, Membrana GmbH, Germany	350 g/L	(Sparenberg et al., 2020)

(*continued on next page*)

Table 2 (*continued*)

Mineral	Solution	Configuration	Membrane	Driving force	Reference
Na_2CO_3•$10H_2O$	150 and 200 g/L Na_2CO_3	Osmotic MD	1 × 5,5 MiniModule™ Liqui-Cel®, Membrana GmbH, Germany		(Luis et al., 2013)
Individual solutions of KCl, $MgSO_4$, Na_2SO_4, NH_4Cl, NaCl		Submerged DCMD	PVDF, Econoty	Tf = 50 °C Tp = 20 °C	(Y. Choi et al., 2019)
$MgNH_4PO_4$•$6H_2O$	Reject water from digester (wastewater treatment)	DCMD	Accurel PP		(C.A.A. Quist-Jensen et al., 2018)
Boric acid	Simulated radioactive wastewater (10–500 mg/L boric acid)	VMD	Polypropylene (PP) (Wochi, WHPP96–21, China) hollow fiber membrane module	Tf = 20–70 °C Vacuum degree = 0.40 to 0.97 atm	(Jia et al., 2017)

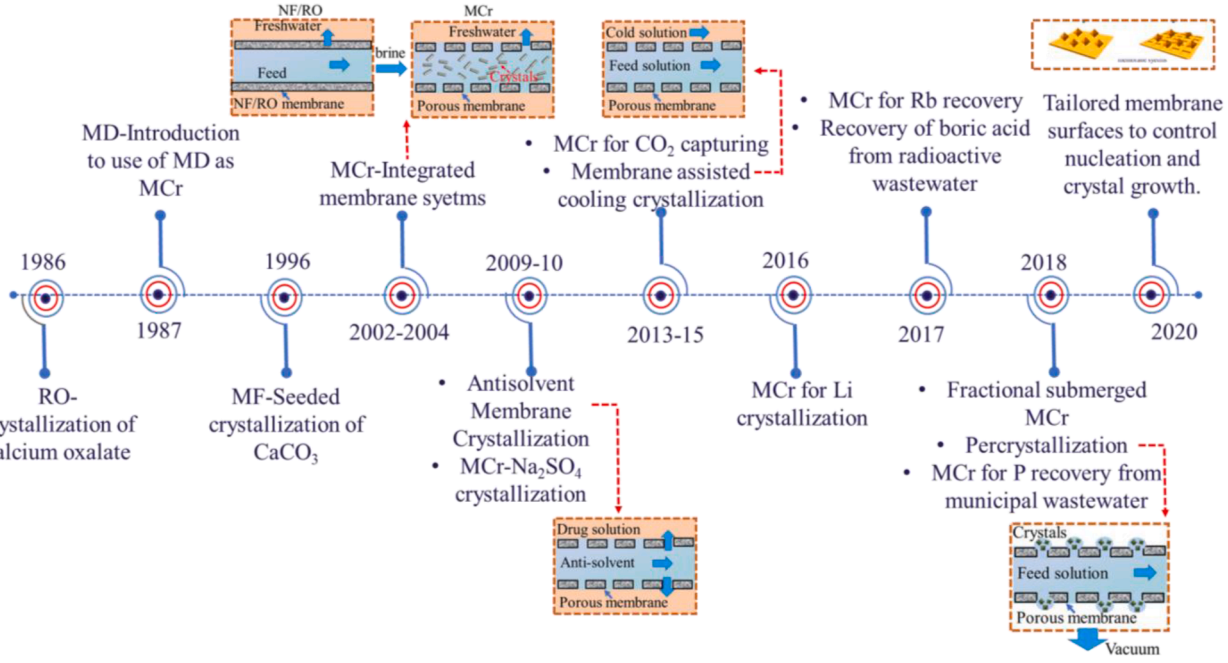

Fig. 3. A timeline of important milestones in development of MCr.

all MD configurations can be used as MCr, but the one to choose depends on feed solution and the operative conditions.

Another example, where MCr can be a tool to increase sustainability, is treatment of industrial wastewater. Perspectives on sustainability and increased restrictions on discharge of industrial wastewater are compelling the industries to treat their wastewaters. Industrial wastewaters are often very complex, in terms of nature and concentration of the contained components, and therefore the treatment options are generally limited and expensive. In this regard, MCr offers an interesting possibility. An interesting example is the wastewater streams containing significant quantities of sodium sulfate (Na_2SO_4), which has been recovered through MCr in some recent studies (*Table 2*). The studies show that different polymorphs of Na_2SO_4 can be recovered, where the anhydrous (thenardite) and decahydrite (mirabilite) forms are the most common. Curcio et al. (Curcio et al., 2010) and Quist-Jensen et al. (Quist-Jensen et al., 2017) found that Na_2SO_4 precipitate as Thenardite when using the DCMD configuration. In contrast, Li et al. (Li et al., 2014) found that Na_2SO_4 crystallizes as Mirabilite when an isothermal osmotic MD configurations is being utilized. This highlights the possibility to alternate polymorphs in MCr by changing MCr configurations, thus the final product can be obtained in required crystalline form by constructing the process according to product requirements. Another interesting aspect of MCr is to sequester and store CO_2 by crystallizing and recovering Na_2CO_3 (Li et al., 2016). This can be a potential solution to limit the greenhouse effects. Recently, MCr is also suggested for efficient phosphorus recovery from municipal wastewater (Quist-Jensen et al., 2018). The study showed an increase in phosphorus recovery from <40% to above 60% from the stream after the digester with respect to the existing technologies. All these studies shows that MCr has potential to recover and recycle metals and minerals from various industrial streams. An overview of different salts recovered from industrial effluents through MCr, along with membranes applied and process conditions, is provided in Table 2.

The membrane surface plays an important role during nucleation and crystal growth. Recently, the crystallization of NaCl through MCr was studied using molecular dynamics and lab-made composite PVDF–graphene membranes as an interactive interface for controlling nucleation-and-growth (Perrotta et al., 2020; Tsai et al., 2018; Perrotta et al., 2020). Similar to salt crystals, the membranes with hydrogel layers have been fabricated for supported heterogeneous support of tailored protein crystallization (Di Profio et al., 2014; Wang et al., 2018; Mirabelli et al., 2018). The hydrogel layer allows to have controlled nano-architecture (mesh size) and different morphologies so that crystals appear at lower protein concentration and have enhanced diffraction features (Di Profio et al., 2014). Another important factor for MCr is that it allows reducing induction times nd therefore it can also be used as a seed generator for various crystallization units (Simone et al., 2018).

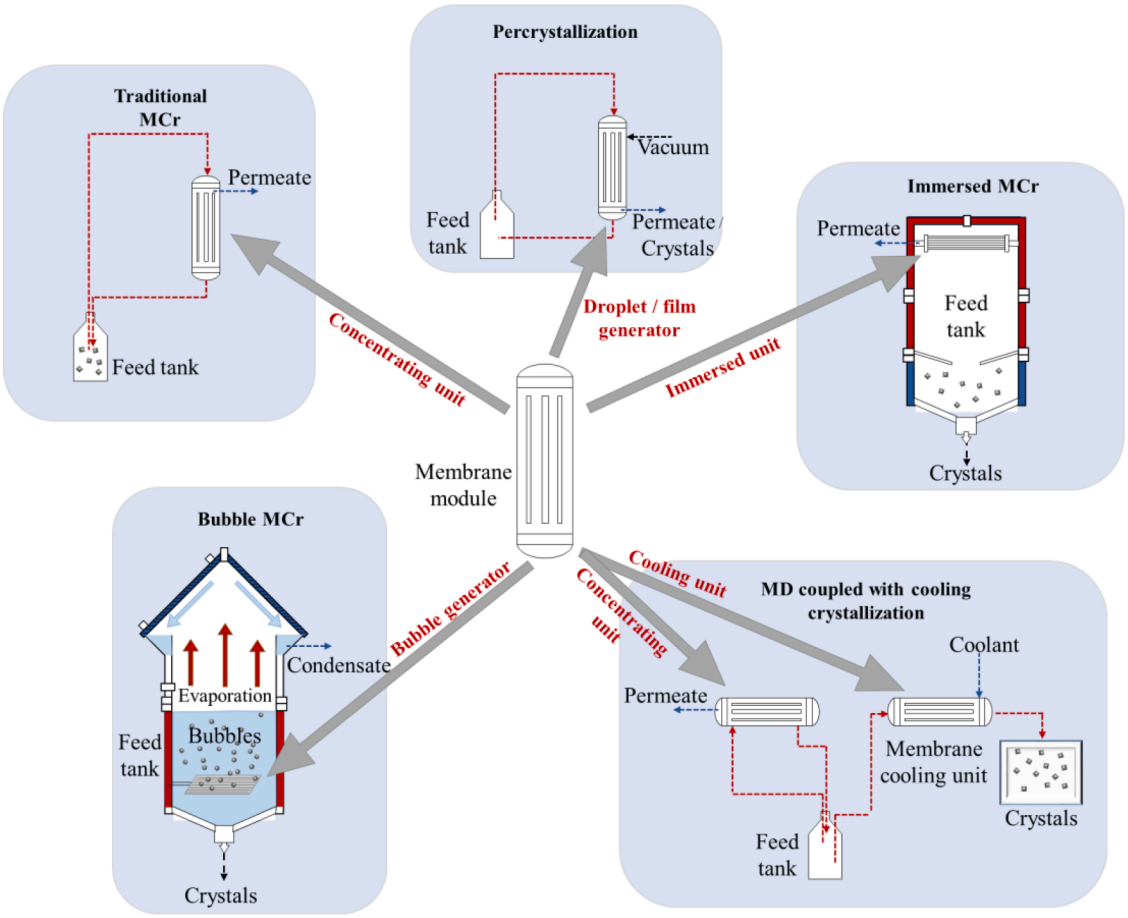

Fig. 4. Schematic overview of new membrane crystallization configurations showing the role of membrane in each configuration.

3. Forward osmosis

3.1. Introduction

3.1.1. Background

Osmosis is the transport of water due to difference in chemical potential of water between two solutions separated by a semipermeable membrane. Presence of solutes reduces the water activity and the chemical potential of water. The osmotic pressure in the solution is defined as the hydraulic pressure required to compensate the reduction of chemical potential by the presence of the solute, and can be calculated with the following equation:

$$\pi = -\frac{RT}{\overline{V}}\ln(a_w) \quad (1)$$

where π is the osmotic pressure of the solution, R is the gas constant, T is the temperature and $\overline{V}$ is the molar volume of water and a_w the water activity. Hence a low water activity (and high solute concentration) leads to a high osmotic pressure of a solution. Osmosis can occur when a feed and draw solution is separated by a semipermeable membrane. Here, water in a feed solution with a high water activity and low solute concentration (hence a higher chemical potential) flows across the membrane into the draw solution with lower water activity and higher solute concentration as shown schematically in Fig. 5. This reduces the gradient in chemical potential across the membrane as water is transported from the feed (elevating $\mu_{w,feed}$ and thereby π_{feed}) to the draw solution (reducing $\mu_{w,draw}$ and thereby π_{draw}). The membrane has a higher permeability of water than solutes, ensuring water permeation and (partial) retention of solutes. The higher the difference in osmotic pressure between the two solutions, $\Delta\pi = \pi_{draw} - \pi_{feed}$, the higher is the water flux, J_w, from feed to draw, whereas a positive hydraulic pressure difference between the solutions, $\Delta P = P_{draw} - P_{feed}$, leads to a reversed flux, i.e. from draw to feed as descried by the following equation (Lee et al., 1981):

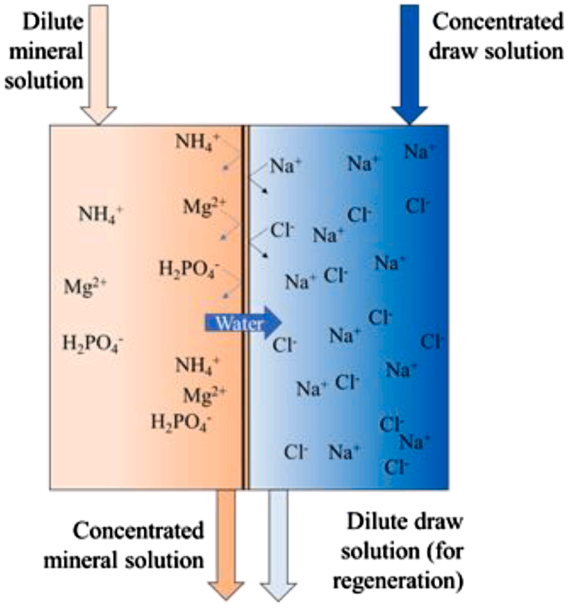

Fig. 5. principle of concentration of nutrients with FO.

$$J_w = A_w(\Delta\pi - \Delta P) \quad (2)$$

Hydraulic pressure is not required for the FO process, but there is instead a requirement for recovery of draw solution due to the reduced driving force between a concentrated and diluted feed and draw with time as illustrated in Fig. 5 (Cath et al., 2006). The following main advantages of using FO for recovery of minerals from waste streams have been reported:

1 FO membranes have high retention of most ions, hence it is possible to concentrate and recover ions from wastewater while extracting clean water from the wastewater (Cath et al., 2006).
2 A high hydraulic pressure is not needed to drive the membrane processes, reducing energy consumption, requirements for membrane physical stability and capital expenses for FO systems (Klaysom et al., 2013).
3 Higher reversibility of fouling compared to pressure driven processes, e.g. RO, resulting in simple cleaning and stable performance. This makes it the method of choice for solutions of high fouling propensity as there are less requirements for pretreatment of the feed (Klaysom et al., 2013; Shaffer et al., 2015; Chun et al., 2017).

A timeline of important milestones for FO has been shown in Fig. 6. It is clear from the figure that, although FO was introduced a long time ago, yet the rapid progress started only after 2000. The main focus of new developments had been the development of suitable draw solutions, designing new configurations and nutrient recovery from wastewater. It was relatively recently that the process started gaining interest for recovery of minerals such as Li as illustrated in the timeline.

3.2. Current developments

3.2.1. Direct concentration of minerals

Numerous studies have investigated the application of FO for concentrating minerals directly in different waste streams for sustainable recovery of minerals and biogas (Ansari et al., 2017). An overview is given in Table 4, summarizing the applied feed and draw solutions, membranes, recovered minerals, solute rejection rates, concentration factors, permeate and reverse salt fluxes. Direct FO concentration for recovery of minerals has been studied on MBR and conventional activated sludge (CAS) effluent, sewage, CAS and MBR sludge, digestates, manure, urine, landfill leachate and whey. The majority of FO research on minerals recovery focus on concentration and recovery of ammonium and phosphate in waste streams, whereas the recovery of metal ions is gaining interest very recently (Wu et al., 2016; Zhao and Liu, 2018; Vital et al., 2018; Cui et al., 2014; Gwak et al., 2018; Li et al., 2018).

Concentration of ammonium and phosphate in sludge and effluent from membrane bioreactor and conventional activated sludge process (AS) has been achieved with synthetic seawater draw solutions (Xue et al., 2016; Xue et al., 2015; Volpin et al., 2018; Hau et al., 2014; Nguyen et al., 2013; Nguyen et al., 2016). Two studies varied volume concentration factor (VCF) of effluent between 2 and 4, leading to a concentration factor (CF) of ammonium of 2.1 in both studies, whereas phosphate CF reached 2.3 and 4, respectively (Xue et al., 2016; Xue et al., 2015). Hence CF of phosphate follows VCF, suggesting a high rejection of phosphate, whereas the ammonium concentration factor is limited by lower rejection. Gao et al. (Gao et al., 2018) reached even higher VCF of 10 on sewer supernatant with concentration factors of phosphate up to 9.4, Calcium and Magnesium 8.2 and 8.6, whereas ammonium only reached a CF of up to 5.3. Again, the ammonium concentration factor does not follow the volume reduction due to low ammonium rejection and precipitation (Kedwell et al., 2019).

Another source of ammonium and phosphate is digestates from anaerobic digestion which can be treated with FO (Camilleri-rumbau et al., 2019; Soler-Cabezas et al., 2018; Ansari et al., 2016; Kedwell et al., 2018). VCF of 5 to 7 has been reached in treating anaerobic digester concentrate and still obtaining high phosphorus and ammonium recovery (> 93%) (Camilleri-rumbau et al., 2019; Soler-Cabezas et al., 2018; Ansari et al., 2016; Kedwell et al., 2018; Vu et al., 2019). In a study by Vu et al. (Vu et al., 2019), a decline in concentration of ammonia and phosphate in digester sludge centrate was observed although reaching 70% water recovery, which was explained by precipitation of phosphate and valorization of ammonia, which was more severe during stirring of the feed suspension. A study of treating digested manure centrate with FO point out that recovery of nutrients may be hampered by the simultaneous retention of heavy metals ($R > 80\%$) and antibiotics (Li et al., 2020). Soler-Cabezas et al. (Soler-Cabezas et al., 2018) also treated sludge concentrate and reached ammonium rejections of only 66% and 85% with Aquaporin and CTA membranes. The large span in reported rates of rejection is explained by the procedures of determining the rejection rate. Eq. (3) is frequently used to calculate rejection, R, from concentration of solute in feed, C_F, and draw, C_D:

$$R = \left(1 - \frac{C_D}{C_F}\right) \quad (3)$$

Nevertheless, this method is not valid for batch FO experiments as a steady state concentration is not reached and solute transported from feed will be diluted in draw, i.e. rejection will depend on draw volume and time/VCF (Kedwell et al., 2019). A more correct determination of rejection rate, independent of feed and draw volumes, VCF and time, can be done by Eq. (4):

$$R = \left(1 - \frac{J_s}{J_w C_F}\right) \quad (4)$$

By selecting $MgCl_2$ draw solutions a high recovery of ammonium and phosphate (> 93% and > 99%) from digested swine wastewater can be ensured even at low a VCF of 2 (Wu et al., 2018). This is explained by the reverse diffusion of magnesium ions leading to co-precipitation of

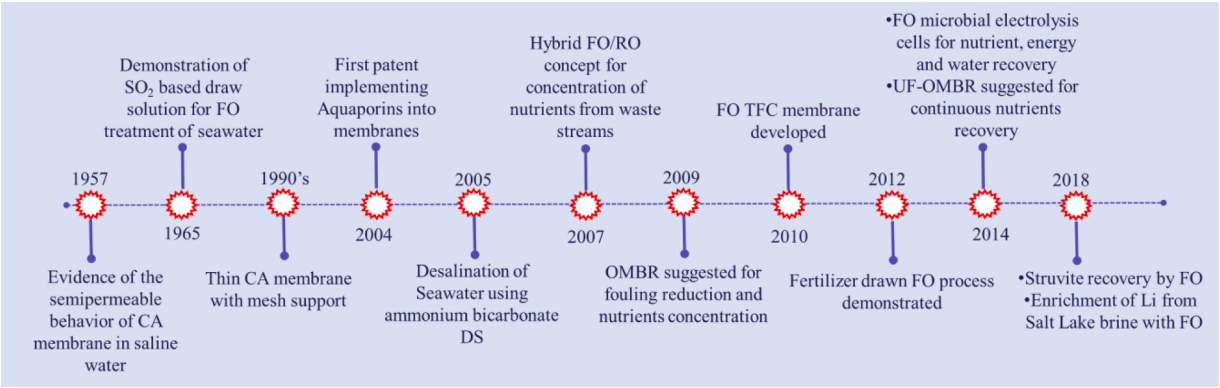

Fig. 6. Key milestones for the development of FO membranes for nutrients and mineral recovery. CA: Cellulose acetate, OMBR: osmotic membrane bioreactor.

ammonium and phosphate as struvite. The concentration by FO treatment enhances recovery, as the same study found that phosphorus recovery with $MgCl_2$ addition and without FO treatment was only 60.7%. Schneider et al. (Schneider et al., 2019) also employed a $MgCl_2$ draw solution for FO concentration of nutrients in swine manure, potato starch and cattle manure. This resulted in TAN rejections up to 97%, which is explained by the low reverse flux of magnesium ions. The magnesium ions are larger than e.g. sodium ions and therefore have lower diffusivity than e.g. Cl^- ions, hence the reverse flux of chloride ions is higher than the reverse flux of magnesium ions, reducing forward flux of ammonium ions. This mechanism is further discussed in Section 6.3.

The beneficial effects of magnesium based draw solution on nutrients recovery have also been demonstrated in Volpin et al. (Volpin et al., 2018) where acidified urine (pH = 4) was concentrated (VCF = 4). Reverse Mg^{2+} flux lead to recovery of 50% ammonium and 40% phosphate through struvite precipitation.

In addition to nutrient recovery, interest has also been observed in applying FO for recovery of valuable metals, e.g. Li, from various streams. Some studies (see Table 3) describe the recovery of heavy metals from contaminated effluents, e.g. acid mine drainage, printed circuit board wastewater and brine. As can be seen from Table 3, FO can reach high rejection of heavy metal ions (>98%) at volume concentration factors > 2 and reasonable fluxes of 11–12 LMH (Wu et al., 2016; Vital et al., 2018) (Li et al., 2018) (Gwak et al., 2018). Zhao et al. (Zhao and Liu, 2018) even reached fluxes at 45–50 LMH by using modified TFC membranes. Landfill leachate is also a source of minerals such as ammonium and phosphate, but also potassium, sodium, magnesium and calcium ions can be recovered (Iskander et al., 2017; Wu et al., 2018). Wu et al. (Wu et al., 2018) treated landfill leachate with high concentrations of magnesium, calcium and ammonium with FO to reach a VCF of 1.6. After this, Calcium was recovered by addition of carbonate (Na_2CO_3) to precipitate carbonate. This was followed by addition of H_3PO_4 to precipitate struvite to reach 95% Mg recovery. FO has also been investigated for the removal and recovery of rare earth elements Cerium, Lanthanum and Dysprosium. With a PA TFC membranes rejection > 90% were achieved (Pramanik et al., 2019). It was also found that the rejection of Dysprosium was significantly higher at higher pH (pH = 7) than lower (pH = 3). However, higher rejection rates of heavy metal ions is needed for efficient removal and recovery of rare earth elements.

In addition, FO has been studied for nutrient mining from milk and dairy wastewater (Chen et al., 2019; Pramanik et al., 2019). Chen et al. (Li et al., 2019) show in a study using a 24 m^2 FO pilot scale system that FO could reach 15% (w/w) whey concentration by a VCF of 2.5 using NaCl solutions (48–57 g/L) (Chen et al., 2019) and 21% (w/w) for skim milk concentration. i.e. FO shows as a viable method to reach high concentration of suspensions due to the low fouling potential as long as the osmotic pressure buildup in the feed suspension does not stop permeation. This is possible for suspensions of large molecular weight substances, as their molar concentration, hence osmotic pressures, will be relatively low compared to salt solutions. The energy consumption for concentration using FO was lower than for RO required that there is no energy required for regeneration of draw. This is possible, if high concentration brines are available as draw solution.

FO clearly has the potential to treat waste streams and recover valuable minerals. However, FO flux is reduced by the elevated osmotic pressure during the continuous concentration of the waste stream, hence the concentration factor is limited by the solution's osmotic pressure and it may not be possible to reach the required concentration for precipitation of certain solutes.

3.2.2. *Hybrid FO systems*

(i) OMBR

In 2009, Achilli et al. (Achilli et al., 2009) proposed an osmotic MBR, replacing the MF membrane with an FO membrane in order to reduce fouling propensity of the MBR, which benefits from independent control of solid retention time (SRT) and hydraulic retention time (HRT) compared to the CAS process. However, by applying FO rather than MF/UF, nutrients and other solutes (e.g. NH4+, PO43−, Ca2+, Mg2+, *K*+) are enriched in the sludge, which is beneficial for nutrients recovery (Qiu and Ting, 2014; Luo et al., 2015; Huang et al., 2015). Other advantages of the osmotic MBR are discharge of water ideally without contaminants (nutrients, trace organic contaminants) (Luo et al., 2015; Cornelissen et al., 2011; Blandin et al., 2018) and lower fouling propensity (Achilli et al., 2009; Linares et al., 2016; Cath et al., 2015). Comparing the OMBR to direct FO treatment of wastewater, OMBR benefits by simultaneous degradation of organic matter (Sun et al., 2016). A schematic outline of the OMBR is given in Fig. 7 (left).

Qiu et al. (Qiu and Ting, 2014) operated a lab scale OMBR for 96 days with a SRT of 50 days and HRT of 15.4 h. Through this period, they reached 98% removal efficiency of ammonium and total organic carbon (TOC). Supernatant was discarded from the bioreactor daily to stabilize salt concentration in the reactor and recover concentrated phosphate. Phosphate was recovered by pH adjustment to 8–9.5 in order to precipitate phosphate with NH4+, Ca2+, Mg2+, *K*+ which are also concentrated in the sludge supernatant. In this way, more than 95% of orthophosphate was recovered, primarily as amorphous calcium phosphate, without addition of calcium or magnesium. A similar study presented in Huang et al. (Huang et al., 2015) also operated a laboratory scale OMBR to treat synthetic wastewater avoided excessive salinity accumulation with intermittent withdrawal and replacement of sludge supernatant. Orthophosphate was recovered by adjusting pH to 8.5 to precipitate and recover phosphate. Over 75 days of operation a 100%, 43% and 96% removal of TOC, ammonium and orthophosphate was reached (Huang et al., 2015).

The main challenges for sustainable operation of the osmotic membrane bioreactor is salinity buildup, which is a consequence of 1) reverse salt flux from draw into the feed solution, and 2) concentration of solutes that are retained in the sludge by the FO membrane (Song et al., 2018). This results in higher conductivity and osmotic pressure and thereby lower flux, sludge de-flocculation, also resulting in lower permeate flux, and eventually inactivation of microorganisms (Huang et al., 2015; Jørgensen et al., 2018; Van De Staey et al., 2015; Holloway et al., 2015; Wang et al., 2016).

(i) MF-OMBR/UF-OMBR

A solution to the accumulation of salts in the OMBR sludge is to integrate a MF/UF membrane in the reactor to form a MF-OMBR/UF-OMBR, outlined in Fig. 7 (right) [190S,195,201–203]. As MF and UF membranes are permeable to solutes, nutrients and emerging organic pollutants are extracted through the MF/UF permeate streams. Hence, integrating both FO and MF/UF membranes into an MBR enables simultaneous concentration and extraction of nutrients as the FO flow relative to MF and excess sludge outtake flow determines the concentration factor of solutes in the sludge. It follows that operation at a high FO flow relative to e.g. MF flow will result in high concentration factor of incoming nutrients, which can then be recovered and precipitated in the MF stream (Blandin et al., 2018). The precipitation of nutrients in MF stream was demonstrated at lab scale by Luo et al. (Luo et al., 2016). Here, sewage was treated with the MF-OMBR, the NaCl draw was regenerated with RO for pure water production while MF permeate was adjusted to pH = 10 to induce calcium phosphate precipitation. Another positive effect is the high rejection of trace organic contaminants, above > 90% (Luo et al., 2015; Blandin et al., 2018; Holloway et al., 2014). Extracting the trace organic contaminants in a concentrated MF stream might be beneficial as degradation (biological and chemical) is more efficient at higher concentrations.

Blandin et al. (Blandin et al., 2018) demonstrated in pilot scale that

Table 3
Studies of direct concentration of minerals with FO.

Feed solution	Draw solution	FO membrane	Main composition of feed	Rejection	VCF	Permeate flux (L m^{-2} h^{-1}, LMH)	Reverse solute flux (g m^{-2} h^{-1}, gmh)	Ref.
MBR effluent	Synthetic seawater	TFC and CTA		> 90% NH_4—N	2.3			(Xue et al., 2015)
MBR effluent	Synthetic seawater	CTA (HTI)	TP: 2.7 ± 0.5 mg/L NH4-N: 10.3 ± 2.4 mg/L		4	4.6		(Xue et al., 2016)
Secondary CAS effluent	Pretreated seawater and synthetic seawater (35 g/L NaCl)	TFC (Toray)	TDS: 336 mg/L NH_4^+ 2.4 mg/L TP 3 mg/L	> 80% NH_4—N		12–22.5	7.6–12.6	(F. Volpin et al., 2018)
Sewage supernatant	NaCl solutions (0.5–4 M)	CTA (HTI)	NH_4—N 42.3 mg/L TP 8.5 mg/L Ca 5.2 mg/L Mg 7.1 mg/L	93.3% NH_4—N 95.4% TP	10			(Gao et al., 2018)
Synthetic MBR sludge	0.7 M EDTA-Na salt	CTA (HTI)	MLSS 8000 mg/L PO4-P 150 mg/L NH4-N 150 mg/L	97% NH_4—N 97% NO_2—N 90% NO_3—N 99% PO_4-P		8.5–4.2	<0.2	(Hau et al., 2014)
Secondary sludge	36 g/L NaCl	CTA (HTI)	MLSS 3000–8000 mg/L PO4-P 100 - 200 mg/L NH4-N 100 - 200 mg/L	96% NH_4—N 98% PO4-P	3.5–7	5.5–2.5		(Nguyen et al., 2013)
Synthetic sludge	0.2 M Na_3PO_4	OsMem TFC-EC	MLSS 3500 ± 24 mg/L PO4-P 100 ± 3 mg/L NH4-N 100 ± 2 mg/L			FO mode: 7.1 PRO mode: 6.7	0.8–1.2	(Nguyen et al., 2016)
Digestates	1.1 M and 3.5 M NaCl	AQP	TS: 20 ± 1.7 g/L NH4-N 2477 mg/L	> 95.5% TAN			3–12	(Camilleri-rumbau et al., 2019)
Raw digester centrate (constant feed concentration)	NaCl	CTA (HTI)		84.7% NH_4—N 85.0% TKN 99.6% PO_4-P				(Holloway et al., 2007)
Digested sludge centrate	saline anion exchange effluent, seawater desalination brine	AQP and CTA	COD 1941 ± 837 mg/L SS 559 ± 343 mg/L NH4-N 886 ± 189 mg/L	66% and 83% NH_4—N		AQP: 3.34 CTA: 2.92		(Soler-Cabezas et al., 2018)
Digested sludge centrate	Seawater	CTA (HTI)	PO4-P 88 ± 5 mg/L TS: 1.13 ± 0.1 mg/L		5	6.4 (initial)		(Ansari et al., 2016)
Digested sludge centrate	Seawater		PO4-P 32 ± 1 mg/L NH_4—N 2200 ± 100 mg/L	> 99% P	7			(Kedwell et al., 2018)
Digested Swine WW	$MgCl_2$	CTA (HTI)	PO4-P 167 ± 2 mg/L NH_4—N 413 ± 0.3 mg/L		2	3.12		(Z. Wu et al., 2018)
Digested manure centrate	1 M NaCl	CTA (HTI) and AQP	TS 9077 ± 88 mg/L TP 70.9 ± 12.8 mg/L NH_4—N 1152 ± 54 mg/L	40% NH_4—N > 80% Heavy metals (Cr, As, Se, Pb, Fe and Mn)		10 (initial)		(Li et al., 2020)
Swine manure, Potato starch, Cattle manure (mesophilic and thermophilic)	0.66 M $MgCl_2$	TFC		80.8–97.0% TAN 98.7–99.8% P		>3 (swine manure and potato starch)		(Schneider et al., 2019)
Anaerobic treated dairy manure	NaCl, $MgCl_2$ and EDTA-2Na (π=90 bar)	TFC		> 98% PO_4-P 70–73% NH_4—N	2.5	19.9 (NaCl), 21.1 ($MgCl_2$) 18.7 (EDTA-2Na)	16.6 (NaCl), 7.7 ($MgCl_2$) 3.7 (EDTA-2Na)	(B.K. Pramanik et al., 2019)
Model anaerobic effluent	NaCl	RO membrane		45.7–88.7% (total acid rejection)		1.9–4.4		(Bakonyi et al., 2020)
Wastewater	NaCl and NaOAc	TFC			10		NaCl: 17.4 NaOAc: 16.6	(A.J. Ansari et al., 2018)
Sewage	$MgCl_2$	AQP	TP 19.5 ± 2 mg/L NH4-N 31 ± 3.2 mg/L		2.3	5.3		(Singh et al., 2019)
Urine	NaCl regenerated with MD		NH4-N 1125 ± 147 mg/L	> 99% NH_4—N				(Liu et al., 2016)
Urine acidified to pH=4	2 M $MgSO_4$	TFC (Toray)			2.5	14 (initial)		(F. Volpin et al., 2018)
Dilute urine	$Mg(NO_3)_2$	TFC (Toray)	PO4-P 281 mg/L TN 4217 mg/L		2			(F. Volpin et al., 2019)
Landfill leachate A: conductivity 31.1	1–3 M NaCl	CTA (HTI)				A: 1.2 B: 3.6	5.4–6.4 gmh	(Iskander et al., 2017)

(*continued on next page*)

Table 4
Characteristics of applied IEM in MCDI.

Feed concentration	Configuration of MCDI	Type of membranes	IEM characteristic	Process conditions	SAC (mg/g)	Charge efficiency (%)	Comments	Ref.
$CaCl_2$ (5 mM)	Solid electrodes	AEM: Neosepta AMX CEM: a) SPPO-based membrane b) Ca-alginate-based membrane c) Neosepta CMX (ASTOM, Japan) d) Neosepta CMB (ASTOM, Japan) e) CMD (Asahi glass, Japan)	a) $Z_{IEC} = 0.013$meq/cm^2, $W = 20.5\%$, δ=70 μm b) $Z_{IEC} = 0.004$meq/cm^2, $W = 45.4\%$, δ=70 μm c) $Z_{IEC} = 0.041$meq/cm^2, $W = 20.7\%$, δ=140 μm d) $Z_{IEC} = 0.059$meq/cm^2, $W = 17.7\%$, δ=230 μm e) $Z_{IEC} = 0.064$meq/cm^2, $W = 25.3\%$, δ=380μm	CV_{ads}=1.2 V CV_{des}=0 V t_{ads}=t_{des}=15min	a) 18.9 b) 18.0 c) 17.2 d) 17.0 e) 18.1	a) 90.4 b) 92.9 c) 87.9 d) 81.8 e) 87.3	–	(Yoon et al., 2019)
a)$K_2Cr_2O_7$ (1.7 mM) b) $K_2Cr_2O_7$ (1.7 mM) + KCl (13.4 mM)	Batch mode, solid electrodes	AEM and CEM from Hangzhou Lvhe Environment Co., Ltd., China	–	CV_{ads}=1.2 V t_{ads}=55 min v = 20 mL/min	a) 155.7 b) 190.8	–		(L. Chen et al., 2019)
NaCl (50 mM)	Single pass, solid electrodes	AEM and CEM from ASTOM, Japan (Neosepta AMX and Neosepta CMX	AMX: $Z_{IEC} = 1.8$meq/cm^2, $W = 23\%$, δ=140 μm CMX: $Z_{IEC} = 1.7$meq/cm^2, $W = 28\%$, δ=170μm	CV_{ads}=1.5 V CV_{des} = 0 V t_{ads}= 15 min t_{des}= 5 min v = 40 mL/min	121.8	–	Water recovery <0.3	(A. Hassanvand et al., 2017)
a)NH_4Cl (30 mM) + NaCl + $CaCl_2$ + glucose b) Real digestate wastewater	Batch mode, flow electrodes	AEM and CEM from IONSEP MC	AEM: Z_{IEC} = 2.2 mol/kg, δ=420 μm CEM: Z_{IEC} = 2.4 mol/kg, δ=420μm	a) CV_{ads}=CV_{des}=1 V t_{ads}=2 h v = 10 mL/min b) CV_{ads}=CV_{des}=1 V t_{ads}=3 h v = 20 mL/min	a) 36 b) -	–	The overall removal efficiencies of Na^+, NH^{4+}, K^+, Ca^{2+} and Mg^{2+} were recorded as 19.7%, 54.4%, 67.9%, 85% and 90%, respectively, with real digestate wastewater	(Sakar et al., 2019)
1 ppm Pb^{2+}, 1 ppm Ca^{2+}, 1 ppm Mg^{2+}	Single pass, solid electrodes	AEM (FAS-PET-130) and CEM (FKS-PET-130) made with PET foil	AEM: Z_{IEC} = 1.0 mmol/g, $W = 13\%$, δ=110 μm CEM: Z_{IEC} = 0.75 mmol/g, $W = 15\%$, δ=110μm	CV_{ads}=1.2 V t_{ads}= 60 min v = 23 mL/min	–	–	Selectivity: Pb/Ca = 7.5 Pb/Mg = 2.8	(Dong et al., 2019)
Ca^{2+} = 160 mg/L Cl^- = 90 mg/L F^- = 1.2 mg/L Mg^{2+} = 50 mg/L Na^+ = 120 mg/L NO^{3-} = 233 mg/L SO_4^{2-} = 40 mg/L	Solid electrodes	Neosepta AM-1 and Neosepta CM-1, Tokuyama Co., Japan	AMX: $Z_{IEC} = 1.8$meq/cm^2, $W = 23\%$, δ=140 μm CMX: $Z_{IEC} = 1.7$meq/cm^2, $W = 28\%$, δ=170μm	CV_{ads}=1.5 V CV_{des}=0.0 V t_{ads}=24 min v = 0.3 L/min	–	–	Average removal = 96% Water recovery = 88% Reduction concentration of nitrades from 233 mg/L to 4.6 mg/L	(Uzun and Debik, 2019)
NaCl= 200 mg/L	Batch mode, solid electrodes	Specific AEM based on bromated PPO (BPPO), quenternized PPO (QPPO)	BPPO: Z_{IEC} = 2.20 mmol/g, $W = 24\%$ QPPO: Z_{IEC} = 1.88 mmol/g, $W = 22.5\%$	CV_{ads}=1.2 V CV_{des}=0.0 V t_{ads}=t_{des}=60 min v = 25 mL/min	8 mg/g	80		(Chang et al., 2018)
NaCl = 1000 mg/L					22.7	83.3		

(*continued on next page*)

Table 4 (*continued*)

Feed concentration	Configuration of MCDI	Type of membranes	IEM characteristic	Process conditions	SAC (mg/g)	Charge efficiency (%)	Comments	Ref.
	Single pass, solid electrodes	AEM: Neosepta AMX, Astom Co., Japan CEM: Neosepta CMX, Astom Co., Japan	AMX: Z_{IEC} = 1.8meq/cm^2, W = 23%, δ=140 μm CMX: Z_{IEC} = 1.7meq/cm^2, W = 28%, δ=170μm	CC_{ads} = 0.1A CC_{des} = 0.0A t_{ads}=t_{des}=400 s v = 30 mL/min				(Choi and Yoon, 2019)
Insulin = 0.4 g/L $ZnCl_2$=360 mg/L	Batch mode, solid electrodes	AEM: Neosepta AMX, Astom Co., Japan CEM: Neosepta CMX, Astom Co., Japan	AMX: Z_{IEC} = 1.8meq/cm^2, W = 23%, δ=140 μm CMX: Z_{IEC} = 1.7meq/cm^2, W = 28%, δ=170μm	CV_{ads}=1.2 V CV_{des}=1.2 V t_{ads}=t_{des}=180 s v = 20 mL/min	–	–	Under the optimal operating condition (operating voltage: 1.2 V, adsorption time: 3 min, flow rate: 20 mL/min) with insulin, 75% of ZnCl2 was removed and most of the (>99%) insulin was recovered.	(Jung et al., 2012)
NaCl=250 ppm	Single pass, flow electrodes	1st pair: Tokuyama CEM I AEM 2nd pair: Nafion CEM, Perfluorinated AEM 3rd pair: SPEEK CEM, QAPPO AEM	–	CC_{ads} = 0.5 mA/cm^2 t_{ads}=t_{des}=120 s v = 16.7 mL/min	–	–	1st pair: salt removal rate = 43.2% 2nd pair: salt removal rate = 51.4% 3rd pair: salt removal rate =57.8%	(Palakkal et al., 2018)
NaCl = 10mM	Single pass, solid electrodes	AEM: Neosepta AMX CEM: sPEEK-87	AMX: Z_{IEC} = 1.8meq/cm^2, W = 23%, δ=140 μm sPEEK-87: Z_{IEC} = 2.3meq/cm^2, W = 47%	CV_{ads}=1.0 V CV_{des}=0.0 V t_{ads}=t_{des}=10 min v = 20 mL/min	16.5	98.6		(Cha et al., 2018)
NaCl = 10mM	Single pass, solid electrodes	AEM: AEP-PEM: crosslinked poly (chloromethylstyrene) with 1-methylimidazole CEM: Neosepta CMX	AEP-PEM: Z_{IEC} = 3.0meq/cm^2, W = 5.0%	CV_{ads}=1.0 V CV_{des}=0.0 V t_{ads}=t_{des}=10 min v = 20 mL/min	16.1	98.3	Pore filling anion exchange membrane	(ul Haq et al., 2018)
NaCl = 5 mM	Single pass, solid electrodes	AEM and CEM: AMX and CMX Neospeta, Eurodia, France	AMX: Z_{IEC} = 1.8meq/cm^2, W = 23%, δ=140 μm CMX: Z_{IEC} = 1.7meq/cm^2, W = 28%, δ=170μm	CV_{ads}=1.2 V CV_{des}=0.0 V t_{ads}=t_{des}=300 s v = 5 mL/min	4.0	–	Cumulative exergy losses at 4 (J/mol water)	(Fritz et al., 2018)
NaCl = 5mM		Neosepta CMC and AMX, Astom Corporation	AMX: Z_{IEC} = 1.8meq/cm^2, W = 23%, δ=140 μm CMX: Z_{IEC} = 1.7meq/cm^2, W = 28%, δ=170μm	CV_{ads}=3.0 V CV_{des}=0.0 V t_{ads}=t_{des}=10 min v = 20 mL/min	85	76	Multi-channel MCDI concept with operating NaCl and $NaClO_4$ as drew solutions	(C. Kim et al., 2018)
NaCl and Na_2SO_4	Single pass, solid electrodes	AEM: quaternized PVA (QPVA) containing pulverized AMBERLITE FPA54	–	CV_{ads}=1.2 V CV_{des}=0.0 V t_{ads}=t_{des}=1.5 h v = 1.0 mL/min	–	68	Salt removal = 58meq/m^2 SO_4^{2-} selectivity=2.25	(Zuo et al., 2018)
NaCl = 10mM	Single pass, flow electrodes	CMX and AMX, Neosepta, ASTOM Co., Japan	AMX: Z_{IEC} = 1.8meq/cm^2, W = 23%, δ=140 μm CMX: Z_{IEC} = 1.7meq/cm^2, W = 28%, δ=170μm	CV_{ads}=1.2 V CV_{des}=0.0 V t_{ads}=t_{des}=15 min v = 2.0 mL/min	21.5	–	Total charge consumption = 3.9C	(Yu et al., 2018)
Humic acids = 50 mg/L NaCl = 75 mg/L	Solid electrodes	Cation and anion exchange membranes (Hangzhou Greenhe Environment Co., Ltd, China)	–	CV_{ads}=1.2 V CV_{des}=−1.2 V t_{ads}=t_{des}=55 min v = 20 mL/min	–	–	Ion removal efficiency = 82%	(Chen et al., 2018)

(*continued on next page*)

Table 4 (*continued*)

Feed concentration	Configuration of MCDI	Type of membranes	IEM characteristic	Process conditions	SAC (mg/g)	Charge efficiency (%)	Comments	Ref.
0.005 M KCl	Solid electrodes	Mosaic membranes produced by mixing NIIPAM with AV-17 anion exchange resin (70 mass%) and KU-2 cation exchanger (30%)	Z_{IEC}=0.96 mmol/g	CV_{ads}=1.4 V t_{ads}=t_{des}=40 min v = 5 mL/min	–	–	Energy consumption = 13.5 Wh/mol	(Volfkovich et al., 2018)
NaCl = 15 mM Na_2SO_4 = 15mM	Solid electrodes	AEM and CEM	AMX: Z_{IEC} = 1.8meq/cm^2, W = 23%, δ=140 μm CMX: Z_{IEC} = 1.7meq/cm^2, W = 28%, δ=170μm	CV_{ads}=1.2 V CV_{des}=−1.2 V t_{ads}=t_{des}=14 min v = 50 mL/min			Water recovery = 66% Selecitivty sulface to chlorides = 1.08	(Tang et al., 2017)
LiCl=10 mM KCl = 10 mM NaCl = 10MM	Batch mode, solid electrodes	Single AEM produced by chemical grafting PVC by EDA	AEM: Z_{IEC} = 3.5 mmol/g, W = 240%, δ=70 μm (A. Siekierka et al., 2018)	CV_{ads}=2.5 V CV_{des}=−2.5 V t_{ads}=t_{des}=30 min v = 66 mL/min	42.1	–	Selectivity toward to lithium	(A. Siekierka et al., 2017; A. Siekierka et al., 2018)
LiCl=20mM	Batch mode, solid electrodes	Single AEM produced by chemical grafting PVDF by EDA	AEM: Z_{IEC} = 4.0 mmol/g, W = 30%, δ=70μm	CC_{ads}=10A/m^2 CC_{des}=−10A/m^2 t_{ads}=t_{des}=10 min v = 66 mL/min	31	92	By application PVDF-EDA24 it is possible to concentrated lithium chloride with 3 times factor.	(Siekierka and Bryjak, 2019)
Na+ = 10,298 mg/L K+ = 102.1 mg/L Li+ = 15.7 mg/L Ca2+ = 63.7 mg/L Mg2+ = 50.3 mg/L Sr 2+ = 33.5 mg/L Cl- = 11,421 mg/L Br- = 128.9 mg/L HCO_3^- = 1462 mg/L B = 156 mg/L Si = 11.4 mg/L	Batch mode, solid electrodes	Single AEM produced by chemical grafting PVC by EDA	AEM: Z_{IEC} = 3.5 mmol/g, W = 240%, δ=70μm [212]	CV_{ads}=2.0 V $CV_{des,1}$ = 0.0 V $CV_{des,2}$=−2.0 V t_{ads}=3 min $t_{des,1}$ = 1 min $t_{des,2}$ = 5 min v = 66 mL/min	800	>100	Selectivity toward lithium	(Siekierka et al., 2020; A. Siekierka et al., 2018)
16 mM P, 8.5 mM NaCl	Solid carbon electrode	n.a.	n.a.	1.2 V in CV mode 1A in CC mode	n.a.	n.a.	Selective P removal	(Huang et al., 2017)
Pd 1–100 mg/L, SO_4 0.9–90.27 mg/L, NH_4 4.36–37.04 mg/L	Batch mode, porous carbon lectrodes	Commercial anion and cation exchange membranes from Astom Corporation (Japan).	n.a	0.9 V			Selective oncentration of Pd	(D.I. Kim et al., 2018)

Z_{IEC} – ion-exchange capacity.
W – water uptake.
δ-thickness.

Table 3 (*continued*)

Feed solution	Draw solution	FO membrane	Main composition of feed	Rejection	VCF	Permeate flux (L m^{-2} h^{-1}, LMH)	Reverse solute flux (g m^{-2} h^{-1}, gmh)	Ref.
mS/cm, B conductivity 3.1 mS/cm								
Landfill leachate	4 M NaCl	CTA (HTI)			1.6	2.1–2.9 (initial)		(S. Wu et al., 2018)
Whey	48–57 g/L NaCl	CTA (FTS-H2O)	Whey 5.9–8.0% (w/w)		2.5	6 (initial)		(G.Q. Chen et al., 2019)
Heavy metal wastewater	2000 ppm Na-Co-CA	Modified TFC membrane		>99.5% (room temperature) >99.7% (60 °C)		11 (room temperature) 16.5 (60 °C)		(Y. Cui et al., 2014)
Synthetic Hg contaminated effluent	NaCl; $MgCl_2$	TFC	20–1000 μg/L $HgCl_2$	> 98%	2			(Wu et al., 2016)
Acid mine drainage	1 M NaCl	TFC	Mg 436 mg/L, Al 293 mg/L, Si 15.3 mg/L, Ca 313 mg/L, Mn 203 mg/L, Fe 13.4 mg/L, Co 2.3 mg/L, Cu 615 mg/L and Zn 68.5 mg/L	Mg 98.9% Al 99.8% Si 97.1% Ca 99.3% Mn 99.6% Fe 100% Co 99.4% Cu: 98.9% Zn 99.5%	2	12		(Vital et al., 2018)
Simulated acid mine drainage		TFC	La 1.2 mg/L Ce 3.3 mg/L Dy 0.4 mg/L	La 91% Ce 91% Dy 97% (AL-FS mode)	5			(B.K. Pramanik et al., 2019)
Cu, Pb and Cd contaminated synthetic wastewater	NaCl	BSA modified TFC membrane	Cu 2 g/L Pb 2 g/L Cd 2 g/L	< 99.4%		45–50		(Zhao and Liu, 2018)
Printed circuit board wastewater	Ni plating solution Pd catalyst	TFC	Ni 5740 mg/L Pd 99.9 mg/L			39.4	Ni 0.43 gMH	(Gwak et al., 2018)
Li contaminated brine	$MgCl_2$	CTA and TFC membranes	Li 780 mg/L Mg 870 mg/L			CTA: 3–9 TFC: 6.5–11.5		(J. Li et al., 2018)
Na_2CO_3 simulating alkaline solution obtained from CO_2 capture by NaOH	NaCl (0.86–5.13 M)	AQP		99.4% purity of Na_2CO_3 $_0$•10 H_2O crystals		3–6	1.23 gMH	(Ye et al., 2016)

AL: Active Layer, AQP: Aquaporin membrane, CTA: Cellulose Triacetate, DS: Draw solution, FS: Feed solution,TFC: Thin Film Composite, HTI: Hydration Technologies I.

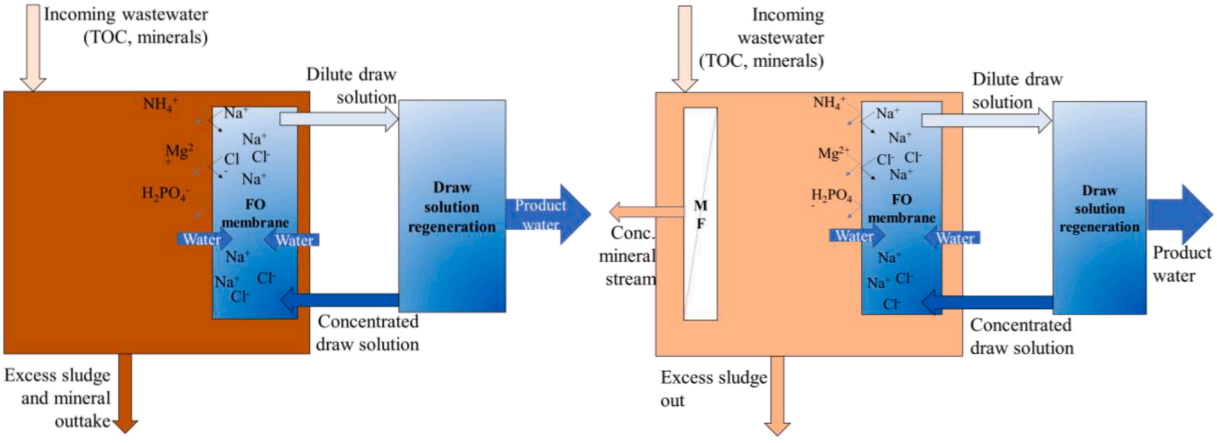

Fig. 7. OMBR (left) and MF/UF-OMBR (right) for simultaneous wastewater treatment and nutrients recovery. The systems have been shown with RO regeneration of draw for potable water reclamation.

the concentration of solutes in the reactor follows the MF/FO flow ratios, as sludge electrical conductivity was higher with higher FO relative to MF flows. However, the higher solute concentrations also results in higher feed osmotic pressure and lower permeate flux. To describe the concentration effect of nutrients and other solutes impermeable to FO but permeable to MF/UF membranes, Jørgensen et al. (Jørgensen et al., 2018) defined the nutrient retention time, NRT, expressed in Eq. (5), which is the time that the solutes spend in the reactor before being extracted.

$$NRT = \frac{V}{Q_{MF} + Q_{Excess}} \quad (5)$$

QMF is the MF flow, QExcess is the excess sludge outtake flow and V is the reactor volume. A similar term, contaminants retention time, CRT, has also been defined (Qiu et al., 2016). Assuming complete retention of nutrients by the FO membrane and no uptake/degradation by the microorganisms, the concentration factor of nutrients in the reactor equals the ratio between NRT and HRT (Jørgensen et al., 2018). Jørgensen et al. operated a MF-OMBR for 47 days with varying NRT and HRT and found correlation between NRT/HRT ratio and concentration of orthophosphate in sludge. However, precipitation occurred in the reactor at dissolved phosphorus concentrations exceeding 40 mg/L. Further concentration of sludge also led to inactivation of microorganisms and sludge deflocculation, reducing permeability, for conductivities > 20 mS/cm. It follows that there is an optimal relationship between NRT and HRT depending on inlet salinity and phosphorus concentration for sustainable operation. Holloway et al. (Holloway et al., 2015) conducted a comparable, 125 day pilot scale study of UF-OMBR treatment of domestic wastewater. The FO flux was stable at 4.8 LMH (on average) due to continuous UF extraction of solutes. Nitrogen removal was carried out by aerobic-anoxic treatment whereas phosphorus was extracted through the UF membrane in concentrations above 50 mg/L. In addition, FO draw solution was continuously recovered with RO to produce potable water. However, nutrients and organic compounds from draw solution accumulated in the draw solution and reverse salt flux from draw to feed elevated sludge conductivity.

Besides from aerobic OMBR, fertilizer drawn anaerobic MF-OMBR has been proposed for producing methane for energy recovery while producing a dilute draw solution for irrigation (Kim et al., 2016; Kim et al., 2017). However, experiments in lab scale have shown that reverse flux of fertilizers to the bioreactor reduces biogas potential. Out of six commercial fertilizers, only mono-ammonium phosphate did not reduce biogas potential due to low reverse salt flux (Kim et al., 2016). In addition, biofouling by the anaerobic sludge is severe compared to aerobic sludge, and reverse salt flux of the fertilizers led to enhanced fouling potential and nutrient accumulation in the sludge (Kim et al., 2017).

A promising solution to reduce fouling in osmotic bioreactors is by the using biofilm OMBR (BF-OMBR), as proposed by Qiu et al. (Qiu et al., 2016). Fixed bed biofilm degrades organic matter and does not require MF/UF membranes to be retained in the MBR. Hence, the system can still be operated at a low HRT (2 h) while maintaining removal efficiency of organics and concentrating nutrients with FO. As the FO membrane is not subject to biomass, a significant reduction in FO fouling was observed for the BF-OMBR when comparing to the MF-OMBR. TOC removal of 90% and ammonium removal > 99% was found in both systems and phosphorus recovery were similar (67.6–81.8% and 63.8–79.6%, respectively).

(i) Microbial electrolysis cells

Nutrient-energy-water recovery from wastewater has been demonstrated with the combination of FO with microbial electrolysis cells (MEC) (Zou et al., 2017; Qin and He, 2014) as illustrated in Fig. 8. Zou et al. (Zou et al., 2017) produce hydrogen gas from synthetic wastewater digestate with MEC by applying an electrical current between an anode chamber and cathode chamber (Fig. 8). The anode chamber contains digestate and exoelectrogens, which are electrochemically active microorganisms degrading COD. As COD is degraded, electrons are transferred from the anode to cathode, while released protons react with ammonia to form ammonium and migrate from the anode chamber to cathode chamber through a cation exchange membrane. In the cathode chamber, ammonium reacts with electrons released from the cathode to form hydrogen gas and ammonia. Thereby, ammonia from wastewater is recovered in the cathode chamber while producing hydrogen gas for energy recovery. Water recovery was obtained by treating the wastewater (anode effluent) with FO while simultaneously concentrating phosphate. The phosphate was then precipitated by adjusting pH and adding magnesium ions. The hybrid system reached a water recovery of $54.2 \pm 1.9\%$, 99.7 ± 13.0 ammonium-N recovery and $79.5 \pm 0.5\%$ phosphorus recovery as struvite (Zou et al., 2017). Potentially, the recovered hydrogen could cover up to 28.1% of the energy supplied to the MEC process through COD and nutrients. This study originated from Qin and He (Qin and He, 2014) where the water recovery with FO was integrated with a different concept; wastewater was used in the anode chamber and ammonium and electrons transferred to the cathode chamber as the exoelectrogens degraded COD in the anode chamber wastewater. Hydrogen was again formed in the cathode chamber and recovered for energy purposes, whereas CO_2 was added to form an ammonium bicarbonate draw solution with the ammonia originating from the wastewater. This could then be used to reduce the wastewater volume by $50.1 \pm 1.7\%$ with forward osmosis.

The MFC-FO system has also been demonstrated to recover water and ammonia from landfill leachate (Qin et al., 2016). There is a synergy between the MEC and FO process in that the MEC reduces salinity and COD content in the leachate, elevating FO flux two-fold (Qin et al., 2016). There are clear benefits of combining MEC and FO, but the hybrid systems are, as with other FO applications, challenged by reverse solute

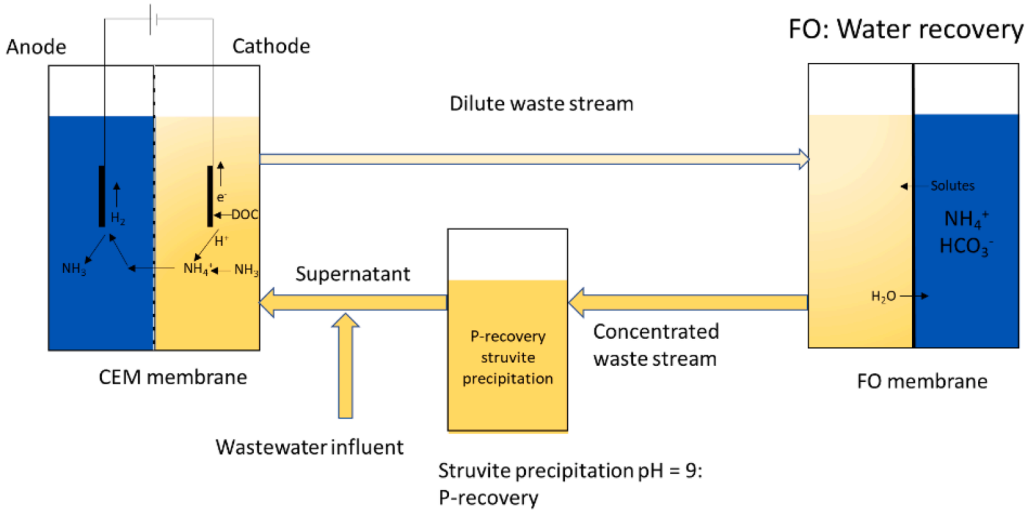

Fig. 8. FO-MEC for simultaneous of energy, ammonia, phosphate and water (Ali et al., 2015).

flux which reduces recovery of nutrients.

Another application of MEC is integration with anaerobic OMBR to form an AnOMEBR (Zhang et al., 2017). An anode immersed in the anaerobic sludge enhances degradation of organic compounds, while a cathode integrated as a spacer near the FO membrane surface reduces fouling and concentration polarization. Hydrogen gas is formed at the cathode increasing the biogas potential of the process. With this, biogas potential of the AnOMEBR has been reported to be 11% higher than conventional AnOMBR and lower concentrations of extracellular polymeric substances reduces sludge fouling propensity. In addition, the reverse diffusion of magnesium and acetate ions was reduced by the electric field (Zhang et al., 2017).

4. Membrane capacitive deionization

4.1. Introduction

Capacitive Deionization (CDI) has emerged as a novel electrosorption technique for removing ions form aqueous solutions (Suss et al., 2015). CDI finds main applications in seawater and brackish water desalination, sewage remediation as well as in potable water softening (Suss et al., 2015) (Porada et al., 2013). The last decade has brought numerous innovations in the CDI field, including theoretical (Suss et al., 2015; Porada et al., 2013; Singh et al., 2018; Biesheuvel et al., 2015; Smith, 2017; He et al., 2018; Härtel et al., 2015), architectural (Tang et al., 2019; Ratajczak et al., 2019; Remillard et al., 2018; Kim et al., 2018; Suss et al., 2012), material (Oladunni et al., 2018) and experimental (Porada et al., 2013; AlMarzooqi et al., 2014) advances. One of the most widespread modification of CDI is covering the surface of porous electrode with ion-exchange membrane (IEM) to make the configuration commonly known as Membrane Capacitive Deionization (MCDI) (Wang et al., 2018; Omosebi et al., 2017). Schematic illustration of traditional MCDI has been shown in Fig. 9. Implementation of ion-exchange membranes on the surface of electrodes prevents the occurrence of an adverse effect of ion re-adsorption during the discharging operations (Suss et al., 2012). The functional groups occluded in IEMs are capable of transporting ions in accordance with their charge, therefore anion-exchange membranes on which the positive functional groups are located will only transport anions. In case of cation-exchange membranes, the effect will be similar, but the functional groups will have a negative charge, which results in the ability to transport cations. The benefits of using ion-exchange membranes are improved adsorption capacity (Hassanvand et al., 2017; Jeon et al., 2013), reduction of energy consumption compared to the conventional CDI process (Fritz et al., 2018) or reduction of the effect of blocking electrodes and thus extending the "life cycle" of electrode materials (Hassanvand et al., 2017).

4.2. Background

Based on electrosorption of the ions, CDI has always been demonstrating the potential of capturing metals from solutions, however, with the perspective of desalination and wastewater treatment. The pioneer in the concept of water desalination, knows as “electrochemical demineralization of water” was Murphy et al. in the early 1960s (Murphy and Caudle, 1967). The mechanism of “electrochemical demineralization” was also widely studied by Evans and Hamilton (Evans et al., 1969). Researchers have attempted to explain the basic mechanism of ion removal using CDI. The breakthrough in understanding the mechanism of demineralization using CDI was the theory of potential-modulated ion sorption proposed in the 1970s by Johnson and colleagues (Oren, 2008). Currently, it is known as the double electrical layer (EDL) theory and has been identified as the actual electro sorption mechanism in the CDI process. The overall progress in CDI research and development remained very slow until first decade of 2000 when research on CDI started gaining moment once again. This renewed interest was mainly driven by the low energy consumption of the process for desalination and wastewater treatment. Modern research on the process of the capacitive deionization are focused on finding new electrode materials, as well as the basic design solutions for capacitive deionization cells. One of the first scientists to use an innovative electrode material in the form of carbonaceous aerogel was Farmer (Farmer et al., 2020). Next, the researches on application of innovative electrode materials were carried out (Porada et al., 2013).

A timeline of MCDI has been shown in Fig. 10. The process was presented by Lee and co-workers in 2006 (Lee et al., 2006) who used the process for desalination of wastewater from a thermal power plant. Over the next years, performance of MCID was benchmarked against traditional CDI (Kim and Choi, 2010) and constant current operational mode was introduced (Zhao et al., 2012). This was followed by an interest in applying MCDI for recovery of different ions from liquid streams as shown in Fig. 9 highlighting the important events in timeline on MCDI. while the theory of accumulation ions into the MCDI was proposed by Bieshuevel in 2010 (Biesheuvel and van der Wal, 2010). In 2015, Gao et al. (Gao et al., 2015) introduced a new method of desalination using CDI. This is a specific kind of CDI where the potential is applied only in desorption step. The modified electrode materials during the acid and amino treatment change their charges which in effect between that material the potential without external electrical field is sufficient to perform the adsorption operation. The opposite modified electrodes with negative and posistive groups were able to generate the electrical potential between them. This potential is called open voltage circuit (Porada et al., 2013) and it is power full tool for self-efficiency operations without external electrical field. This phenomenon find application in Inverted-Capacitive Deionization (Gao et al., 2015). The -COO-

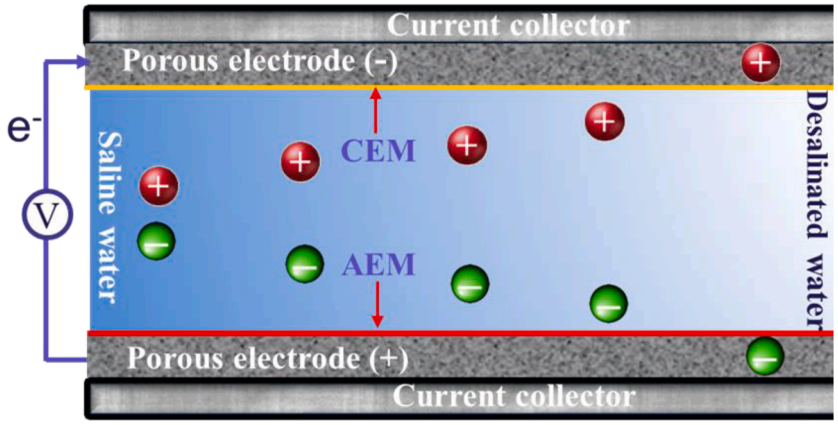

Fig. 9. A schematic illustration of MCDI.

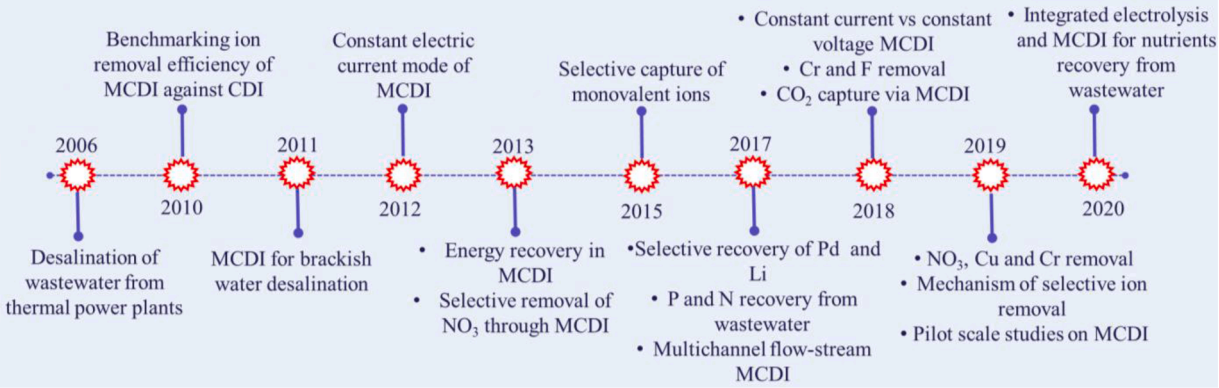

Fig. 10. A timeline of important milestones in MCDI.

groups were grafted onto the cathode material, while -NH^{2+} groups appeared in the anode material. Inspired from the energy storage field such as batteries and super capacitors, a highly promising approach is to replace one of the two capacitive electrode (porous electrode) with a battery electrode (Faradaic electrode) for a novel desalination technique referred to as Hybrid Capacitive Deionization (HCDI) (Lee et al., 2014).]. Unlike a HCDI cell combing a battery electrode (e.g., sodium manganese oxide) and a capacitive electrode (e.g., porous carbon), a desalination battery cell is composed of two different battery electrodes (one for cation Faradaic intercalation/de-intercalation and the other for anion Faradaic intercalation/de-intercalation). The concept of desalination battery was first proposed and demonstrated by Pasta et al. with the cell consisting of an Ag negative electrode and a $Na_2Mn_5O_{10}$ positive electrode (Pasta et al., 2012). Nowadays, the specific applications of HCDI are being investigated. Siekierka et al. presented in 2018 HCDI with selective adsorbent of lithium ions. By manipulation electrical mode during charge and discharge steps was possible to release lithium ions with 73% efficiency in separate flux (Siekierka et al., 2020).

4.2.1. *MCDI in minerals recovery*

Generally, the CDI technologies are applied for softening water, removal of hardness and brackish water desalination. However, application of IEM in CDI system created the possibility to concentrate, release and recover minerals and salts from aqueous solutions (Oren, 2008; Li and Zou, 2011). Moreover, targeted or selective ion removal is also being investigated by some research groups (Kim et al., 2019; Wang et al., 2019; Li et al., 2019; Wang and Lin, 2019; Dong et al., 2019; Siekierka, 2019; Siekierka et al., 2017; Siekierka et al., 2018). An overview of various studies on recovery of metals from solution by applying MCDI has been provided in Table 4. It is evident from the table that MCDI has been applied to remove a wide range of metals including Pd, Li, Cu, K, Mg etc. Similar to CDI, MCDI has been conventionally applied with the main objective of desalination or wastewater treatment. In desalination, MCDI has been used to treat ground water (Uzun and Debik, 2019; Tang et al., 2017) or low-salinity waters (Chen et al., 2018; Palakkal et al., 2018). For wastewater and water treatment applications, MCDI has been applied for the removal of nutrients (Sakar et al., 2019) and heavy metals (Chen et al., 2019). Due to the unique capability of the process of selectively capturing targeted ions form the solution, an increasing interest in developing the process for resource recovery from liquid stream has been witnessed. Recovery of Li from low concentration solution has been the focus of recent studies (Siekierka and Bryjak, 2019; Siekierka and Bryjak, 2017) due to increasing demand of Li for energy storage applications. Although, in both studies [211, 212], model low concentration (10–20 mM) LiCl solutions were applied, yet in the latter, the relative adsorption of Li was compared with of K and Na by using the model solutions of these ions having the same molar concentration. It was found that adsorption of Li on specifically designed electrode was significantly higher than K and Na, demonstrating the capability of MCDI to selectively adsorb Li.

MCDI exhibits better deionization performance than CDI due to application of IEMs. The charged functional groups on IEM selectively allow the penetration of counter ions blocking that of co-ions (Biesheuvel and van der Wal, 2010). Hence, IEM effectively alleviates co-ion repulsion, resulting in enhanced deionization performances (Yoon et al., 2019). However, the effect of IEM characteristics (e.g., ion exchange capacity, water uptake, electrical resistance) on process performance has not been systemically investigated in the MCDI field. Even in MCDI research applying novel functional ion-exchange materials, the basic analysis of IEM has not been presented. Hence, the aim of numerous research activities under MCDI performances as well as IEM for MCDI is to investigate the effects of the characteristics of CEM and AEM on MCDI performances and to develop new membranes for MCDI applications. Yoon et al. studied the influence of CEM on MCDI performance based on the CEM characteristic (Yoon et al., 2019). SAC (SAC – salt adsorption capacity in mg/g unit, this is a general amount of captured salt per weight of used elecrode), maximum average deionization rate (MADR), and charge efficiency were chosen to demonstrate the MCDI performance. Among them, MADR was most significantly affected by changes in CEM, indicating that the properties of the CEM contributed to the rate capability of MCDI (i.e., MADR) rather than capacity capability (i.e., SAC and charge efficiency). Application of commercial type IEM can affect the MCDI performances and their possibility to minerals recovery. By manipulating the ion-exchange capacity and thickness of the applied IEM, the adsorption rate can be characterized by high fluctuation of values of SAC and time of charging and discharging with the same desalinated effect. However, this effect is strongly dependent upon the feed composition and concentration as well as the electrical modes. SAC is directly influenced by the concentration of feed solution. With higher concentration of minerals in flow channel, the SAC is higher. By manipulating the MCDI stack, it is possible to recover minerals from solutions, selective capture anions and cations as well as totally remove salt and concentrate it in separate compartments. The MCDI process exhibit enormous flexibility of many kind of applications. Additionally, in accordance with ELDs theory by insertion MCDI can recover 30–80% of consumed energy (Fritz et al., 2018).

5. Comparison of MCr, MCDI and FO

5.1. *Fouling*

In a broader sense, fouling is defined as the process of deposition of particles or solute at the membrane surface or inside the pores such that the membrane performance is deteriorated (Field, 2020). It is generally considered as one of the major obstacles in applications of membrane technology (Bacchin et al., 2006). Fouling increases the resistance to mass transport across the membrane causing a decrease in flux, increases the pressure drop, and reduces the lifetime of the membrane.

Intensive fouling may also require rigorous chemical cleaning or membrane replacement, thus contributing to the overall operational cost of the plant (Te Lin et al., 2010). There are several types of fouling encountered in membrane processes such as colloidal, biological, organic and scaling. Depending upon the applied process and solution characteristics, one type of fouling can be more significant compared to the others.

5.1.1. Membrane crystallization

Only very few studies have addressed fouling investigation specifically in MCr (Jiang et al., 2019), however, it is very intuitive that fouling phenomena in MCr will be similar but more severe than those observed in MD. Due to high concentrations of the salt solutions generally treated through MD, scaling has been reported as the most severe problem (Warsinger et al., 2015). All three categories of scaling, namely alkaline, non-alkaline and uncharged molecular scaling, occur in MD (Laqbaqbi et al., 2017). From a mechanistic point of view, scaling occurs due to the precipitation of salts at the membrane surface under supersaturation conditions. In case of seawater desalination, NaCl causes the most scaling at membrane surface (Ali et al., 2015) (Laqbaqbi et al., 2017) applied for MD. $CaSO_4$, $CaCO_3$, $Ca_3(PO_4)_2$, $BaSO_4$ and $MgSO_4$ have been identified as the other main scale causing salts (Warsinger et al., 2015) (Lee et al., 2018). Scaling is influenced by various factors including operating temperature, cross flow velocity, pH, nature of the feed solution, membrane surface characteristics (hydrophobicity, roughness, contact angle) and distribution of flow within the module (Warsinger et al., 2015) (Nghiem and Cath, 2011) (Bush et al., 2018). Concentration and temperature polarization can also promote scaling at the membrane surface by inducing supersaturation (Duong et al., 2015) (Julian et al., 2018).

In addition to scaling, biofouling is also a concern for MD. However, this is mainly restricted to food processing and related applications (Warsinger et al., 2015). In case of desalination, high feed salinity combined with high feed temperature reduces the intensity of biofouling in MD compared to pressure driven processes (Krivorot et al., 2011). Organic fouling, originating from the interaction of membrane with solutions containing humic acid, alginate acid, protein, polysaccharides and some low molecular weight species, has also been reported in MD (Khayet and Mengual, 2004) (Khayet et al., 2004) (Naidu et al., 2014). Organic fouling significantly increases with the hydrophobicity of the membrane due to stronger interaction of hydrophobic content of natural organic matter with the membrane surface (DiGiano and Nilson, 2013). The presence of multivalent cations and high concentration of electrolytes such as NaCl favors the aggregation of humic acid and increase the rate of fouling (Yuan and Zydney, 2000). There is a mixed opinion about the reversibility of organic fouling in MD (Khayet and Mengual, 2004) (Srisurichan et al., 2005) (Naidu et al., 2014).

Intensity and rate of membrane fouling in MD is expected to be more pronounced for applications where the feed solution has a high organic content (Drioli et al., 2015; Shirazi and Kargari, 2015) such as municipal or dairy wastewater and various industrial process streams. However, studies on MD lack systematic investigations of the effect of organics on membrane fouling. In some studies, severe membrane fouling comprising of protein (Gryta et al., 2006) and other organics (Zarebska et al., 2014), has been observed which can reduce membrane hydrophobicity. Such observations indicate the need for developing improved membranes and pretreatment steps for controlling fouling and membrane damage when considering MD for wastewater treatment and related applications (García et al., 2018). In case of whey and skim milk processing, protein, lactose and mineral based fouling has been observed (Kezia et al., 2015; Hausmann et al., 2014; Hausmann et al., 2013).

There are certain other phenomena in MD that have the similar effect as fouling on process performance. Pore wetting causes the flux decline and deteriorates the permeate quality at the same time (Velioğlu et al., 2018; Warsinger et al., 2017). In case of partial wetting, the temperature at the pore mouth can be significantly lower than that at the surface and increases the temperature polarization which in turn can induce scaling of salts, with positive temperature solubility, inside the pore (Elshkaki et al., 2018). Temperature polarization in MD can be regarded as the counterpart of concentration polarization in low pressure driven processes (Ali et al., 2013) and must be minimized for the same reasons.

5.1.2. Forward osmosis

In FO, both sides of the membrane are in contact with solutions having fouling or scaling potential. For wastewater treatment applications, one side of the membrane is in contact with impaired water containing organics in high concentration, thus organic fouling and, subsequent biofouling, are obviously the dominant issues for this side of the membrane (Le-Clech et al., 2006). The rate and extent of organic fouling is strongly influenced by the interactions among the foulants as well as between foulants and membrane surface (Mi and Elimelech, 2008). In case of asymmetric membranes with the active layer facing the draw solution, intense biofouling and scaling of various salts at the substrate has been reported (Zhang et al., 2012). Permeation drag, hydrodynamic shear and calcium binding were also found to be influential parameters for organic fouling. In some studies, the scale formation at the membrane surface facing the draw solution has also been observed (Phuntsho et al., 2014).

FO fouling propensity has been reported to be low with high reversibility (90–100% flux restoration) by physical cleaning (Xue et al., 2016; Gao et al., 2018; Ansari et al., 2016; Lotfi et al., 2017; Lee et al., 2010; Mi and Elimelech, 2010; Baoxia and Elimelech, 2010). For example, Xue et al. (Xue et al., 2016) saw only a 5% reduction in flux over a two months continuous enrichment of nutrients from treated municipal wastewater. For treatment of sewage, Gao et al. (Gao et al., 2018) reached 90% flux recovery by air-water washing and 96% recovery by chemical cleaning (1% w/w NaOCl), whereas Ansari et al. (Ansari et al., 2018) reached complete restoration of flux by a combination of ultrasonic and high crossflow cleaning after treatment of digester concentrate. Fouling is reported as deposition of organic foulants, but Phunthso et al. (Phuntsho et al., 2014) observed that reverse salt flux of di-ammonium phosphate fertilizer draw solutions led to scaling on the membrane surface. Grafting polyamidoamine dendrimers to TFC membranes also show significant antifouling capacity while elevating ammonium rejection (Bao et al., 2019; X. Bao et al., 2019).

There is yet no consensus on the explanation behind the low fouling propensity in FO compared to pressure driven membrane processes such as RO. One explanation is that a less compact and more reversible fouling layer is formed in FO, whereas in RO for example the gradient in hydraulic pressure across the membrane promotes a more compact fouling layer (Holloway et al., 2007; Mi and Elimelech, 2008; Lee et al., 2010). However, this is questioned in other studies (Siddiqui et al., 2018; Tow and Lienhard V, 2017) suggesting that the lower fouling in FO is simply a result of lower permeate flux, transporting less foulants to be deposited on the membranes.

Another central parameter reducing permeance in FO is concentration polarization (CP) (McCutcheon and Elimelech, 2006). External CP (ECP) is the local dilution of draw solution and concentration of feed solution near the membrane surfaces facing draw solution and feed, respectively. ECP reduces the effective osmotic gradient and its intensity increases with permeate flux. In addition, an elevated concentration of solutes at the membrane surface may result in precipitation of salts of low solubility leading to scaling and flux decline. By elevating the crossflow velocity the thickness of the laminar layer along the membrane can be decreased thereby reducing CP. In addition, internal CP (ICP) inside the membrane material (e.g. in the support layer of asymmetric membranes) reduces the effective osmotic gradient. ICP is dilutive when active layer faces the feed solution (a configuration referred to as FO mode), and concentrative if the support layer faces the draw solution (PRO mode). Therefore, it is beneficial to reduce support layer thickness to reduce ICP and to operate at a relatively high crossflow velocity, typically up to 9 cm/s to reduce ECP (Ansari et al., 2015;

McCutcheon et al., 2005). However, high flow velocities also lead to more energy consumption.

5.1.3. MCDI

The studies on fouling in MCDI are scarce and most of the existing literature gives an overview of fouling in CDI (Hassanvand et al., 2017) where it directly affects the carbon electrodes and reduces the salt removal efficiency. However, it is anticipated that fouling on IEM of MCDI should deteriorate the process performance to a lesser extent than what is observed for CDI electrodes (Hassanvand et al., 2017). In general, IEMs are prone to colloidal, organic and biofouling (Mikhaylin and Bazinet, 2016). Additionally, the precipitation of dissolved salts on membrane surface also causes scaling. In a recent study (Wang et al., 2019), it was demonstrated that for a mixed solution containing calcium and bovine serum albumin, the presence of bovine serum albumin decreased the fouling when calcium concentration was below a threshold value (0.5–3 mM). However, above 5 mM, the presence of bovine serum albumin caused more fouling compared to the single component solution. Thus the concentration of calcium in the solution influenced the adsorption of bovine serum albumin at membrane surface, thus controlling the rate of fouling. It was also inferred that combining ultrasonic and chemical cleaning was effective in restoring the membrane efficiency. More importantly, the study concludes that cause of severe fouling in MCDI is scaling of inorganic salts instead of organic fouling.

In another study (Chen et al., 2018), organic fouling caused by humid acid and sodium alginate at electrode and IEM of MCDI were investigated. Na^{+} and Ca^{2+} were used as the sample ions in the solutions. It was found that presence of either of the organic compounds reduces the adsorption of Na and also increases energy consumption significantly. More detrimental effects were observed for humic acid which reduced Na adsorption by 5.3 mg per cycle and increased energy consumption by 57%. For the solutions with the same conductivity and organic concentration, higher fouling potential and energy consumption was observed for Ca^{2+} containing solutions compared to Na^{+} solutions. Fouling analysis revealed adsorption of organics on the electrodes and adsorption as well as penetration at the membrane surface. It was recommended that the feed solutions should undergo appropriate pretreatments before being fed into the MCDI unit. These are only preliminary investigation and knowledge on fouling in MCDI remains very limited at this stage and further research efforts are needed to explore this phenomenon.

5.2. Concentration ranges

5.2.1. Membrane crystallization

MCr can be operated in a wide range of solution concentrations. As shown in *Table 2*, MCr has been applied for recovery of minerals from the solution containing ions in concentrations ranging from a few hundred ppm to several hundred g/L. The conventional direct contact configuration of the process, however, is not suitable for highly soluble salts such as LiCl (Quist-jensen et al., 2016) which shows positive solubility with temperature. At high solution concentrations, such salts exhibit high osmotic pressures, thus in order to keep their vapor pressure above that of the permeate side, solution temperature has to be increased which also increases solubility of the salts, thus achieving supersaturation becomes challenging. For such solutions, relatively less explored MCr configurations, such as vacuum MCr can be more suitable. Recovery of salts in MCr is based upon supersaturation and crystallization is achieved through selective migration of water vapors through the membrane. For highly soluble salts solutions with low initial concentrations, MCr could be high-energy consumption solution.

5.2.2. Forward osmosis

As evident from Table 3, FO has mainly been applied for enrichment or recovery of nutrients-phosphorus and ammonia-from wastewater. Phosphorous concentration reported in these studies does not exceed a few hundred ppm and the ammonia concentration is also generally less than 1000 ppm. However, it should be noted that the wastewater streams treated through FO have very high load of organic contents. The motivation for applying FO in these applications is mainly driven by the prospect of low energy demand and low fouling propensity. In many of these studies, a draw solution either economically concentratable (e.g. seawater) or directly usable for external applications (e.g. for fertigation) has been applied which makes the overall economics of the process feasible. Also the recovered nutrient might have low solubility in the feed solution (i.e. the solubility of struvite in water at 25 °C is ~170 ppm), thus precipitation can be achieved at low overall solution concentration. The ability of FO to concentrate the solutions to saturation levels has been well documented in various studies (Iskander et al., 2017; S. Wu et al., 2018; Z. Wu et al., 2018). However, for solutions containing highly soluble salts, the osmotic gradient generated by the draw solution may not be enough to achieve supersaturation of salts of interest on feed side. In addition, CP reduces effective osmotic gradient between highly concentrated solutions and thereby reduces flux. Thus, FO is more promising candidate for precipitation of low to medium range soluble minerals.

5.2.3. MCDI

MCDI and CDI have been demonstrated for desalination of low-to-moderate-salinity solutions such as brackish water, low-salinity wastewater, and surface water having salt concentrations below 5000 ppm (Zhao et al., 2012). For these applications, MCDI and CDI are considered as alternatives to conventional desalination processes because they may require less energy and lower investments. CDI and MCDI have not yet been employed for seawater desalination due to the high salinity level and the relatively low salt removal capacity (SRC) of the charged electrodes. This is very much evident from Table 5 where the concentrations of various ions in feed solutions are of order of a few mM. In a recent study (Tang et al., 2019), however, it has been demonstrated that the salt removal capacity of MCDI can be enhanced by applying an over-potential (OP). An OP-MCDI system with mesoporous electrodes demonstrated an eight-fold increase in salt removal capacity compared to an OP-CDI system operating on a 0.5 M NaCl solution. However, the high solution concentration and applied voltage increases the energy demand and reduce the long term stability. It is therefore essential to address these issues before MCDI or CDI can be used for large-scale applications (Tang et al., 2019).

The literature reviewed in this paper combined with other studies (Tsai et al., 2017), has been used to plot the suitable concentration ranges for the various processes as shown in Fig. 11. RO has been included as examples of traditional desalination processes. It is evident that seawater RO is mainly applied to achieve the final solution concentrations up to 50 g/L. MCr can be applied to achieve supersaturation of several different solutions (Table 2) with concentration ranging from seawater to more than 350 g/L. However, for the feed solutions with relatively low concentration, RO can be used as a pre-concentration step due to its low energy consumption and MCr can be applied to further concentrate the retentate from RO. FO has been applied for low to medium concentration feed solutions. As discussed earlier, FO has the potential to achieve high solution concentrations. However, high concentrations require the application of draw solutions with high osmotic pressures (such as high-concentrated salt solutions) which might not be economically viable, particularly if draw solution recovery is also required. MCDI is suitable when the initial concentration of the required minerals in solution is very low and far from saturation.

5.3. Recovery from multicomponent solutions

5.3.1. Membrane crystallization and forward osmosis

In natural liquid streams as well as in wastewater, multiple ions are present simultaneously. Salts or metals are commercially attractive only

Table 5
A qualitative comparison of MCr, FO and MCDI.

	MCr	FO	MCDI
Driving force	Vapor pressure difference caused by temperature gradient	Gradient in osmotic pressure	External electrical field
Fouling	Scaling, organic fouling for feed solutions containing organics	Organic fouling, biofouling, scaling	scaling of IEM and deterioration of electrode structure
Energy consumption	High (typically 600–1000 kWh/m^3) without energy recovery	High if draw solution recovery is required	Low (0.5–3 kWh/$m^{3)}$ depending upon feed concentration
Type of energy	Mainly thermal, electric energy only for circulation of the solutions	Electric for circulation of feed and draw solution within the system (thermal energy may also be needed depending upon the draw solution recovery system)	Electric
Separation of salts from mixture	Suitable pretreatments are needed	Suitable pretreatments are needed	Potential to selectively capture the desired ion
Concentration ranges	70,000->350, 000 ppm	10–5000 ppm (excluding the concentration of organics which can be upto several thousand ppm)	20–5000 ppm
Overall disadvantage	Not a good candidate to recover high soluble salts from low concentrated solutions, high energy consumption without considering energy recovery, pore wetting, additional crystal recovery systems required	Regeneration of draw solution, limitation of feed concentration factor by osmotic pressure buildup, accumulation of feed solutes in draw, internal concentration polarization, unable to selectively separate targeted components	Limited feed concentration, issues with desorption step, low readiness level, membrane/electrode fouling issues

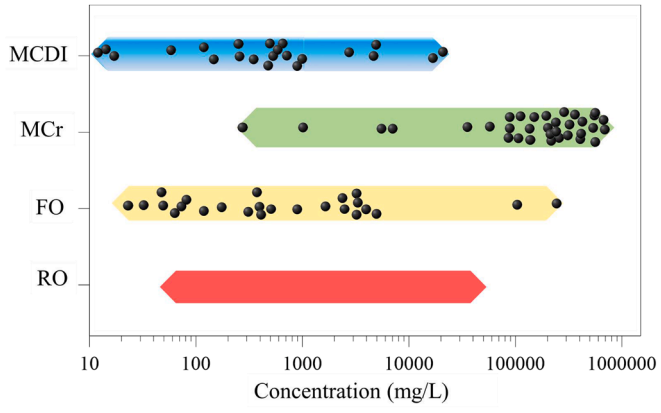

Fig. 11. Operational ranges of conventional (reverse osmosis, electrodialysis) and less-explored (membrane crystallization, forward osmosis and capacitive deionization) processes (taken from Table 2, *Table 3* and Table 4). Each circle represents the initial or final concentration of the feed stream used in the referred studies. RO has been included as a representative of conventional membrane-based desalination process.

when recovered in a pure form. Recovery in both MCr and FO is dependent upon the precipitation induced through supersaturation. Thus, some undesired salts/minerals start precipitating before the targeted salt or at some stage of precipitation, multiple salts start co-precipitating as shown in Fig. 12(a) for saturation of Li in Li brine (Hyun et al., 2020). Thus, selective separation or precipitation of the required salts from such mixture is a big challenge (Drioli et al., 2017; Ali et al., 2018). This aspect has not been highlighted in many studies on MCr as well as FO as those studies have been either performed mainly as proof-of-the-concept of minerals recovery from various brines (Ali et al., 2015; Ji et al., 2010; Mericq et al., 2010) or a single salt solution has been used to simulate brine (Edwie and Chung, 2013) (Ali et al., 2015). At high freshwater recovery factors, co-precipitation is expected to occur as indicate in other studies (Quist-jensen et al., 2016; Ali et al., 2018). Since minerals recovery in MCr and FO is controlled by supersaturation, it will be the salt with the lowest saturation that will precipitate first (Ye et al., 2013). It implies that more valuable minerals such as rare earth metals, which are present in different brines in minor quantities, are difficult to extract only by MCr or FO.

In order to overcome this challenge, integration of MCr and FO with other suitable processes is proposed. In some studies (Wu et al., 2018; Macedonio et al., 2013; Quist-jensen et al., 2016), the undesired co-precipitating salts are removed prior to the concentration step through chemical precipitation. The removal of co-precipitating ions has several advantages. For instance, the removal can prevent scale formation at the membrane surface in subsequent FO or MCr processes. FO has also been integrated to enhance the productivity of chemical crystallization by concentrating the solution containing desired crystals. The undesired ions generally also react with the chemical agent, which is expensive in many cases, thus increasing the process cost. For example, for magnesium recovery from landfill leachate in form of struvite, H_3PO_4 is added as the external chemical agent which also reacts with calcium present in the landfill leachate to form undesired calcium phosphate (Wu et al., 2018). The precipitation of undesired salts is generally achieved through addition of another relatively cheaper salt. For instance, calcium in the example is removed through addition of sodium carbonate. This aspect helps in reducing cost and improving the quality of the recovered product.

In addition to chemical treatments, physical treatments such as membrane filtration have also been applied to achieve the precipitation of only undesired salt. For minerals recovery from seawater brine, multivalent ions have been separated from monovalent ions using NF (Quist-jensen et al., 2016). Separate MCr units have been considered for treating NF and RO retentate for separate precipitation of multivalent and monovalent ions salts, respectively. In another study (Hyun et al., 2020), NF was applied to remove multivalent ions from Li brine which significantly delayed the precipitation of multivalent ions as shown in Fig. 12(b) and (c), thus allowing to achieve higher concentration of Li in the solution. However, this approach has two main drawbacks: NF membranes do not reject the multivalent ions completely thus, along with monovalent ions, some multivalent ions are also present in NF permeate. Secondly, even if a complete rejection of multivalent ions by NF is assumed, co-precipitation of several monovalent and multivalent ions salts still happens in each of the MCr units applied at NF permeate and retentate, respectively. This is attributed to the fact that NF membrane does not differentiate between the ions with same charge. Thus, conventional membrane-based solutions do not seem very promising for efficient recovery of desired salts/metals from complex multicomponent solutions such as seawater brine and produced water. As an alternative, integration of MCr with chemical adsorption has been suggested for recovery of Rb from brine (Naidu et al., 2017; Choi et al., 2019).

It has also been observed that the presence of other ions and organic matter can influence thermodynamics, kinetics, structure and purity of the required salts (Macedonio et al., 2013; Ji et al., 2010; Chong and Sheikholeslami, 2001). The crystallization of NaCl from seawater RO brine containing organic matter showed reduction in growth rate,

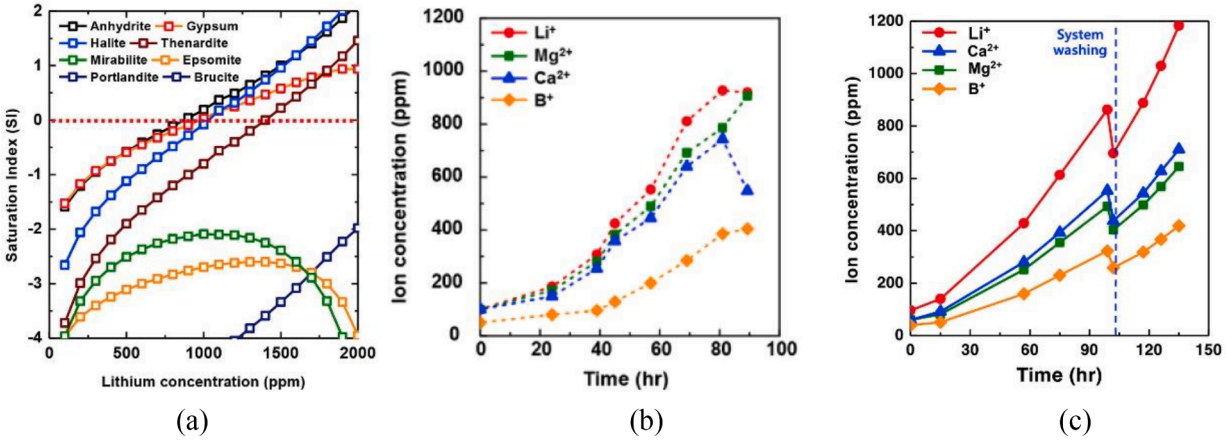

Fig. 12. (a) Saturation index of different salts when concentrating Li brines. At overall Li concentration of around 900, which is well below the minimum required concentration (6000 ppm) of Li to realize its recovery, other slats (anhydrite, gypsum, halite) start precipitaing (SI>0). (b) concentration of Li obtained (app. 900 ppm) before start of precipitaion of unwanted multivalent ions from untreated solution. (c) concentration of Li achieved (app 1200 ppm) after nanofiltration based pretreatment of Li brine.

suppression of cubic structure and smaller size compared to crystallization from artificial brine (Ji et al., 2010). Other ions in the brine also affect the morphology of the crystals as for instance making the cubic NaCl crystals more elongated (Macedonio et al., 2013; Ji et al., 2010). SO_4 ions have proven to impact the structure of Na_2CO_3, whereas NO_3^- and Cl^- showed no effect (Ye et al., 2013). However, the current literature lacks comprehensive protocols on precipitation of desired ions from multicomponent solution.

5.3.2. MCDI

Specific configurations of MCDI have been reported as solutions for selective removal of desired salts from multicomponent solutions in recent literature. In MCDI, ions first get adsorbed at the IEM and subsequently, these adsorbed ions move to the surface of the carbon electrode (Kim et al., 2013). It means that ion exchange membrane acts as an essential gateway the ions have to pass through before reaching the electrode. This allows tuning the selectivity of MCDI system towards certain ions by applying ion exchange membranes which offer selective adsorption of those ions. The behavior of selectivity nature in MCDI is governed by perm-selectivity phenomenon which enables the selective permeations of ions through the IEMs (Nativ et al., 2019). Nativ et al. (Nativ et al., 2018) investigated separation of mono- and di-valent ions using a flow electrode capacitive deionization (FCDI) system operated with a thin-film composite NF membrane (NF270) (Nativ et al., 2018). It was observed that the NF-FCDI process operated with equimolar solutions of monovalent and divalent ions is capable of selective separation of anions (perm selectivity of 1.28–7.03 between Cl^- and SO_4^{2-}), but incapable of separating cations (perm selectivity of 0.69–1.04 between Na^+ and Mg^{2+}).

MCDI has also been tested for removal of lead (Pb^{2+}) from water containing calcium and magnesium (Dong et al., 2019). The authors observed higher preferential removal and discharge of lead by using AEM compared to baseline CDI. In another study (Kim et al., 2013), MCDI was applied to selectively remove nitrate ions from a 5 mM NaCl + 2 mM $NaNO_3$ solution where AMX membranes demonstrated a selectivity coefficient of 4.37. Selective removal of nitrate could be enhanced by reducing the applied current; however, reduction in applied current also decreased the desalination rate. It was concluded that a new composite electrode should be developed to increase the selectivity at high desalination rates. For a description of the mechanism of bivalent ion selective removal compared to monovalent ions, see (Wang and Lin, 2019). As an alternative to suitable IEMs, a novel hybrid capacitive MCDI has been proposed for selective recovery of lithium from geothermal water where the lithium comprised only 0.07% of the total salts present in the solution with a TDS value of 23.4 g/L. (Siekierka et al., 2018) (Siekierka et al., 2020). The 'magic part' of the applied set-up was a cathode made of a lithium selective material which preferentially adsorbed lithium from the solution containing multiple ions including Mg^{2+}, Na^+, K^+, Ca^{2+}, Sr^{2+}, BR^-, Cl^-, HCO_3^-, B and Si. As a result of desorption, the process generated a lithium rich stream containing 73% of the lithium adsorbed by the electrode. The reported energy demand of the process was only 0.83 Whg^{-1} of the adsorbed salt.

MCDI was also tested for simultaneous ammonia removal and deionization of wastewater containing other ions including Mg^{+2}, Na^+, K^+ and Ca^{+2} by using enhanced flow channel MCDI (Sakar et al., 2019). Real digestate wastewater applied in the study contained 2.3 g/l overall concentration of these ions (individual concentrations were 709, 120, 1277.8, 183.7 and 48 ppm for NH_4^+, Mg^{+2}, Na^+, K^+ and Ca^{+2}). The overall removal of Mg^{+2}, Ca^{+2}, K^+ and NH_4^+ was recorded as 90.4%, 85%, 67.9% and 54.4%. It was observed that the electrosorption of NH_4^+, depended on hydrated radius, charge valance, affinity and concentration of the other ions.

5.4. Energy consumption and type of energy input

5.4.1. Membrane crystallization

Operation of MCr requires electric and/or thermal energy input. Electric energy is generally applied to operate the pumps. Thermal input, which can also be supplied through electric energy, though it is an expensive option, is used to heat the solution to be treated. In the field of desalination and wastewater treatment, MCr is in general used at temperatures ranging from 30 to 85 °C as shown in Table 2, which is below conventional distillation. The low temperatures makes it possible to use low-grade heat for operation, which can reduce the cost of the processes significantly. Schwantes et al. reported output ratios of 2.4–3–4 and specific energy requirements of 170–300 kWh/m^3 for full-scale desalination demonstration plants utilizing a parallel multi MD-module setup (Schwantes et al., 2013). Dow et al. tested DCMD in pilot-scale using waste heat and found an average thermal energy consumption of 1500 kWh/m^3 (Dow et al., 2016). However, as also reported by Khayet (Khayet, 2013), energy requirements for MD reported in the literature vary over a broad span ranging from 1 to 9100 kWh/m^3. The discrepancy in the observed energy consumption is associated with several factors including membrane type (Ali et al., 2019), applied configuration (Criscuoli et al., 2008), module design (Ali et al., 2018) (Ali et al., 2015), heat recovery system (Ali et al., 2018) and the availability of low-grade heat such as solar energy (Khayet, 2013). Energy reduction in MCr is achieved through three main routes: development of better

membranes, improved and optimized process designs including modules and new configurations aiming at improved energy recovery.

MCr can be operated in direct contact and vacuum configurations. Condensation of water vapors for both these configurations requires some cooling system which can remove the latent heat of the vapors. In direct contact configuration, the cooling is provided through an electric cooler which removes the heat absorbed by the cooling media (generally a pure water stream) from the vapors. In vacuum configuration, the heat is removed from the vapor by using a cooling liquid stream such as liquid nitrogen. However, the energy requirements associated with the cooling have been generally neglected while calculating overall energy requirements of the system (Al-Obaidani et al., 2008; Ali et al., 2016) which results into underestimation of the net specific energy requirements of MCr systems.

5.4.2. Forward osmosis

Generally there are lower electric energy requirements of FO compared to RO as there is no need for feed stream pressurization in FO (Chen et al., 2019). The overall energy consumption in FO is associated with two steps: i. circulation of feed and draw solution; ii. draw solution recovery/regeneration. The main energy consumption or cost in FO for production of clean water is associated with draw solution regeneration, however, many studies on FO, lack the discussion on the energy associated with draw solution recovery system leading to a false perception of FO being more energy efficient than RO (Long et al., 2020). Thus, in addition to low reverse salt flux and high permeate flux, economics of draw solution recovery is an important parameter for feasible implementations of the process. Draw solution recovery systems can be driven by different energy types including thermal (solar as well as waste heat), electric (pressure drive membrane processes), chemical (inducing precipitation) and magnetic fields (for magnetic separation) (Long et al., 2020). There are also directly usable draw solutions, such as saccharide and liquid fertilizers, which can be used as a product somewhere else without recovery (Shan et al., 2012; Su et al., 2012; Xie et al., 2015).

Since draw solution recovery is achieved through various approaches, energy requirements and final cost in FO is a function of draw solution recovery system applied. For example, for an FO-RO system for nutrients recovery where RO has been applied for draw solution recovery, the FO process has been modelled to consume 25% of the energy and RO the remaining 75% of the specific energy consumption of approximately 4 kWh/m^3 (Holloway et al., 2007). Yangali-Quintanilla et al. (Yangali-Quintanilla et al., 2011) compared the energy consumption of a combined FO - low pressure RO (FO-LPRO) system with conventional high pressure RO for treatment of secondary wastewater effluent and found that the FO-LPRO system had energy consumption of 1.5 kWh/m^3 compared to 2.5 kWh/m^3 for RO. However, due to high FO membrane costs, the FO-LPRO process is only economically feasible compared to RO if FO can deliver a permeate flux above 5.5 LMH. This is in accordance with the study of Aydiner et al. (Aydiner et al., 2014), finding higher capital expenses for FO-RO treatment of whey due to FO membrane cost but shorter payback time explained by high water recovery and low energy consumption. In another study describing water recovery from landfill leachate (Iskander et al., 2017), the maximum energy consumption was in the range of 0.276 ± 0.033 kW h m^{-3}, however, the energy consumption for draw solution recovery was not been included into the analysis. For an ammonia-carbon dioxide FO desalination system, where the draw solution was concentrated through distillation, the specific electric energy consumption has been calculated to be 0.24 kWh/m^3 (McGinnis and Elimelech, 2007). For the same system, the energy requirements for draw solution recovery have been calculated in the range of 3.31 to 7.4 kWh/m^3 (Moon and Lee, 2012).

Thermal energy driven draw solution recovery techniques mainly apply low grade energy to recover draw solutions. These techniques include application of gas and volatile compounds (McCutcheon et al., 2005; McGinnis and Elimelech, 2007; Achilli et al., 2010), phase transition materials (Li et al., 2011; Kim et al., 2016; Cai et al., 2015) and MD. The first technique utilizes low grade energy to decompose the solute into gas phases which can be reused as draw solution. For instance, ammonium bicarbonate containing solutions generate high osmotic pressure and decompose into NH_3 and CO_2 upon heating. Though this technique can significantly save energy (SEC as low as 0.25 kWh/m^3 of freshwater), the reverse salt flux is high in this case and water quality is compromised (Stone et al., 2013). Phase transition materials, as the name suggests, change the phase from liquid to solid or vice versa with change in temperature or pH. These materials are potentially interesting candidates as low energy draw solution recovery systems (SEC as low as 1.80 kWh/m^3), yet the produced water may require further treatment (Darvishmanesh et al., 2017; Cai and Hu, 2016). Another approach for draw solution recovery is MD, which is an interesting candidate when low-grade thermal energy is available (Zhang et al., 2014; Volpin et al., 2019), however, the expected energy consumptions are in the same range as discussed in above paragraphs on energy consumption for MCr.

In chemical energy driven draw solution recovery systems, multivalent inorganic salts such as $Al_2(SO_4)_3$, $MgSO_4$ and $CuSO_4$ have been traditionally applied (Alnaizy et al., 2013; Alnaizy et al., 2013; Environ et al., 2011). Such salts bring the energy consumption of the recovery process significant low, however, solute recovery involved generally pH adjustment or metathesis reaction. In both cases, the addition of chemicals generate additional cost and environmental related issues which should be taken into account when comparing the benefits of these techniques with traditional electric energy driven technologies. Additionally, the presence of heavy metals in the recovered water even in trace quantities will be fatal for practical implementation of the technology. While applying FO for minerals recovery, the potential of these technologies to achieve saturation concentrations on feed side also needs further investigations.

5.4.3. MCDI

Compared to MCr, MCDI requires only one type of energy source i.e. electricity. The energy consumption of MCDI is approximately 0.1 – 0.2 kWh/m^3 of purified water, which compares favorably to the energy use of 0.86 – 1.55 kWh m^3 deionized water for RO treatment of brackish water. In another study (Zhao et al., 2013), energy consumption in MCDI was quantified as function of influent concentration, flow rate and water recovery. Experimental laboratory scale data demonstrated that MCDI, with energy consumption less than 1 kWh/m^3, is more energy efficient than RO at salinity levels lower than 60 mM to extract freshwater. For a more concentrated solution (0.5 M NaCl), Tang et al. (Tang et al., 2019) estimated an energy consumption of 83.2 kWh/m^3 by using a modified MCDI system. By implementing an energy recovery system as an integral part of MCDI, the overall thermodynamic energy consumption of the process can be as low as 0.26 kWh/m^3 of the freshwater produced (Długołęcki et al., 2013), however, the experimentally measured values are much higher indicating the perquisite to improve the thermodynamic efficiency of the process. It should also be noted that adsorbed minerals in MCDI are discharged from the electrode in form of a concentrate liquid stream which requires further processing for separation of salts. Energy consumption for such processes has not been considered in literature and should be included when calculating the overall energy consumption of the process.

Lee at al. demonstrated the feasibility of desalinating secondary effluent from a domestic wastewater treatment plant (DWTP) using membrane capacitive deionization (MCDI) for reclamation purposes. Removal of the ions was easily performed by the electrostatic field-assisted deionization process. The use of MCDI for low-salinity wastewater reclamation demonstrated favorable energy performance with a low volumetric energy input and a molar energy input of 0.12 kWh/m^3 and 0.03 kWh/mole, respectively; and the energy efficiency of this system can be further improved by energy recovery or incorporation of energy-producing processes. These results indicate the benefits of using MCDI as part of the treatment processes for the reclamation of

wastewater with low salinity (Lee et al., 2019).

A summary of various parameters compared in this section has been provided in Table 5.

6. Technology readiness

6.1. MCr

Recently there has been some progress in commercializing MCr systems. Thus, Memswift, a Singapore based company, is supplying MCr systems for resource recovery and to approach zero liquid discharge in wastewater treatment. However, not much detail is available about the systems applied or current projects undertaken by the company. For commercializing MD, several promoters and developers have emerged. Modified air gap membrane distillation process, now commercialized as Memstill, was licensed to Aquastill and Keppel Seghers. In addition to AGMD systems, the company also provides DCMD and liquid gap membrane distillation modules and has installed several pilot units at various locations during 2006–2011 (Thomas et al., 2017). Memsys, now acquired by New Concepts Holdings Limited (NCHL), is another example. The company develops Vacuum Multi Effect Membrane Distillation (V-MEMD) modules and has installed several pilot units (the maximum capacity of 50m^3/day) in many countries.

6.2. FO

The use of FO for recovery of nutrients and other ions has been studied mainly at the bench scale, but there are also studies demonstrating the technology in pilot and small pilot scale, showing that it is simple to scale up from bench to pilot scale (Cath et al., 2010) (Hancock et al., 2011) (Chen et al., 2019; Lotfi et al., 2015) (Phuntsho et al., 2016). Hancock et al. (Hancock et al., 2011) studied the treatment of domestic wastewater with a combined FO-RO system at 26.5 m^3/d using CTA membranes for FO and three seawater RO membrane units to recover the NaCl draw solution. The pilot scale investigation showed a constant high rejection of trace organic contaminants over 40 days of operation. Despite of the high rejection, contaminant accumulation in the draw solution was observed over time. A similar system was used to purify secondary wastewater effluent (Cath et al., 2010). In this study, a stable water flux was observed, and there was high flux restoration with physical and chemical cleaning. Again, pollutant accumulation in the draw solution was observed as the ammonia and nitrate concentrations increased over the period of operation. In fertilizer drawn FO (20.2 m^2 CTA membrane) coupled with NF (7.9 m^2) draw solution regeneration, there was again observed high stable/recoverable water permeability during the period of operation and the process was limited by accumulation of feed salts in draw and reverse flux of nutrients from draw to feed (Phuntsho et al., 2016).

6.3. MCDI

Despite being a very young process, significant interest has been observed in developing MCDI technology for desalination and wastewater treatment. A Dutch company, Volte offers MCDI units (CapDI©) with production capacity up to 30GPM. Recently MCDI has been combined with photovoltaic (PV) panels and battery storage to ensure salt recovery though MCDI in a green and sustainable way (Tan et al., 2018). The possibility of designing and powering MCDI technology with PV panels coupled with battery storage has been investigated using a prototype system capable of electrode charging currents in excess of 100 A and product volumes on the order of 5 m^3/day (Tan et al., 2018). Guidelines for the design of systems able to operate for 24 h without grid connection are provided. The energy consumption of an MCDI prototype plant with various influent flow rates and charging currents has been evaluated and the relationship between these parameters explored such that an in-built system controller could be used to dynamically adjust the operating conditions of the process so as to increase the system effective operation time (Tan et al., 2018).

7. Challenges and future research directions

7.1. MCr

MCr has been developed at laboratory scale during the last 30 years and its proof-of-concept for many different solutions and recovery schemes has been proved. Despite being a new concept, it is a very promising technology for resource recovery from different effluents. It provides several advantages with respect to conventional methodologies including controlled nucleation and crystal growth, uniform crystal size distribution, tunable polymorph selection etc. The results achieved in previous studies on MCr prove that a wide range of applications are possible ranging from inorganic salts in desalination and wastewater treatment (Table 2) to crystallization of biomolecules. The scalability of membrane operations, in particular, is advantageous. For instance in the crystallization of single molecules for diffraction analysis, the equipment should be at a small scale. The opposite applies to applications in desalination where e.g. a single plant might need to process hundreds of cubic meters brine per day. This provides another positive aspect to membrane crystallizers, i.e. for the recovery of rare and expensive minerals from brine or other wastewater sources as a contribution to the existing mining industry (Quist-Jensen et al., 2018). However, a number of research targets are required to achieve to enable the successful commercial scale implementation of MCr related to long-term and continues operation as discussed below.

7.1.1. Membrane development

Membrane properties, such as hydrophobicity, porosity and pore size are all important for MCr performance and commercialization (Cui et al., 2018). Commercial membranes typically used in MCr are normally fabricated for low pressure-driven filtration processes such as microfiltration (see Table 2) rather than for temperature-driven processes (Al-Obaidani et al., 2008). However, driving force and separation requirements in MD and MCr are different from low pressure driven membrane operations. Therefore, membranes have to be developed taking into consideration the specific mechanism of MCr. As seen from the previous studies, materials such as PVDF, PP and PTFE are mainly used. In general fluoropolymers have low surface tension, high thermal stability and chemical resistance making them suited for membrane operations (Cui et al., 2014) (Liu et al., 2011). In addition to conventional materials, new types of polymers such as HALAR and Hyflon offer distinct advantages for membranes for MD/MCr applications due to their inherently high hydrophobic character (Gugliuzza and Drioli, 2007). New membrane synthesis routes, such as sequential electrospinning and electrospraying in combination with thermal treatment and integration of superhydrophobic character of membrane surfaces with anti-deformable pores, have also been proven affective in producing robust hydrophobic membranes (Zhu et al., 2020; Zhu et al., 2020). Future studies should also focus on preparing membranes utilizing green solvents to strengthen the sustainability of MD and MCr (Cui et al., 2013). Therefore, the entire lifespan of the membranes (cradle to cradle) including their long-term stability at extreme concentrations and high temperatures should be a very important factor during further development and commercialization of MCr. For simultaneous production of energy, raw materials and freshwater through MCr, as suggested in the literature (Ali et al., 2018), the membrane pore size, hydrophobicity and mechanical strength should be designed to tolerate the applied hydrostatic pressure on permeate side. It has been well demonstrated that different polymorphs of a single compound can be obtained by tuning the membrane features and operative conditions in MCr, however, current literature seriously lack of systematic investigation of this aspect. Thus, the membrane synthesis techniques able to prepare the membranes with specific surface features can be of central

importance in future studies on MCr.

Ideal membranes for MD should also exhibit minimum thermal conduction to reduce the undesired conductive heat transfer across the membrane. Naturally, MCr membranes are also expected to demonstrate excellent anti-scaling character. Anti-scaling features can be achieved by tuning the surface properties of the membranes as well as selecting suitable materials (Ali et al., 2015; Boo et al., 2016), however, further research efforts are required to better understand the relationship between surface properties and anti-scaling behavior. Due to the prospective role of MD/MCr in aqueous solution containing oil content (oil and gas industry, wastewater from olive oil mills, bilge water etc.) membranes showing omniphobic characteristics (repellence to water and oil) are also expected to gain significant importance (Lu et al., 2019).

7.1.2. Understanding and mitigation of fouling

As stated earlier, membrane surface scaling is an important issue for MCr. In addition to scaling, membrane pore wetting is also considered an issue with equally detrimental, or even more severe effects. There is accumulating evidence that scaling increases wetting issues (Gryta, 2007; Gryta, 2000). However, intrusion of saline solution into the pore, followed by evaporation, will result in formation of scales within the pores. While surface scaling can be removed using traditional methods (rinsing with water or appropriate chemical agents); the scaling within the pores might require more rigorous treatments such as backwashing with appropriate cleaning agents (Warsinger et al., 2017). Thus it is crucial to develop strategies and protocols to avoid wetting issues in MCr. For a long time it was believed that sufficient hydrophobicity of the membrane, appropriate pore size and low pressure drop within the feed channel are sufficient to mitigate the wetting in MD/MCr (Warsinger et al., 2015). However, is has become clear now that also operation mode (intermittent or continuous) as well as operating conditions play role in inducing pore wetting (Jacob et al., 2019). However, further research is needed to explore more dimensions of this phenomenon. This aspect is particularly important when considering solar energy-which is intermittent by nature- to drive MD/MCr.

For scaling and fouling control, the effect of membrane design parameters (e.g. surface roughness and pore size) need to be investigated. This aspect will become more crucial when applying MCr for food, pharmaceutics and chemical productions where current understanding of membrane fouling/scaling is even more limited compared than desalination. Some salt scaling can be controlled by appropriate operative conditions such as feed temperatures and flow rates which can either delay the salt precipitation or can wash the precipitating salts away from the membrane. Temperature control within the membrane module (taking into account the temperature polarization) and in the feed tank is also very important to avoid membrane surface scaling. Moreover, suitable membrane module alignment (vertical or horizontal) and appropriate cleaning procedures are other examples of issues which have to be addresses for successful and efficient operation of MCr.

7.1.3. Separation of salts from multicomponent solutions

Another limitation towards commercialization of MCr is the separation of the desired precipitants in multicomponent solutions. The difficulty of separating the desired mineral from a multicomponent mixture is also a bottleneck in further extending the applications of MCr for recovery of various minerals from different streams. In current literature, mainly single salts have been obtained by MCr from multicomponent solutions. Until now, the main focus of MCr has been on recovery of Na, Ca, Mg, with some studies on Rb and Li. Estimations on the order of precipitation have been carried out by thermodynamic modeling (Macedonio et al., 2013; Quist-Jensen et al., 2016) and show promising results for recovery of more valuable elements from seawater RO brine than for instance NaCl. However, the main challenge in recovery of individual salts and components of low concentration in e.g. seawater or produced water is the unavailability of effective protocols to separate them from a multicomponent solution as discussed in detail in Section 5.3 (Quist-Jensen et al., 2016). New physical (membrane processes, better crystallization protocols etc.) as well as chemical treatments should be integrated with MCr to tackle the problem of co-precipitation of undesired salts and ensure that more valuable and targeted compounds such as Zn, Cu, Mn and other ions listed in Table 1 can be recovered from unconventional resources. Future research directions should comprehend analysis of targeted ions for specific purposes for instance battery technologies to secure correct mineral purity, crystal size and size distribution etc. New physical (membrane processes, better crystallization protocols etc.) as well as chemical treatments should be integrated with MCr to tackle the problem of co-precipitation of undesired salts. Methods of avoiding co-precipitation has been described in Section 5.3 as integration of NF and MCr to separated monovalent ions from bivalent ions and integration of MCr and adsorption for Rb recovery. To further extend the MCr research, temperature and pH variations might also be considered to separate ions as well as MCr / MCDI and MCr / adsorption hybrid systems are likely to solve the limitation of MCr to target more valuable compounds in low concentrations from multicomponent solutions.

7.1.4. Efficient crystal recovery system to avoid scaling and fiber blocking

For stable operation of MCr, efficient crystal recovery systems needs to be developed and build in order to avoid scaling and fiber blocking. One solution can be the integration of MCr units with MF/UF units to ensure continuous separation of the crystals from solution.

7.1.5. Membrane module design

In traditional MD, module design is mainly aimed at improving hydrodynamic within the module (Ali et al., 2015; Yang et al., 2012) or devising better energy recovery arrangements (Guillén-burrieza et al., 2012; Singh and Sirkar, 2012). In case of MCr, additional focus should be on mitigation of scaling/fouling at the membrane surface. This potentially can be achieved by devising the module that offer more shear at membrane surface and following the membrane geometries which allow easy separation/washing of crystals from membrane surface. Also specific modules for MD and MCr needs to be developed taking into account the length of the modules (Ali et al., 2016), characteristics of the membranes (Ali et al., 2016) and flow patterns (Ali et al., 2015) to obtain enhanced flux, high energy efficiency and low temperature polarization.

7.2. FO

7.2.1. Draw solution recovery

The main challenge for widespread use of FO for recovery of minerals is the membrane cost as well as low permeability towards water and high permeability towards undesired solutes. As the feed stream is not pressurized in FO, the energy requirements of FO as such is low compared to RO (Chen et al., 2019). However, the energy costs for FO is associated with draw solution regeneration as discussed in Section 5.4. A common draw solute is NaCl, which can be recovered with RO or MD, requiring hydraulic pressure or a temperature gradient, respectively, which elevates expenses for the FO process (Chung et al., 2012; Lutchmiah et al., 2014). As an alternative, some studies have focused on draw solutions that does not require re-concentration. This can be seawater or RO brine, which can then be discharged back to the sea after a given dilution factor has been reached (Kedwell et al., 2018; Cath et al., 2010; Vu et al., 2018). Hence, energy for regeneration is not required and pure water is transported directly to the sea. The only energy costs required is energy for circulation of the draw and feed suspensions. Similarly, concentrated fertilizer solutions have been investigated as possible draw solutions (Kim et al., 2016). However, these scenarios hold true in very specific circumstances and more general draw solution recovery methods still need to be discovered.

7.2.2. Solute rejection

Feed solute permeability is also a critical parameter for FO as a high permeability will result in loss of solutes from feed and accumulation in the draw solution (Luo et al., 2016). FO membranes have shown high rejection of trace organic contaminants present in wastewater, almost complete rejection for charged, whereas hydrophobic and uncharged contaminants have lower rejection (Holloway et al., 2014). In nutrients recovery, FO operation show high phosphate rejection; all studies in Table 3 show rejections above 95%, even up to 99.8%. There is significantly lower rejection of ammonia and ammonium ranging from 99% down to 62% (Hau et al., 2014; Chen et al., 2014). This is explained by the lower hydrodynamic radius and molecular weight and thereby higher diffusivity through the membrane of ammonium and ammonia compared to phosphate ions (Kedwell et al., 2019). Ammonia and ammonium rejection depends on pH, as it is present as uncharged ammonia at high pH values ($pK_a = 9.24$) with lower hydrodynamic radius (180 pm) than ammonium ions (330 pm), hence ammonia/ammoniums nitrogen rejection decreases with increasing pH (Kedwell et al., 2019; Kedwell et al., 2018). Another explanation for low rejection of ammonium is the bidirectional diffusion across FO membranes, meaning that a high reverse cation flux induces high solute flux from feed to draw (Kedwell et al., 2019; Lu et al., 2014; Hancock and Cath, 2009). For an ammonium ion to diffuse from draw to feed, a positively charged ion is required to diffuse from draw to feed in order to keep electro neutrality across the membrane. It follows that one solution to enhance rejection of ions is to reduce reverse salt flux by selecting draw solutes with lower reverse salt fluxes, e.g. $MgSO_4$ or CH_3COOMg, or even uncharged solutes such as glucose. Because of the bidirectional transport of ions, RO rejection of solutes may be higher than FO rejection as there are no ions present in RO permeate to facilitate the bidirectional transport of ions. In a recent review, other strategies to reduce reverse solute flux are presented, of which pressure and electrolysis assisted osmosis are promising (Zou et al., 2019).

7.2.3. FO membrane permeability enhancement

The above-mentioned challenges place demands for further development of FO membranes to reduce their permeability towards solutes and elevate water permeability. One attempt is by surface modification. FO membranes have been modified to be positively charged, e.g. by grafting amine groups on the membranes, e.g. polyethyleneimine (PEI) (Bao et al., 2019; Lu et al., 2014; Bao et al., 2019; Qiu and He, 2019). This elevates rejection of cations, e.g. heavy metals, sodium and ammonium ions thereby enhancing retention of nutrients and reducing reverse salt flux. Surface modification also reduced reverse salt flux and pure water flux and made the membranes less prone to fouling. In addition, development of FO membranes with high retention of small cations also enables the recovery and removal of heavy metals from waste streams (Hamid et al., 2020; Saeedi-Jurkuyeh et al., 2020). E.g., the synthesis of thin-film nanocomposite FO membranes modified by graphene oxide and polyethylene glycol enables rejection of Pb, Cd and Cr og 99.9%, 99.7% and 98.3%, respectively, while having a water flux of 34.3 LMH (2 M NaCl draw solution (Saeedi-Jurkuyeh et al., 2020). Another promising approach is by synthesis of a swellable PA-BSA active layer in the TFC membrane to create water channels with high water and low solute permeability (Zhao and Liu, 2018). Alternatively, high water permeability and rejection of minerals is ensured by efficient implementation of water channels - aquaporin proteins -as aquaporins have excellent water permeability and solute rejection (Tang et al., 2015; Kumar et al., 2007). In principle this allows for high flux operation and 100% rejection of solutes if the proteins are embedded in a matrix with no permeability towards solute (Tang et al., 2015; Kumar et al., 2007). The Danish company Aquaporin A/S produces Aquaporin FO hollow fiber membranes consisting of polyethersulfone (PES) porous support layers coated with a PA active layer containing vesicles housing multiple aquaporin channels. Hence, water permeability depends on the number of vesicles and aquaporins per area of membrane surface (Zhao et al., 2012). As an alternative to aquaporins, other studies have also demonstrated that carbon nanotubes and aluminosilicate nanotubes can be embedded into FO TFC membranes to enhance water permeability without elevating solute permeability (Li et al., 2018; Shi et al., 2019; Wang et al., 2013).

7.2.4. FO membrane configuration

Currently, FO membranes have mainly been studied in a flat sheet configuration. However, for FO to be feasible for full scale operation, it is essential that the membranes can be installed with a low footprint. This will be accomplished by the development of tubular FO membranes and by the application of hollow fiber membranes which have a high surface area per volume compared to flat sheet membranes. Tubular FO membranes are still under development, but Aquaporin, Toyobo and Samsung Cheil Industries have already developed hollow fiber FO membranes (Ren and McCutcheon, 2018; Shibuya et al., 2015; Majeed et al., 2015).

7.3. MCDI

As MCDI is very new process, a huge margin of improvement exists in various structural elements, better understanding of the process when applied for different applications as discussed below.

7.3.1. Ion exchange membranes

A significant improvement in energy efficiency of MCDI can be achieved by integration of highly ion conductive ion-exchange membranes with the electrodes, which may lead to significant reduction of the electrical resistance. The critical properties of IEMs are related with high ionic conductivity and current densities, which enhance mass transfer and rate of removal of the salts (Pawlowski et al., 2019). Reduction in cell resistance with improved IEMs allows maintaining a low cell voltage at a constant high current density and this minimizes undesired side reactions such as electrochemical splitting of water molecules. As membranes for MCDI act just as a conformal layer for ion selectivity and do not partition liquid compartment like electordialysis, therefore thickness for MCDI membranes need to be optimized. Compared to traditional IEMs applied, membranes must demonstrate excellent selective permeability to desired ions when considering MCDI for selective removal of ions. The membrane should also demonstrate lower swelling potential when applied in aqueous solutions (Pawlowski et al., 2019). Another important challenge is related with optimal ion exchange factor that allows transporting ions through the membranes as well as might increase the kinetics of adsorption and desorption phenomena or effect the permselectivity (Wang et al., 2019).

7.3.2. Electrodes

The second critical challenge for MCDI is electrodes. In general, electrodes for MCDI should demonstrate high electrical conductivity, hierarchically porous structure, good wettability, and large surface areas. Electrodes have been built from different materials, starting from basic activated carbon, where accumulation of ions are related with electrical double layer, and ending on the Faradic materials (Yu et al., 2019; Luo et al., 2018), where ions are adsorbed or desorbed according with Faradaic reactions while the electric double layer effect can be neglected. Carbon has been the most extensively applied material as electrode because of its high stability combined with low price. However, the adsorption capacity of traditional carbon electrode is limited and therefore, further efforts should be devoted to enhance adsorption capacity of these electrodes, for instance by using different modification techniques such as element doping, metal oxide modification, chemical treatment and surface coating. In addition to applying typical carbon based electrodes, the use of other materials such polymers, ceramics and metals (off course complying with the fundamental requirements of an electrode including electrical conductivity and formation of bicontinuous porous network) should also be considered for electrode

applications. Application of advanced materials tools may allow the formation of transparent, flexible and highly specific adsorption by using such materials. Replacement of the traditional electrosorption with a reversible chemical reaction can be another potential gateway of increasing the adsorption efficiency of electrodes. General absorption of various types of ions at electrode is another important factor hindering the applications of MCDI for selective adsorption of ions from a mixed solution, thus more research endeavors should be devoted to enhance the selective adsorption capacity of the electrodes (Yang et al., 2019) (Palakkal et al., 2018). Suitable pore size and pore size distribution of electrode material must also be identified to achieve optimum performance of the electrode. In addition to innovative materials for electrodes, advanced electrode design can also play vital role in improving the performance of MCDI system.

7.3.3. Development as a multifunctional process

Initially, CDI and MCDI technologies were developed as desalination techniques for production of fresh water from brackish water or lower salinity solutions. More recently, the focus of applications has broadened from freshwater production to metals recovery and even energy production. By manipulating dedicatedly materials, like selective IEMs (Palakkal et al., 2018) or electrode materials, the selective removal of ions gain the greater potential (Pan et al., 2018). Additionally, MCDI process and its modification are characterized by lower energy consumption in comparison with pressure-driven or evaporated technologies. This fact push up the MCDI techniques as an economical and environmentally friendly processes suitable for production of water, metals recovery and energy production. Hence, the future study on development of MCDI should consider the multifunctional character of this process and should clearly target the final applications to develop the entire process around that.

8. Concluding remarks

Interesting progress is taking place in developing alternative green technologies for recovery of raw materials including metals, minerals and nutrients from alternative non-traditional resources. New membrane operation including MCr, FO and MCDI are gaining substantial interest for recovery of dissolved components from various liquid streams. The review of current literature clearly indicates that MCr can be used in many diverse applications ranging from salts recovery from brine to the crystallization of protein and macromolecules. FO has gained more popularity for nutrient recovery from wastewater, though some applications for recovery of metals and minerals have also been demonstrated recently at lab-scale. MCDI, as a technology, is less mature compared to MCr and FO and is gaining momentum for targeted recovery of specific ions from the solutions. MCr and FO require development of appropriate pretreatment strategies (NF, adsorption etc.) to achieve the precipitation of desired salts, whereas MCDI has potential to selectively capture the desired ions from the solution provided the suitable membranes and electrodes are available. Another important limitation of MCDI is that it is suitable only for minerals recovery from low concentration (20–5000 ppm) solutions. Thus, the process is attractive for recovery of high soluble components present in very low concentration in solutions. MCr, on the other hand, is more suitable to precipitate the salts from high-concentrated solutions including seawater RO brine. Due to potentially low fouling, FO becomes a favorable choice for recovery of compounds, with low to medium solubility (50–30,000 ppm), from solutions containing a high organic load.

Due to traditionally different applications and different types of the membranes applied in FO and MCr, the nature of the fouling in the two processes is different. In MCr, scaling has been identified as the main type of fouling whereas organic fouling has been observed mainly when applying the process for wastewater treatment, concentration of food products and related applications. There is very less information available on biofouling in MCr, probably due to the fact that high temperature and salt concentration of the feeds normally applied in MCr may significantly reduce the extent of biofouling. In FO, on the other hand, organic and biofouling have been mainly observed and scaling is less evident. Very limited information is available on fouling in MCDI, where scaling has affected applied IEM and has caused deterioration of activated carbon structure. To realize the commercial applications of MCr, FO and MCDI for resource recovery from liquid streams, better and more effective fouling/scaling mitigation strategies need to be developed for all the processes.

High values of energy consumption (typically 600–1000 kWh/m^3) have been reported for MCr, highlighting the importance of developing efficient energy recovery protocols. SEC for FO is strongly dependent upon the method applied for draw solution recovery and process is more attractive for applications which do not involve draw solution recovery due to very low energy consumption under this condition. Better draw solution recovery techniques need to be developed to extend the applications of the process. In MCDI, low SEC values (0.5–3 kWh/m^3) have been reported for low concentration solutions, however, SEC increases significantly with increase in feed concentration. It is important to point out that in MCr, mainly thermal energy is used which can be provided by a source of low-grade energy such as solar or geothermal, and electric energy is required only for circulation of the solutions. MCDI, on the other hand, is completely driven with electric energy input. From process point of view, MCr and FO suffer from pore wetting and reverse salt flux, respectively. MCDI has issues with desorption step and limited adsorption of the desired component. These drawbacks highlight the importance of developing better membranes for all the three processes considered in current study.

Declaration of Competing Interest

The author declare that they have no known competing financial interests or personal relationships that could have appeared to influence the work reported in this paper.

References

Achilli, A., Cath, T.Y., Childress, A.E., 2010. Selection of inorganic-based draw solutions for forward osmosis applications. J. Memb. Sci. 364, 233–241. https://doi.org/10.1016/j.memsci.2010.08.010.

Achilli, A., Cath, T.Y., Marchand, E.A., Childress, A.E., 2009. The forward osmosis membrane bioreactor: a low fouling alternative to MBR processes. Desalination 238, 10–21. https://doi.org/10.1016/j.desal.2008.02.022.

Ali, A., Aimar, P., Drioli, E., 2015c. Effect of module design and flow patterns on performance of membrane distillation process. Chem. Eng. J. 277, 368–377. https://doi.org/10.1016/j.cej.2015.04.108.

Ali, A., Criscuoli, A., Macedonio, F., Drioli, E., 2019b. A comparative analysis of fl at sheet and capillary membranes for membrane distillation applications. Desalination 456, 1–12. https://doi.org/10.1016/j.desal.2019.01.006.

Ali, A., Tsai, J.-H.J.-H., Tung, K.-L.K.-L., Drioli, E., Macedonio, F., 2018e. Designing and optimization of continuous direct contact membrane distillation process. Desalination 426, 97–107. https://doi.org/10.1016/j.desal.2017.10.041.

Ali, A., Jacobsen, J.H., Jensen, H.C., Christensen, M.L., Quist-jensen, C.A., 2019a. Treatment of wastewater solutions from anodizing industry by membrane distillation and membrane crystallization. Appl. Sci. https://doi.org/10.3390/app9020287.

Ali, A., Macedonio, F., Drioli, E., Aljlil, S., Alharbi, O.A., 2013. Experimental and theoretical evaluation of temperature polarization phenomenon in direct contact membrane distillation. Chem. Eng. Res. Des. 91, 1966–1977. https://doi.org/10.1016/j.cherd.2013.06.030.

Ali, A., Quist-Jensen, C.A., Macedonio, F., Drioli, E., 2015b. Application of membrane crystallization for minerals' recovery from produced water. Membranes (Basel) 5. https://doi.org/10.3390/membranes5040772.

Ali, A., Quist-Jensen, C.A., Macedonio, F., Drioli, E., 2016b. On designing of membrane thickness and thermal conductivity for large scale membrane distillation modules. J. Membr. Sci. Res. 2.

Ali, A., Quist-Jensen, C.A.A., Macedonio, F., Drioli, E., 2016a. Optimization of module length for continuous direct contact membrane distillation process. Chem. Eng. Process. Process Intensif. 110, 188–200. https://doi.org/10.1016/j.cep.2016.10.014.

Ali, A., Quist-Jensen, C.A.C.A., Drioli, E., Macedonio, F., 2018c. Evaluation of integrated microfiltration and membrane distillation/crystallization processes for produced water treatment. Desalination 434, 161–168. https://doi.org/10.1016/j.desal.2017.11.035.

Ali, A., Quist-jensen, C.A.C.A., Macedonio, F., Drioli, E., 2015a. Application of membrane crystallization for minerals' recovery from produced water. Membranes (Basel) 5, 772–792. https://doi.org/10.3390/membranes5040772.
Ali, A., Tsai, J.-.H., Tung, K.-.L., Drioli, E., Macedonio, F., 2018d. Designing and optimization of continuous direct contact membrane distillation process. Desalination 426, 97–107. https://doi.org/10.1016/j.desal.2017.10.041.
Ali, A., Tufa, R.A., Macedonio, F., Curcio, E., Drioli, E., 2018b. Membrane technology in renewable-energy-driven desalination. Renew. Sustain. Energy Rev. 81 https://doi.org/10.1016/j.rser.2017.07.047.
Ali, A., Tufa, R.A.R.A., Macedonio, F., Curcio, E., Drioli, E., 2018a. Membrane technology in renewable-energy-driven desalination. Renew. Sustain. Energy Rev. 81, 1–21. https://doi.org/10.1016/j.rser.2017.07.047.
Ali, S.H., Giurco, D., Arndt, N., Nickless, E., Brown, G., Demetriades, A., Durrheim, R., Enriquez, M.A., Kinnaird, J., Littleboy, A., Meinert, L.D., Oberhänsli, R., Salem, J., Schodde, R., Schneider, G., Vidal, O., Yakovleva, N., 2017. Mineral supply for sustainable development requires resource governance. Nature 543, 367–372. https://doi.org/10.1038/nature21359.
AlMarzooqi, F.A., Al Ghaferi, A.A., Saadat, I., Hilal, N., 2014. Application of Capacitive Deionisation in water desalination: a review. Desalination 342, 3–15. https://doi.org/10.1016/j.desal.2014.02.031.
Alnaizy, R., Aidan, A., Qasim, M., 2013a. Journal of Environmental Chemical Engineering Copper sulfate as draw solute in forward osmosis desalination. Biochem. Pharmacol. 1, 424–430. https://doi.org/10.1016/j.jece.2013.06.005.
Alnaizy, R., Aidan, A., Qasim, M., Alnaizy, R., Aidan, A., Qasim, M., 2013b. Draw solute recovery by metathesis precipitation in forward osmosis desalination osmosis desalination. Chem. Commun. 37–41. https://doi.org/10.1080/19443994.2013.770238.
Al-Obaidani, S., Curcio, E., Macedonio, F., Di Profio, G., A-Hinai, H., Drioli, E., 2008. Potential of membrane distillation in seawater desalination: thermal efficiency, sensitivity study and cost estimation. J. Memb. Sci. 323, 85–98.
Ansari, A.J., Hai, F.I., Guo, W., Ngo, H.H., Price, W.E., Nghiem, L.D., 2015. Selection of forward osmosis draw solutes for subsequent integration with anaerobic treatment to facilitate resource recovery from wastewater. Bioresour. Technol. 191, 30–36. https://doi.org/10.1016/j.biortech.2015.04.119.
Ansari, A.J., Hai, F.I., He, T., Price, W.E., Nghiem, L.D., 2018b. Physical cleaning techniques to control fouling during the pre-concentration of high suspended-solid content solutions for resource recovery by forward osmosis. Desalination 429, 134–141. https://doi.org/10.1016/j.desal.2017.12.011.
Ansari, A.J., Hai, F.I., Price, W.E., Drewes, J.E., Nghiem, L.D., 2017. Forward osmosis as a platform for resource recovery from municipal wastewater - A critical assessment of the literature. J. Memb. Sci. 529, 195–206. https://doi.org/10.1016/j.memsci.2017.01.054.
Ansari, A.J., Hai, F.I., Price, W.E., Nghiem, L.D., 2016. Phosphorus recovery from digested sludge centrate using seawater-driven forward osmosis. Sep. Purif. Technol. 163, 1–7. https://doi.org/10.1016/j.seppur.2016.02.031.
Ansari, A.J., Hai, F.I., Price, W.E., Ngo, H.H., Guo, W., Nghiem, L.D., 2018a. Assessing the integration of forward osmosis and anaerobic digestion for simultaneous wastewater treatment and resource recovery. Bioresour. Technol. 260, 221–226. https://doi.org/10.1016/j.biortech.2018.03.120.
Ates, N., Uzal, N., 2018. Removal of heavy metals from aluminum anodic oxidation wastewaters by membrane filtration. Environ. Sci. Pollut. Res. 25, 22259–22272. https://doi.org/10.1007/s11356-018-2345-z.
Aydiner, C., Sen, U., Topcu, S., Sesli, D., Ekinci, D., Altinay, A.D., 2014. Techno-economic investigation of water recovery and whey powder production from whey using UF/RO and FO/RO integrated membrane systems. Desalin. Water Treat. 52, 1–11.
Azoury, R., Garside, J., Robertson, W.G., 1986. Crystallization processes using reverse osmosis. J. Cryst. Growth 79, 654–657.
P. Bacchin, P. Aimar, R.W. Field, Review Critical and sustainable fluxes : theory, experiments and applications, Journal of Membrane Science, 2 (2006) 42–69.
Backman, C.M., 2008. Global supply and demand of metals in the future. J. Toxicol. Environ. Heal. - Part A Curr. Issues. 71, 1244–1253. https://doi.org/10.1080/15287390802209582.
Baker, Richard, 2020. Membrane Technology and Applications, Second Edition. John Wiley & Sons, Ltd, p. 204AD. https://doi.org/10.1002/0470020393.
Bakonyi, Á.B, P., Galambos, I., Katalin, B., 2020. Separation of volatile fatty acids from model anaerobic e ffl uents using various membrane technologies. Membranes (Basel) 10, 252. https://doi.org/10.3390/membranes10100252.
Bao, X., Wu, Q., Shi, W., Wang, W., Yu, H., Zhu, Z., Zhang, X., Zhang, Z., Zhang, R., Cui, F., 2019a. Polyamidoamine dendrimer grafted forward osmosis membrane with superior ammonia selectivity and robust antifouling capacity for domestic wastewater concentration. Water Res 153, 1–10. https://doi.org/10.1016/j.watres.2018.12.067.
Bao, X., Wu, Q., Shi, W., Wang, W., Zhu, Z., Zhang, Z., Zhang, R., Zhang, B., Guo, Y., Cui, F., 2019b. Dendritic amine sheltered membrane for simultaneous ammonia selection and fouling mitigation in forward osmosis. J. Memb. Sci. 584, 9–19. https://doi.org/10.1016/j.memsci.2019.04.063.
Bao, X., Wu, Q., Shi, W., Wang, W., Zhu, Z., Zhang, Z., Zhang, R., Zhang, X., Zhang, B., Guo, Y., Cui, F., 2019c. Insights into simultaneous ammonia-selective and anti-fouling mechanism over forward osmosis membrane for resource recovery from domestic wastewater. J. Memb. Sci. 573, 135–144. https://doi.org/10.1016/j.memsci.2018.11.072.
Baoxia, M.I., Elimelech, M., 2010. Gypsum scaling and cleaning in forward osmosis: measurements and mechanisms. Environ. Sci. Technol. 44, 2022–2028. https://doi.org/10.1021/es903623r.
Bardi, U., 2010. Extracting Minerals from Seawater: an Energy Analysis. Sustainability 2, 980–992. https://doi.org/10.3390/su2040980.
Bi Cai, L., Lian Sheng, H., Rui, M., Juan Juan, S., 2015. Research of acid mine wastewater treatment technology. J. Chem. Pharm. Res. 7, 1011–1017.
Biesheuvel, P.M., Hamelers, H.V.M., Suss, M.E., 2015. Theory of water desalination by porous electrodes with immobile chemical charge. Colloids Interface Sci. Commun. 9, 1–5. https://doi.org/10.1016/J.COLCOM.2015.12.001.
Biesheuvel, P.M., van der Wal, A., 2010. Membrane capacitive deionization. J. Memb. Sci 346, 256–262. https://doi.org/10.1016/j.memsci.2009.09.043.
G. Blandin, C. Gautier, M. Sauchelli, H. Monclús, I. Rodriguez-roda, J. Comas, Retro fitting membrane bioreactor (MBR) into osmotic membrane bioreactor (OMBR): A pilot scale study, Chemical Engineering Journal, 339 (2018) 268–277.
Boo, C., Lee, J., Elimelech, M., 2016. Engineering surface energy and nanostructure of microporous films for expanded membrane distillation applications. Environ. Sci. Technol. 50, 8112–8119. https://doi.org/10.1021/acs.est.6b02316.
Bouchrit, R., Boubakri, A., Mosbahi, T., Hafiane, A., Bouguecha, S.A.T., 2017. Membrane crystallization for mineral recovery from saline solution: study case Na2SO4 crystals. Desalination 412, 1–12. https://doi.org/10.1016/j.desal.2017.02.021.
Brika, B., Omran, A.A., Dia Addien, O., 2016. Chemical elements of brine discharge from operational Tajoura reverse osmosis desalination plant. Desalin. Water Treat. 57, 5345–5349. https://doi.org/10.1080/19443994.2014.1003330.
Bush, J.A., Vanneste, J., Gustafson, E.M., Waechter, C.A., Jassby, D., Turchi, C.S., Cath, T.Y., 2018. Prevention and management of silica scaling in membrane distillation using pH adjustment. J. Memb. Sci. 554, 366–377. https://doi.org/10.1016/j.memsci.2018.02.059.
Cai, Y., Hu, X.M., 2016. A critical review on draw solutes development for forward osmosis. Desalination 391, 16–29. https://doi.org/10.1016/j.desal.2016.03.021.
Cai, Y., Shen, W., Wei, J., Chong, H., Wang, R., Krantz, W.B., Fane, G., Hu, X., 2015. Environmental Science using responsive ionic liquid draw solutes †. Environ. Sci. Water Res. Technol. 1, 341–347. https://doi.org/10.1039/c4ew00073k.
Camilleri-rumbau, M.S., Soler-cabezas, J.L., Christensen, K.V., Norddahl, B., Mendoza-roca, J.A., Vincent-vela, M.C., 2019. Application of aquaporin-based forward osmosis membranes for processing of digestate liquid fractions. Chem. Eng. J. 371, 583–592. https://doi.org/10.1016/j.cej.2019.02.029.
Cath, T.Y., Childress, A.E., Elimelech, M., 2006. Forward osmosis: principles, applications, and recent developments. J. Memb. Sci. 281, 70–87. https://doi.org/10.1016/j.memsci.2006.05.048.
Cath, T.Y., Hancock, N.T., Lundin, C.D., Hoppe-jones, C., Drewes, J.E., 2010. A multi-barrier osmotic dilution process for simultaneous desalination and purification of impaired water. J. Memb. Sci. 362, 417–426. https://doi.org/10.1016/j.memsci.2010.06.056.
Cath, T.Y., Holloway, R.W., Achilli, A., 2015. The osmotic membrane bioreactor: a critical review. Environ. Sci. Water Res. Technol. 1, 581–605. https://doi.org/10.1039/C5EW00103J.
Cha, J.-.H., ul Haq, O., Choi, J.-.H., Lee, Y.-.S., 2018. Sulfonated poly(ether ether ketone) ion-exchange membrane for membrane capacitive deionization applications. Macromol. Res. 26, 1273–1275. https://doi.org/10.1007/s13233-019-7043-2.
Chabanon, E., Mangin, D., Charcosset, C., 2016. Membranes and crystallization processes: state of the art and prospects. J. Memb. Sci. 509, 57–67. https://doi.org/10.1016/j.memsci.2016.02.051.
Chang, J., Tang, K., Cao, H., Zhao, Z., Su, C., Li, Y., Duan, F., Sheng, Y., 2018. Application of anion exchange membrane and the effect of its properties on asymmetric membrane capacitive deionization. Sep. Purif. Technol. 207, 387–395. https://doi.org/10.1016/J.SEPPUR.2018.06.063.
Chen, G., Lu, Y., Krantz, W.B., Wang, R., Fane, A.G., 2014a. Optimization of operating conditions for a continuous membrane distillation crystallization process with zero salty water discharge. J. Memb. Sci. 450, 1–11. https://doi.org/10.1016/j.memsci.2013.08.034.
Chen, G.Q., Artemi, A., Lee, J., Gras, S.L., Kentish, S.E., 2019a. A pilot scale study on the concentration of milk and whey by forward osmosis. Sep. Purif. Technol. 215, 652–659. https://doi.org/10.1016/j.seppur.2019.01.050.
Chen, L., Gu, Y., Cao, C., Zhang, J., Ng, J.-.W., Tang, C., 2014b. Performance of a submerged anaerobic membrane bioreactor with forward osmosis membrane for low-strength wastewater treatment. Water Res 50, 114–123. https://doi.org/10.1016/J.WATRES.2013.12.009.
Chen, L., Wang, C., Liu, S., Hu, Q., Zhu, L., Cao, C., 2018. Investigation of the long-term desalination performance of membrane capacitive deionization at the presence of organic foulants. Chemosphere 193, 989–997. https://doi.org/10.1016/J.CHEMOSPHERE.2017.11.130.
Chen, L., Wang, C., Liu, S., Zhu, L., 2019b. Investigation of adsorption/desorption behavior of Cr(VI) at the presence of inorganic and organic substance in membrane capacitive deionization (MCDI). J. Environ. Sci. (China). 78, 303–314. https://doi.org/10.1016/j.jes.2018.11.005.
Choi, J.-.H., Yoon, D.-.J., 2019. The maximum allowable charge for operating membrane capacitive deionization without electrode reactions. Sep. Purif. Technol. 215, 125–133. https://doi.org/10.1016/J.SEPPUR.2019.01.003.
Choi, Y., Naidu, G., Jeong, S., Lee, S., Vigneswaran, S., 2018. Fractional-submerged membrane distillation crystallizer (F-SMDC) for treatment of high salinity solution. Desalination 440, 59–67. https://doi.org/10.1016/j.desal.2018.01.027.
Choi, Y., Naidu, G., Lee, S., Vigneswaran, S., 2019b. Effect of inorganic and organic compounds on the performance of fractional-submerged membrane distillation-crystallizer. J. Memb. Sci. 582, 9–19. https://doi.org/10.1016/j.memsci.2019.03.089.
Choi, Y., Ryu, S., Naidu, G., Lee, S., 2019c. Separation and purification technology integrated submerged membrane distillation-adsorption system for rubidium

recovery. Sep. Purif. Technol. 218, 146–155. https://doi.org/10.1016/j.seppur.2019.02.050.
Choi, Y., Ryu, S., Naidu, G., Lee, S., Vigneswaran, S., 2019a. Integrated submerged membrane distillation-adsorption system for rubidium recovery. Sep. Purif. Technol. 218, 146–155. https://doi.org/10.1016/j.seppur.2019.02.050.
Chong, T.H., Sheikholeslami, R., 2001. Thermodynamics and kinetics for mixed calcium carbonate and calcium sulfate precipitation. Chem. Eng. Sci. 56, 5391–5400. https://doi.org/10.1016/S0009-2509(01)00237-8.
Chun, Y., Mulcahy, D., Zou, L., Kim, I.S., 2017. A short review of membrane fouling in forward osmosis processes. Membranes (Basel) 7, 1–23. https://doi.org/10.3390/membranes7020030.
Chung, T.S., Li, X., Ong, R.C., Ge, Q., Wang, H., Han, G., 2012. Emerging forward osmosis (FO) technologies and challenges ahead for clean water and clean energy applications. Curr. Opin. Chem. Eng. 1, 246–257. https://doi.org/10.1016/j.coche.2012.07.004.
Cornelissen, E.R., Harmsen, D., Beerendonk, E.F., Qin, J.J., Oo, H., De Korte, K.F., Kappelhof, J.W.M.N., 2011. The innovative Osmotic Membrane Bioreactor (OMBR) for reuse of wastewater. Water Sci. Technol. 63, 1557–1565. https://doi.org/10.2166/wst.2011.206.
Criscuoli, A., Concetta, M., Drioli, E., 2008. Evaluation of energy requirements in membrane distillation. Chem. Eng. Process. Process Intensif. 47, 1098–1105. https://doi.org/10.1016/j.cep.2007.03.006.
Cui, Y., Ge, Q., Liu, X.-Y., Chung, T.-C., 2014a. Novel forward osmosis process to effectively remove heavy metal ions. J. Memb. Sci 467, 188–194. https://doi.org/10.1016/j.memsci.2011.11.018.
Cui, Z., Drioli, E., Lee, Y.M., 2014b. Recent progress in fluoropolymers for membranes. Prog. Polym. Sci. 39, 164–198. https://doi.org/10.1016/j.progpolymsci.2013.07.008.
Cui, Z., Hassankiadeh, N.T., Lee, S.Y., Lee, J.M., Woo, K.T., Sanguineti, A., Arcella, V., Lee, Y.M., Drioli, E., 2013. Poly(vinylidene fluoride) membrane preparation with an environmental diluent via thermally induced phase separation. J. Memb. Sci. 444, 223–236. https://doi.org/10.1016/j.memsci.2013.05.031.
Cui, Z., Li, X., Zhang, Y., Wang, Z., Gugliuzza, A., Militano, F., Drioli, E., Macedonio, F., 2018. Testing of three different PVDF membranes in membrane assisted-crystallization process: influence of membrane structural-properties on process performance. Desalination 440, 68–77. https://doi.org/10.1016/j.desal.2017.12.038.
Curcio, E., Criscuoli, A., Drioli, E., 2001. Membrane crystallizers. Ind. Eng. Chem. Res 40, 2679–2684.
Curcio, E., Ji, X., Quazi, A.M., Barghi, S., Di Profio, G., Fontananova, E., Macleod, T., Drioli, E., 2010. Hybrid nanofiltration–membrane crystallization system for the treatment of sulfate wastes. J. Memb. Sci. 360, 493–498. https://doi.org/10.1016/j.memsci.2010.05.053.
Darvishmanesh, S., Pethica, B.A., Sundaresan, S., 2017. Forward osmosis using draw solutions manifesting liquid-liquid phase separation. Desalination 421, 23–31. https://doi.org/10.1016/j.desal.2017.05.036.
Dawoud, M.A., Al Mulla, M.M., 2012. Environmental impacts of seawater desalination : arabian gulf case study. Int. J. Environ. Sustain. 1, 22–37.
De-Bashan, L.E., Bashan, Y., 2004. Recent advances in removing phosphorus from wastewater and its future use as fertilizer (1997-2003). Water Res 38, 4222–4246. https://doi.org/10.1016/j.watres.2004.07.014.
Di Profio, G., Polino, M., Nicoletta, F.P., Belviso, B.D., Caliandro, R., Fontananova, E., De Filpo, G., Curcio, E., Drioli, E., 2014. Tailored Hydrogel Membranes for Efficient Protein Crystallization. Adv. Funct. Mater. 24, 1582–1590. https://doi.org/10.1002/adfm.201302240.
Di Profio, G., Tucci, S., Curcio, E., Drioli, E., 2007. Controlling polymorphism with membrane-based crystallizers : application to form I and II of Paracetamol. Chem. Mater. 19, 2386–2388.
DiGiano, F.A., Nilson, J.A., 2013. Influence of NOM composition on nanofiltration. J. Am. Water Work. Assoc. 88, 53–66.
Długołęcki, P., van der Wal, A., van der Wal, A., 2013. Energy recovery in membrane capacitive deionization. Environ. Sci. Technol. 47, 4904–4910. https://doi.org/10.1021/es3053202.
Dong, Q., Guo, X., Huang, X., Liu, L., Tallon, R., Taylor, B., Chen, J., 2019. Selective removal of lead ions through capacitive deionization: role of ion-exchange membrane. Chem. Eng. J. 361, 1535–1542. https://doi.org/10.1016/J.CEJ.2018.10.208.
Dow, N., Gray, S., Li, J., Zhang, J., Ostarcevic, E., Liubinas, A., Atherton, P., Roeszler, G., Gibbs, A., Duke, M., 2016. Pilot trial of membrane distillation driven by low grade waste heat: membrane fouling and energy assessment. Desalination 391, 30–42. https://doi.org/10.1016/j.desal.2016.01.023.
Drioli, E., Ali, A., Macedonio, F., 2015. Membrane distillation: recent developments and perspectives. Desalination 356. https://doi.org/10.1016/j.desal.2014.10.028.
Drioli, E., Ali, A., Macedonio, F., 2017. Membrane operations for process intensification in desalination. Appl. Sci. 7 https://doi.org/10.3390/app7010100.
Drioli, E., Curcio, E., Criscuoli, A., Di Profio, G., 2004. Integrated system for recovery of CaCO3, NaCl and MgSO4•7H2O from nanofiltration retentate. J. Memb. Sci. 239, 27–38. https://doi.org/10.1016/j.memsci.2003.09.028.
Drioli, E., Curcio, E., di Profio, G., 2005. State of the art and recent progresses in membrane contactors. Chem. Eng. Res. Des. 83, 223–233. https://doi.org/10.1205/cherd.04203.
Drioli, E., Di Profio, G., Curcio, E., 2012b. Progress in membrane crystallization. Curr. Opin. Chem. Eng. 1, 178–182. https://doi.org/10.1016/j.coche.2012.03.005.
Drioli, E., Macedonio, F., Ali, A., 2012a. Membrane distillation: basic aspects and applications. J. Memb. Sci. A Journal of Membrane Science Virtual Special Issu http://www.journals.elsevier.com/journal-of-membrane-science/virtual-special-issues/membrane-distillation-basic-aspects-and-applications/.
Dudka, S., Adriano, D.C., 2010. Environmental impacts of metal ore mining and processing: a review. J. Environ. Qual. 26, 590. https://doi.org/10.2134/jeq1997.00472425002600030003x.
Duong, H.C., Gray, S., Duke, M., Cath, T.Y., Nghiem, L.D., 2015. Scaling control during membrane distillation of coal seam gas reverse osmosis brine. J. Memb. Sci. 493, 673–682. https://doi.org/10.1016/j.memsci.2015.07.038.
Duong, T., Xie, Z., Ng, D., Hoang, M., 2013. Ammonia removal from aqueous solution by membrane distillation. Water Environ. J. 27, 425–434. https://doi.org/10.1111/j.1747-6593.2012.00364.x.
Edwie, F., Chung, T.-S., 2013. Development of simultaneous membrane distillation–crystallization (SMDC) technology for treatment of saturated brine. Chem. Eng. Sci. 98, 160–172. https://doi.org/10.1016/j.ces.2013.05.008.
Elements in short supply, 2011. Nat. Mater 10, 157. https://doi.org/10.1038/nmat2985.
Elshkaki, A., Graedel, T.E., Ciacci, L., Reck, B.K., 2018. Resource demand scenarios for the major metals. Environ. Sci. Technol. 52, 2491–2497. https://doi.org/10.1021/acs.est.7b05154.
Environ, E., Liu, Z., Bai, H., Lee, J., Sun, D.D., 2011. A low-energy forward osmosis process to produce drinking water. Energy Environ. Sci. 4, 2582–2585. https://doi.org/10.1039/c1ee01186c.
European Commission, 2018. Raw materials, metals, Minerals and Forest-Based Industrie. https://ec.europa.eu/growth/sectors/raw-materials/policy-strategy_en.
Evans, S., Accomazzo, M.A., Accomazzo, J.E., 1969. Electrochemically controlled ion exchange. J. Electrochem. Soc. 116, 307. https://doi.org/10.1149/1.2411821.
Fakhru'l-Razi, A., Pendashteh, A., Abdullah, L.C., Biak, D.R.A., Madaeni, S.S., Abidin, Z. Z., 2009. Review of technologies for oil and gas produced water treatment. J. Hazard. Mater. 170, 530–551. https://doi.org/10.1016/j.jhazmat.2009.05.044.
Farmer, J C, Fix, D V, Mack, G V, Pekala, R W, and Poco, J F. Fri , The use of capacitive deionization with carbon aerogel electrodes to remove inorganic contaminants from water, United States. doi:10.2172/80970. https://www.osti.gov/servlets/purl/80970.
Field, R., 2020. Fundamentals of Fouling. In: Nunes, K.-V.P., Pereira, S. (Eds.), Membr. Water Treat. WILEY-VCH Verlag GmbH & Co. KGaA, Weinheim n.d.
Fritz, P.A., Zisopoulos, F.K., Verheggen, S., Schroën, K., Boom, R.M., 2018. Exergy analysis of membrane capacitive deionization (MCDI). Desalination 444, 162–168. https://doi.org/10.1016/J.DESAL.2018.01.026.
Gao, X., Omosebi, A., Landon, J., Liu, K., 2015. Enhanced salt removal in an inverted capacitive deionization cell using amine modified microporous carbon cathodes. Environ. Sci. Technol. 49, 10920–10926. https://doi.org/10.1021/acs.est.5b02320.
Gao, Y., Fang, Z., Liang, P., Huang, X., 2018. Direct concentration of municipal sewage by forward osmosis and membrane fouling behavior. Bioresour. Technol. 247, 730–735.
García, J.V., Dow, N., Milne, N., Zhang, J., Gray, S., Duke, M., 2018. Membrane distillation trial on textile wastewater containing surfactants using hydrophobic and hydrophilic-coated polytetrafluoroethylene. Membranes (Basel) 8, 1–15. https://doi.org/10.3390/membranes8020031.
Ge, Z., Chen, X., Huang, X., Ren, Z.J., 2018. Capacitive deionization for nutrient recovery from wastewater with disinfection capability. Environ. Sci. Water Res. Technol. 4, 33–39. https://doi.org/10.1039/c7ew00350a.
Graedel, T.E., Harper, E.M., Nassar, N.T., Reck, B.K., 2013. On the materials basis of modern society. Proc. Natl. Acad. Sci. 112, 6295–6300. https://doi.org/10.1073/pnas.1312752110.
Gryta, M., 2000. Concentration of saline wastewater from the production of heparin. Desalination 129, 35–44.
Gryta, M., 2002. Concentration of NaCl solution by membrane distillation integrated with crystallization. Sep. Sci. Technol. 37, 3535–3558. https://doi.org/10.1081/SS-120014442.
M. Gryta, Separation science and technology concentration of nacl solution by membrane distillation integrated with crystallization, (2007) 37–41. doi:10.1081/SS-120014442.
Gryta, M., Tomaszewska, M., Grzechulska, J., Morawski, A.W., 2001. Membrane distillation of NaCl solution containing natural organic matter. J. Memb. Sci. 181, 279–287. https://doi.org/10.1016/S0376-7388(00)00582-2.
Gryta, M., Tomaszewska, M., Karakulski, K., 2006. Wastewater treatment by membrane distillation. Desalination 198, 67–73. https://doi.org/10.1016/j.desal.2006.09.010.
Gugliuzza, a., Drioli, E., 2007. PVDF and HYFLON AD membranes: ideal interfaces for contactor applications, J. Memb. Sci. 300, 51–62. https://doi.org/10.1016/j.memsci.2007.05.004.
Guillén-burrieza, E., Zaragoza, G., Miralles-cuevas, S., Blanco, J., 2012. Experimental evaluation of two pilot-scale membrane distillation modules used for solar desalination. J. Memb. Sci. 409–410, 264–275. https://doi.org/10.1016/j.memsci.2012.03.063.
Gwak, G., Kim, D.I., Hong, S., 2018. New industrial application of forward osmosis (FO): precious metal recovery from printed circuit board (PCB) plant wastewater. J. Memb. Sci. 552, 234–242. https://doi.org/10.1016/j.memsci.2018.02.022.
Hamid, M.F., Abdullah, N., Yusof, N., Ismail, N.M., Ismail, A.F., Salleh, W.N.W., Jaafar, J., Aziz, F., Lau, W.J., 2020. Effects of surface charge of thin-film composite membrane on copper (II) ion removal by using nanofiltration and forward osmosis process. J. Water Process Eng. 33 https://doi.org/10.1016/j.jwpe.2019.101032.
Hancock, N.T., Cath, T.Y., 2009. Solute coupled diffusion in osmotically driven membrane processes. Environ. Sci. Technol. 43, 6769–6775. https://doi.org/10.1021/es901132x.
Hancock, N.T., Xu, P., Heil, D.M., Bellona, C., Cath, T.Y., 2011. Comprehensive bench- and pilot-scale investigation of trace organic compounds rejection by forward

osmosis. Environ. Sci. Technol. 45, 8483–8490. https://doi.org/10.1021/es201654k.
Härtel, A., Janssen, M., Samin, S., van Roij, R., 2015. Fundamental measure theory for the electric double layer: implications for blue-energy harvesting and water desalination. J. Phys. Condens. Matter. 27, 194129 https://doi.org/10.1088/0953-8984/27/19/194129.
Harvey, F., 2013. Demand for metals likely to increase tenfold, study says. Guard. https://www.theguardian.com/environment/2013/apr/2. https://www.theguardian.com/environment/2013/apr/24/demand-metals-increase.
Hassanvand, A., Chen, G.Q., Webley, P.A., Kentish, S.E., 2017b. Improvement of MCDI operation and design through experiment and modelling: regeneration with brine and optimum residence time. Desalination 417, 36–51. https://doi.org/10.1016/J.DESAL.2017.05.004.
Hassanvand, A., Wei, K., Talebi, S., Chen, G.Q., Kentish, S.E., 2017a. The role of Ion exchange membranes in membrane capacitive deionisation. Membranes (Basel) 7, 54. https://doi.org/10.3390/membranes7030054.
Hau, N.-.T., Chen, S., Nguyen, C.N., Huang, K.Z., Ngo, H.H., Guo, W., 2014. Exploration of EDTA sodium salt as novel draw solution in forward osmosis process for dewatering of high nutrient sludge. J. Memb. Sci. 455, 305–311. https://doi.org/10.1016/j.memsci.2013.12.068.
Hausmann, A., Sanciolo, P., Vasiljevic, T., Kulozik, U., Duke, M., 2014. Performance assessment of membrane distillation for skim milk and whey processing. J. Dairy Sci 97, 56–71. https://doi.org/10.3168/jds.2013-7044.
Hausmann, A., Sanciolo, P., Vasiljevic, T., Weeks, M., Schroën, K., Gray, S., Duke, M., 2013. Fouling mechanisms of dairy streams during membrane distillation. J. Memb. Sci. 441, 102–111. https://doi.org/10.1016/j.memsci.2013.03.043.
He, F., Biesheuvel, P.M., Bazant, M.Z., Hatton, T.A., 2018. Theory of water treatment by capacitive deionization with redox active porous electrodes. Water Res 132, 282–291. https://doi.org/10.1016/J.WATRES.2017.12.073.
R.W. Holloway, A.E. Childress, K.E. Dennett, T.Y. Cath, Forward osmosis for concentration of anaerobic digester centrate, Water Research, 41 (2007) 4005–4014. doi:10.1016/j.watres.2007.05.054.
Holloway, R.W., Regnery, J., Nghiem, L.D., Cath, T.Y., 2014. Removal of trace organic chemicals and performance of a novel hybrid ultrafiltration-osmotic membrane bioreactor. Environ. Sci. Technol. 48, 10859–10868. https://doi.org/10.1021/es501051b.
Holloway, R.W., Wait, A.S., da Silva, A.F., Herron, J., Schutter, M.D., Lampi, K., Cath, T.Y., 2015. Long-term pilot scale investigation of novel hybrid ultrafiltration-osmotic membrane bioreactors. Desalination 363, 64–74.
Huang, L., Lee, D., Lai, J.-.Y., 2015. Forward osmosis membrane bioreactor for wastewater treatment with phosphorus recovery. Bioresour. Technol. 198, 418–423.
Huang, X., He, D., Tang, W., Kovalsky, P., Waite, T.D., 2017. Investigation of pH-dependent phosphate removal from wastewaters by membrane capacitive. Environ. Sci. Water Res. Technol. 3, 875–882. https://doi.org/10.1039/c7ew00138j.
Hyun, S., Hoon, J., Ju, S., Tae, J., Hyun, H., Ali, A., Quist-jensen, C.A., Macedonio, F., Drioli, E., Moo, Y., 2020. Lithium recovery from artificial brine using energy-efficient membrane distillation and nanofiltration. J. Memb. Sci. 598, 117683 https://doi.org/10.1016/j.memsci.2019.117683.
Iskander, S.M., Zou, S., Brazil, B., Novak, J.T., He, Z., 2017. Energy consumption by forward osmosis treatment of landfill leachate for water recovery. Waste Manag 63, 284–291. https://doi.org/10.1016/j.wasman.2017.03.026.
Jacob, P., Zhang, T., Laborie, S., Cabassud, C., 2019. Influence of operating conditions on wetting and wettability in membrane distillation using Detection of Dissolved Tracer Intrusion (DDTI). Desalination 468, 114086. https://doi.org/10.1016/j.desal.2019.114086.
Jeon, S., Park, H., Yeo, J., Yang, S., Cho, C.H., Han, M.H., Kim, D.K., 2013. Desalination via a new membrane capacitive deionization process utilizing flow-electrodes. Energy Environ. Sci. 6, 1471. https://doi.org/10.1039/c3ee24443a.
Jeppesen, T., Shu, L., Keir, G., Jegatheesan, V., 2009. Metal recovery from reverse osmosis concentrate. J. Clean. Prod. 17, 703–707.
Ji, X., Curcio, E., Al Obaidani, S., Di Profio, G., Fontananova, E., Drioli, E., Al, S., Di, G., Fontananova, E., Drioli, E., 2010. Membrane distillation-crystallization of seawater reverse osmosis brines. Sep. Purif. Technol. 71, 76–82. https://doi.org/10.1016/j.seppur.2009.11.004.
Jia, F., Li, J., Wang, J., 2017. Recovery of boric acid from the simulated radioactive wastewater by vacuum membrane distillation crystallization. Ann. Nucl. Energy. 110, 1148–1155. https://doi.org/10.1016/j.anucene.2017.07.024.
Jiang, X., Lu, D., Xiao, W., Li, G., Zhao, R., Li, X., He, G., Ruan, X., 2019. Interface-based crystal particle autoselection via membrane crystallization: from scaling to process control. AIChE J 65, 723–733. https://doi.org/10.1002/aic.16459.
Jones, E., Qadir, M., van Vliet, M.T.H., Smakhtin, V., mu Kang, S., 2019. The state of desalination and brine production: a global outlook. Sci. Total Environ. 657, 1343–1356. https://doi.org/10.1016/j.scitotenv.2018.12.076.
Jørgensen, M.K., Sørensen, J.H., Quist-Jensen, C.A., Christensen, M.L., 2018b. Wastewater treatment and concentration of phosphorus with the hybrid osmotic microfiltration bioreactor. J. Memb. Sci. 559 https://doi.org/10.1016/j.memsci.2018.05.001.
Jørgensen, M.K.M.K., Sørensen, J.H.J.H., Quist-Jensen, C.A.C.A., Christensen, M.L.M.L., 2018a. Wastewater treatment and concentration of phosphorus with the hybrid osmotic microfiltration bioreactor. J. Memb. Sci. 559, 107–116.
Julian, H., Lian, B., Li, H., Liu, X., Wang, Y., Leslie, G., Chen, V., 2018. Numerical study of CaCO3 scaling in submerged vacuum membrane distillation and crystallization (VMDC), J. Memb. Sci. 559, 87–97. https://doi.org/10.1016/j.memsci.2018.04.050.
Jung, S.-.M., Choi, J.-.H., Kim, J.-.H., 2012. Application of capacitive deionization (CDI) technology to insulin purification process. Sep. Purif. Technol. 98, 31–35. https://doi.org/10.1016/J.SEPPUR.2012.06.005.
Kedwell, K.C., Christensen, M.L., Quist-Jensen, C.A., Jørgensen, M.K., 2019. Effect of reverse sodium flux and pH on ammoniacal nitrogen transport through biomimetic membranes. Sep. Purif. Technol. 217, 40–47. https://doi.org/10.1016/j.seppur.2019.02.001.
Kedwell, K.C., Quist-Jensen, C.A., Giannakakis, G., Christensen, M.L., 2018. Forward osmosis with high-performing TFC membranes for concentration of digester centrate prior to phosphorus recovery. Sep. Purif. Technol. 197, 449–456. https://doi.org/10.1016/j.seppur.2018.01.034.
Kezia, K., Lee, J., Weeks, M., Kentish, S., 2015. Direct contact membrane distillation for the concentration of saline dairy effluent. Water Res 81, 167–177. https://doi.org/10.1016/j.watres.2015.05.042.
Khayet, M., 2013. Solar desalination by membrane distillation : dispersion in energy consumption analysis and water production costs (a review). Desalination 308, 89–101. https://doi.org/10.1016/j.desal.2012.07.010.
Khayet, M., Mengual, J.I., 2004. Effect of salt concentration during the treatment of humic acid solutions by membrane distillation. Desalination 168, 373–381. https://doi.org/10.1016/j.desal.2004.07.023.
Khayet, M., Velázquez, A., Mengual, J.I., 2004. Direct contact membrane distillation of humic acid solutions. J. Memb. Sci. 240, 123–128. https://doi.org/10.1016/j.memsci.2004.04.018.
Kim, C., Srimuk, P., Lee, J., Aslan, M., Presser, V., 2018c. Semi-continuous capacitive deionization using multi-channel flow stream and ion exchange membranes. Desalination 425, 104–110. https://doi.org/10.1016/J.DESAL.2017.10.012.
Kim, C., Srimuk, P., Lee, J., Presser, V., 2018d. Enhanced desalination via cell voltage extension of membrane capacitive deionization using an aqueous/organic bi-electrolyte. Desalination 443, 56–61. https://doi.org/10.1016/J.DESAL.2018.05.016.
Kim, D.I., Gwak, G., Dorji, P., He, D., Phuntsho, S., Hong, S., Shon, H., 2018a. Palladium recovery through membrane capacitive deionization from metal plating wastewater. ACS Sustain. Chem. Eng. 6, 1692–1701. https://doi.org/10.1021/acssuschemeng.7b02923.
Kim, J., Jain, A., Zuo, K., Verduzco, R., Walker, S., Elimelech, M., Zhang, Z., Zhang, X., Li, Q., 2019. Removal of calcium ions from water by selective electrosorption using target-ion specific nanocomposite electrode. Water Res 160, 445–453. https://doi.org/10.1016/j.watres.2019.05.016.
Kim, J., Kang, H., Choi, Y., Ah, Y., Lee, J., 2016b. Thermo-responsive oligomeric poly (tetrabutylphosphonium styrenesulfonate) s as draw solutes for forward osmosis (FO) applications. Desalination 381, 84–94. https://doi.org/10.1016/j.desal.2015.11.013.
Kim, J., Kim, J., Hong, S., 2018b. Recovery of water and minerals from shale gas produced water by membrane distillation crystallization. Water Res 129, 447–459. https://doi.org/10.1016/j.watres.2017.11.017.
Kim, J., Kwon, H., Lee, S., Lee, S., Hong, S., 2017a. Membrane distillation (MD) integrated with crystallization (MDC) for shale gas produced water (SGPW) treatment. Desalination 403, 172–178. https://doi.org/10.1016/j.desal.2016.07.045.
Kim, Y., Chekli, L., Shim, W., Phuntsho, S., Li, S., Ghaffour, N., Leiknes, T., Shon, H.K., 2016a. Selection of suitable fertilizer draw solute for a novel fertilizer-drawn forward osmosis – anaerobic membrane bioreactor hybrid system. Bioresour. Technol. 210, 26–34. https://doi.org/10.1016/j.biortech.2016.02.019.
Kim, Y., Choi, J., 2010. Enhanced desalination efficiency in capacitive deionization with an ion-selective membrane. Sep. Purif. Technol. 71, 70–75. https://doi.org/10.1016/j.seppur.2009.10.026.
Kim, Y., Li, S., Chekli, L., Phuntsho, S., Ghaffour, N., Leiknes, T., Shon, H.K., 2017b. Influence of fertilizer draw solution properties on the process performance and microbial community structure in a side-stream anaerobic fertilizer-drawn forward osmosis – ultrafiltration bioreactor. Bioresour. Technol. 240, 149–156. https://doi.org/10.1016/j.biortech.2017.02.098.
Kim, Y.J., Kim, J.H., Choi, J.H., 2013. Selective removal of nitrate ions by controlling the applied current in membrane capacitive deionization (MCDI). J. Memb. Sci. 429, 52–57. https://doi.org/10.1016/j.memsci.2012.11.064.
Klaysom, C., Cath, T.Y., Depuydt, T., Vankelecom, I.F.J., 2013. Forward and pressure retarded osmosis: potential solutions for global challenges in energy and water supply. Chem. Soc. Rev 42, 6959–6989. https://doi.org/10.1039/c3cs60051c.
Ko, C.-C.C.C., Ali, A., Drioli, E., Tung, K.-L.K.L., Chen, C.-H.C.H., Chen, Y.-R.Y.R., Macedonio, F., 2018. Performance of ceramic membrane in vacuum membrane distillation and in vacuum membrane crystallization. Desalination 440, 48–58. https://doi.org/10.1016/j.desal.2018.03.011.
Krivorot, M., Kushmaro, A., Oren, Y., Gilron, J., 2011. Factors affecting biofilm formation and biofouling in membrane distillation of seawater. J. Memb. Sci. 376, 15–24. https://doi.org/10.1016/j.memsci.2011.01.061.
Krohns, S., Schafnitzel, M., Tuma, A., Reller, A., Kolotzek, C., Helbig, C., Thorenz, A., 2017. Benefits of resource strategy for sustainable materials research and development. Sustain. Mater. Technol. https://doi.org/10.1016/j.susmat.2017.01.004.
Kumar, M., Grzelakowski, M., Zilles, J., Clark, M., Meier, W., 2007. Highly permeable polymeric membranes based on the incorporation of the functional water channel protein Aquaporin Z. PNAS 104, 20719–20724. https://doi.org/10.1073/pnas.0708762104.
Laqbaqbi, M., Sanmartino, J., Khayet, M., García-Payo, C., Chaouch, M., 2017. Fouling in membrane distillation, osmotic distillation and osmotic membrane distillation. Appl. Sci. 7, 334. https://doi.org/10.3390/app7040334.
Le-Clech, P., Chen, V., Fane, T.A.G., 2006. Fouling in membrane bioreactors used in wastewater treatment. J. Memb. Sci. 284, 17–53. https://doi.org/10.1016/j.memsci.2006.08.019.

Lee, D.H., Ryu, T., Shin, J., Ryu, J.C., Chung, K.S., Kim, Y.H., 2017. Selective lithium recovery from aqueous solution using a modified membrane capacitive deionization system. Hydrometallurgy 173, 283–288. https://doi.org/10.1016/j.hydromet.2017.09.005.

Lee, J., Kim, S., Kim, C., Yoon, J., 2014. Hybrid capacitive deionization to enhance the desalination performance of capacitive techniques. Energy Environ. Sci. 7, 3683–3689. https://doi.org/10.1039/C4EE02378A.

Lee, J.-.B., Park, K.-.K., Eum, H.-.M., Lee, C.-.W., 2006. Desalination of a thermal power plant wastewater by membrane capacitive deionization. Desalination 196, 125–134. https://doi.org/10.1016/J.DESAL.2006.01.011.

Lee, J.G., Jang, Y., Fortunato, L., Jeong, S., Lee, S., Leiknes, T.O., Ghaffour, N., 2018. An advanced online monitoring approach to study the scaling behavior in direct contact membrane distillation. J. Memb. Sci. 546, 50–60. https://doi.org/10.1016/j.memsci.2017.10.009.

Lee, K.L., Baker, R.W., Lonsdale, H.K., 1981. Membranes for power generation by pressure-retarded osmosis. J. Memb. Sci. 8, 141–171. https://doi.org/10.1016/S0376-7388(00)82088-8.

Lee, M., Fan, C.S., Chen, Y.W., Chang, K.C., Te Chiueh, P., Hou, C.H., 2019. Membrane capacitive deionization for low-salinity desalination in the reclamation of domestic wastewater effluents. Chemosphere 235, 413–422. https://doi.org/10.1016/j.chemosphere.2019.06.190.

Lee, S., Boo, C., Elimelech, M., Hong, S., 2010. Comparison of fouling behavior in forward osmosis (FO) and reverse osmosis (RO). J. Memb. Sci. 365, 34–39. https://doi.org/10.1016/j.memsci.2010.08.036.

Li, D., Zhang, X., Yao, J., Simon, P., Wang, H., 2011. Stimuli-responsive polymer hydrogels as a new class of draw agent for forward osmosis desalination w. Chem. Commun. 1710–1712. https://doi.org/10.1039/c0cc04701e.

Li, G., Cai, W., Zhao, R., Hao, L., 2019. Electrosorptive removal of salt ions from water by membrane capacitive deionization (MCDI): characterization, adsorption equilibrium, and kinetics. Environ. Sci. Pollut. Res. 26, 17787–17796. https://doi.org/10.1007/s11356-019-05147-5.

Li, H., Zou, L., 2011. Ion-exchange membrane capacitive deionization: a new strategy for brackish water desalination. Desalination 275, 62–66. https://doi.org/10.1016/j.desal.2011.02.027.

Li, J., Wang, M., Zhao, Y., Yang, H., Zhong, Y., 2018a. Enrichment of lithium from salt lake brine by forward osmosis. R. Soc. Open Sci. 5, 1–8. https://doi.org/10.1098/rsos.180965.

Li, W., Van der Bruggen, B., Luis, P., 2014. Integration of reverse osmosis and membrane crystallization for sodium sulphate recovery. Chem. Eng. Process. Process Intensif. 85, 57–68. https://doi.org/10.1016/j.cep.2014.08.003.

Li, W., Van der Bruggen, B., Luis, P., 2016. Recovery of Na2CO3and Na2SO4from mixed solutions by membrane crystallization. Chem. Eng. Res. Des. 106, 315–326. https://doi.org/10.1016/j.cherd.2015.12.022.

Li, X., Qin, Y., Liu, R., Zhang, Y., Yao, K., 2012. Study on concentration of aqueous sulfuric acid solution by multiple-effect membrane distillation. Desalination 307, 34–41. https://doi.org/10.1016/j.desal.2012.08.023.

Li, Y., Xu, Z., Xie, M., Zhang, B., Li, G., Luo, W., 2020. Resource recovery from digested manure centrate: comparison between conventional and aquaporin thin-film composite forward osmosis membranes. J. Memb. Sci. 593, 117436 https://doi.org/10.1016/j.memsci.2019.117436.

Li, Y., Zhao, Y., Tian, E., Ren, Y., 2018b. Preparation and characterization of novel forward osmosis membrane incorporated with sulfonated carbon nanotubes. RSC Adv. 8, 41032–41039. https://doi.org/10.1039/C8RA08900K.

Linares, R.V., Li, Z., Yangali-Quintanilla, V., Li, Q., Vrouwenvelder, J.S., Amy, G.L., Ghaffour, N., 2016. Hybrid SBR–FO system for wastewater treatment and reuse: operation, fouling and cleaning. Desalination 393, 31–38. https://doi.org/10.1016/j.desal.2016.03.015.

Lisbona, D.F., Somerfield, C., Steel, K.M., 2012. Treatment of spent pot-lining with aluminum anodizing wastewaters: selective precipitation of aluminum and fluoride as an aluminum hydroxyfluoride hydrate product. Ind. Eng. Chem. Res. 51, 12712–12722. https://doi.org/10.1021/ie3013506.

Liu, F., Hashim, N.A., Liu, Y., Abed, M.R.M., Li, K., 2011. Progress in the production and modification of PVDF membranes. J. Memb. Sci. 375, 1–27. https://doi.org/10.1016/j.memsci.2011.03.014.

Liu, Q., Liu, C., Zhao, L., Ma, W., Liu, H., Ma, J., 2016. Integrated forward osmosis-membrane distillation process for human urine treatment. Water Res 91, 45–54. https://doi.org/10.1016/j.watres.2015.12.045.

Liu, Z., Zhang, Y., Lu, X., Wang, X., Zhao, X., 2018. Study of the bubble membrane crystallization process for zero-brine discharge. J. Memb. Sci. 563, 584–591. https://doi.org/10.1016/j.memsci.2018.06.021.

Q. Long, Y. Jia, J. Li, J. Yang, F. Liu, J. Zheng, B. Yu, Recent advance on draw solutes development in, (n.d.) (2020) 7–11. doi:10.3390/pr6090165.

Lotfi, F., Chekli, L., Phuntsho, S., Hong, S., Choi, J.Y., Shon, H.K., 2017. Understanding the possible underlying mechanisms for low fouling tendency of the forward osmosis and pressure assisted osmosis processes. Desalination 421, 89–98. https://doi.org/10.1016/j.desal.2017.01.037.

F. Lotfi, S. Phuntsho, T. Majeed, K. Kim, D.S. Han, A. Abdel-wahab, H.K. Shon, Thin film composite hollow fibre forward osmosis membrane module for the desalination of brackish groundwater for fertigation, 364 (2015) 108–118. doi:10.1016/j.desal.2015.01.042.

Lu, K.J., Chen, Y., Chung, T.S., 2019b. Design of omniphobic interfaces for membrane distillation – A review. Water Res 162, 64–77. https://doi.org/10.1016/j.watres.2019.06.056.

Lu, K.J., Cheng, Z.L., Chang, J., Luo, L., Chung, T.S., 2019a. Design of zero liquid discharge desalination (ZLDD) systems consisting of freeze desalination, membrane distillation, and crystallization powered by green energies. Desalination 458, 66–75. https://doi.org/10.1016/j.desal.2019.02.001.

Lu, X., Boo, C., Ma, J., Elimelech, M., 2014. Bidirectional diffusion of ammonium and sodium cations in forward osmosis: role of membrane active layer surface chemistry and charge. Environ. Sci. Technol. 48, 14369–14376. https://doi.org/10.1021/es504162v.

Luis, P., Van Aubel, D., Van der Bruggen, B., 2013. Technical viability and exergy analysis of membrane crystallization: closing the loop of CO2 sequestration. Int. J. Greenh. Gas Control. 12, 450–459. https://doi.org/10.1016/j.ijggc.2012.11.027.

Luo, L., Zhao, J., Chung, T.S., 2018a. Integration of membrane distillation (MD) and solid hollow fiber cooling crystallization (SHFCC) systems for simultaneous production of water and salt crystals. J. Memb. Sci. 564, 905–915. https://doi.org/10.1016/j.memsci.2018.08.001.

T. Luo, S. Abdu, M. Wessling, Selectivity of ion exchange membranes: a review, (2018). doi:10.1016/j.memsci.2018.03.051.

Luo, W., Hai, F.I., Kang, J., Price, W.E., Nghiem, L.D., Elimelech, M., 2015. The role of forward osmosis and microfiltration in an integrated osmotic-microfiltration membrane bioreactor system. Chemosphere 136, 125–132. https://doi.org/10.1016/j.chemosphere.2015.04.082.

Luo, W., Hai, F.I., Price, W.E., Guo, W., Ngo, H.H., Yamamoto, K., Nghiem, L.D., 2016. Phosphorus and water recovery by a novel osmotic membrane bioreactor-reverse osmosis system. Bioresour. Technol. 200, 297–304. https://doi.org/10.1016/j.biortech.2015.10.029.

Lutchmiah, K., Verliefde, A.R.D., Roest, K., Rietveld, L.C., 2014. Forward osmosis for application in wastewater treatment : a review. Water Res 58, 179–197. https://doi.org/10.1016/j.watres.2014.03.045.

Macedonio, F., a. A. Quist-Jensen, C., Al-harbi, O., Alromaih, H., a. A. Al-jlil, S., Al Shabouna, F., Drioli, E., Al Shabouna, F., Drioli, E., 2013. Thermodynamic modeling of brine and its use in membrane crystallizer. Desalination 323, 83–92. https://doi.org/10.1016/j.desal.2013.02.009.

Macedonio, F., Katzir, L., Geisma, N., Simone, S., Drioli, E., Gilron, J., 2011. Wind-Aided Intensified eVaporation (WAIV) and Membrane Crystallizer (MCr) integrated brackish water desalination process: advantages and drawbacks. Desalination 273, 127–135. https://doi.org/10.1016/j.desal.2010.12.002.

Magalhães, J.M., Silva, J.E., Castro, F.P., Labrincha, J.A., 2005. Physical and chemical characterisation of metal finishing industrial wastes. J. Environ. Manage. 75, 157–166. https://doi.org/10.1016/j.jenvman.2004.09.011.

Majeed, T., Phuntsho, S., Sahebi, S., Kim, J.E., Khee, J., Kim, K., Shon, H.K., 2015. Influence of the process parameters on hollow fiber-forward osmosis membrane performances. Desalin. Water Treat. 3994, 817–828. https://doi.org/10.1080/19443994.2014.916232.

McCutcheon, J.R., Elimelech, M., 2006. Influence of concentrative and dilutive internal concentration polarization on flux behavior in forward osmosis. J. Memb. Sci. 284, 237–247. https://doi.org/10.1016/j.memsci.2006.07.049.

McCutcheon, J.R., McGinnis, R.L., Elimelech, M., 2005. A novel ammonia-carbon dioxide forward (direct) osmosis desalination process. Desalination 174, 1–11. https://doi.org/10.1016/j.desal.2004.11.002.

McGinnis, R.L., Elimelech, M., 2007. Energy requirements of ammonia-carbon dioxide forward osmosis desalination. Desalination 207, 370–382. https://doi.org/10.1016/j.desal.2006.08.012.

Mericq, J.P., Laborie, S., Cabassud, C., 2010. Vacuum membrane distillation of seawater reverse osmosis brines. Water Res 44, 5260–5273. https://doi.org/10.1016/j.watres.2010.06.052.

Mi, B., Elimelech, M., 2008. Chemical and physical aspects of organic fouling of forward osmosis membranes. J. Memb. Sci. 320, 292–302. https://doi.org/10.1016/j.memsci.2008.04.036.

Mi, B., Elimelech, M., 2010. Organic fouling of forward osmosis membranes: fouling reversibility and cleaning without chemical reagents. J. Memb. Sci. 348, 337–345. https://doi.org/10.1016/j.memsci.2009.11.021.

Mikhaylin, S., Bazinet, L., 2016. Fouling on ion-exchange membranes: classification, characterization and strategies of prevention and control. Adv. Colloid Interface Sci. 229, 34–56. https://doi.org/10.1016/j.cis.2015.12.006.

Mirabelli, V., Majidi Salehi, S., Angiolillo, L., Belviso, B.D., Conte, A., Del Nobile, M.A., Di Profio, G., Caliandro, R., 2018. Enzyme crystals and hydrogel composite membranes as new active food packaging material. Glob. Challenges. 2, 1700089 https://doi.org/10.1002/gch2.201700089.

Mogollón, J.M., Beusen, A.H.W., Van Grinsven, H.J.M., Westhoek, H., Bouwman, A.F., 2018. Future agricultural phosphorus demand according to the shared socioeconomic pathways. Glob. Environ. Chang. 50, 149–163. https://doi.org/10.1016/j.gloenvcha.2018.03.007.

Moon, A.S., Lee, M., 2012. Energy consumption in forward osmosis desalination compared to other desalination techniques. Int. Sch. Sci. Res. Innov. 6, 421–423.

Motuzas, J., Yacou, C., Madsen, R.S.K., Fu, W., Wang, D.K., Julbe, A., Vaughan, J., Diniz da Costa, J.C., 2018. Novel inorganic membrane for the percrystallization of mineral, food and pharmaceutical compounds. J. Memb. Sci. 550, 407–415. https://doi.org/10.1016/j.memsci.2017.12.077.

Munk, L.A., Hynek, S.A., Bradley, D.C., Boutt, D., Labay, K., Jochens, H., 2016. Lithium brines : a global perspective chapter 14 lithium brines : a global perspective. in: Rev. Econ. Geol. 339–365.

Murphy, G.W., Caudle, D.D., 1967. Mathematical theory of electrochemical demineralization in flowing systems. Electrochim. Acta. 12, 1655–1664. https://doi.org/10.1016/0013-4686(67)80079-3.

Naidu, G., Jeong, S., Hasan, A., Fane, A.G., Kandasamy, J., Vigneswaran, S., 2017. Rubidium extraction from seawater brine by an integrated membrane distillation-selective sorption system. Water Res 123, 321–331. https://doi.org/10.1016/j.watres.2017.06.078.

Naidu, G., Jeong, S., Kim, S.J., Kim, I.S., Vigneswaran, S., 2014. Organic fouling behavior in direct contact membrane distillation. Desalination 347, 230–239. https://doi.org/10.1016/j.desal.2014.05.045.
National Research Council, 2008. Minerals, Critical Minerals, and the U.S. Economy. National Academies Press, Washington DC.
Nativ, P., Fridman-Bishop, N., Gendel, Y., 2019. Ion transport and selectivity in thin film composite membranes in pressure-driven and electrochemical processes. J. Memb. Sci. 46–55. https://doi.org/10.1016/j.memsci.2019.04.041.
Nativ, P., Lahav, O., Gendel, Y., 2018. Separation of divalent and monovalent ions using flow-electrode capacitive deionization with nanofiltration membranes. Desalination 425, 123–129. https://doi.org/10.1016/j.desal.2017.10.026.
Nghiem, L.D., Cath, T., 2011. A scaling mitigation approach during direct contact membrane distillation. Sep. Purif. Technol. 80, 315–322. https://doi.org/10.1016/j.seppur.2011.05.013.
Nguyen, C.N., Hau Thi, N., Su-thing, H., Shiao-shing, C., Ngo, H.H., Guo, W., Ray, S.S., Hsu, H.-.T., 2016. Exploring high charge of phosphate as new draw solute in a forward osmosis – membrane distillation hybrid system for concentrating high-nutrient sludge. Sci. Total Environ. 557–558, 44–50. https://doi.org/10.1016/j.scitotenv.2016.03.025.
Nguyen, N.C., Chen, S., Yang, H., Hau, N.T., 2013. Application of forward osmosis on dewatering of high nutrient sludge. Bioresour. Technol. 132, 224–229. https://doi.org/10.1016/j.biortech.2013.01.028.
Oladunni, J., Zain, J.H., Hai, A., Banat, F., Bharath, G., Alhseinat, E., 2018. A comprehensive review on recently developed carbon based nanocomposites for capacitive deionization: from theory to practice. Sep. Purif. Technol. 207, 291–320. https://doi.org/10.1016/j.seppur.2018.06.046.
Omosebi, A., Gao, X., Holubowitch, N., Li, Z., Landon, J., Liu, K., 2017. Anion exchange membrane capacitive deionization cells. J. Electrochem. Soc. 164, E242–E247. https://doi.org/10.1149/2.0461709jes.
Oren, Y., 2008. Capacitive deionization (CDI) for desalination and water treatment — Past, present and future (a review). Desalination 228, 10–29. https://doi.org/10.1016/J.DESAL.2007.08.005.
V.M. Palakkal, J.E. Rubio, Y.J. Lin, C.G. Arges, Low-resistant ion-exchange membranes for energy efficient membrane capacitive deionization, 6 (2018) 13778–13786. doi: 10.1021/acssuschemeng.8b01797.
Pan, J., Zheng, Y., Ding, J., Gao, C., Van der Bruggen, B., Shen, J., 2018. Fluoride removal from water by membrane capacitive deionization with a monovalent anion selective membrane. Ind. Eng. Chem. Res. 57, 7048–7053. https://doi.org/10.1021/acs.iecr.8b00929.
Pasta, M., Wessells, C.D., Cui, Y., La Mantia, F., 2012. A desalination battery. Nano Lett 12, 839–843. https://doi.org/10.1021/nl203889e.
Pawlowski, S., Crespo, J.G., Velizarov, S., 2019. Profiled ion exchange membranes: a comprehensible review. Int. J. Mol. Sci. 20 https://doi.org/10.3390/ijms20010165.
Pérez-González, A, Urtiaga, A M, Ibáñez, R., Ortiz, I., 2012. State of the art and review on the treatment technologies of water reverse osmosis concentrates. Water Res 46, 267–283. https://doi.org/10.1016/j.watres.2011.10.046.
Perrotta, M.L., Macedonio, F., Giorno, L., Jin, W., Drioli, E., Gugliuzza, A., Tocci, E., 2020b. Molecular insights on NaCl crystal formation approaching PVDF membranes functionalized with graphene. Phys. Chem. Chem. Phys. 22, 7817–7827. https://doi.org/10.1039/d0cp00928h.
Perrotta, M.L., Macedonio, F., Tocci, E., Giorno, L., Drioli, E., Gugliuzza, A., 2020a. Graphene stimulates the nucleation and growth rate of NaCl crystals from hypersaline solution via membrane crystallization. Environ. Sci. Water Res. Technol. 6, 1723–1736. https://doi.org/10.1039/c9ew01124b.
Phuntsho, S., Kim, J.E., Johir, M.A.H., Hong, S., Li, Z., Ghaffour, N., Leiknes, T., Shon, H. K., 2016. Fertiliser drawn forward osmosis process: pilot-scale desalination of mine impaired water for fertigation. J. Memb. Sci. 508, 22–31. https://doi.org/10.1016/j.memsci.2016.02.024.
Phuntsho, S., Lotfi, F., Hong, S., Shaffer, D.L., Elimelech, M., Shon, H.K., 2014. Membrane scaling and flux decline during fertiliser-drawn forward osmosis desalination of brackish groundwater. Water Res 57, 172–182. https://doi.org/10.1016/j.watres.2014.03.034.
M.P. Pina, R. Mallada, Enhanced protein crystallization on Na fi on membranes modi fied by low-cost surface patterning techniques, (2020). doi:10.1021/acs.cgd.9b00969.
Porada, S., Zhao, R., van der Wal, A., Presser, V., Biesheuvel, P.M., 2013. Review on the science and technology of water desalination by capacitive deionization. Prog. Mater. Sci. 58, 1388–1442. https://doi.org/10.1016/J.PMATSCI.2013.03.005.
Pramanik, B.K., Hai, F.I., Ansari, A.J., Roddick, F.A., 2019a. Mining phosphorus from anaerobically treated dairy manure by forward osmosis membrane. J. Ind. Eng. Chem. 78, 425–432. https://doi.org/10.1016/j.jiec.2019.05.025.
Pramanik, B.K., Hai, F.I., Roddick, F.A., 2019c. Ultraviolet/persulfate pre-treatment for organic fouling mitigation of forward osmosis membrane: possible application in nutrient mining from dairy wastewater. Sep. Purif. Technol. 217, 215–220. https://doi.org/10.1016/j.seppur.2019.02.016.
Pramanik, B.K., Shu, L., Jegatheesan, J., Shah, K., Haque, N., Bhuiyan, M.A., 2019b. Rejection of rare earth elements from a simulated acid mine drainage using forward osmosis: the role of membrane orientation, solution pH, and temperature variation. Process Saf. Environ. Prot. 126, 53–59. https://doi.org/10.1016/j.psep.2019.04.004.
Profio, G.D.I., Stabile, C., Caridi, A., Curcio, E., Drioli, E., 2009. Antisolvent membrane crystallization of pharmaceutical compounds. J. Pharm. Sci. 98, 4902–4913. https://doi.org/10.1002/jps.
Qin, M., He, Z., 2014. Self-supplied ammonium bicarbonate draw solute for achieving wastewater treatment and recovery in a microbial electrolysis cell-forward osmosis-coupled system. Environ. Sci. Technol. Lett 1, 437–441. https://doi.org/10.1021/ez500280c.
Qin, M., Molitor, H., Brazil, B., Novak, J.T., He, Z., 2016. Recovery of nitrogen and water from landfill leachate by a microbial electrolysis cell-forward osmosis system. Bioresour. Technol. 200, 485–492. https://doi.org/10.1016/j.biortech.2015.10.066.
Qiu, G., Law, Y.M., Das, S., Ting, Y.P., 2015. Direct and complete phosphorus recovery from municipal wastewater using a hybrid microfiltration-forward osmosis membrane bioreactor process with seawater brine as draw solution. Environ. Sci. Technol. 49, 6156–6163. https://doi.org/10.1021/es504554f.
Qiu, G., Ting, Y.P., 2014. Direct phosphorus recovery from municipal wastewater via osmotic membrane bioreactor (OMBR) for wastewater treatment. Bioresour. Technol. 170, 221–229. https://doi.org/10.1016/j.biortech.2014.07.103.
Qiu, G., Zhang, S., Raghavan, D.S.S., Das, S., Ting, Y., 2016. The potential of hybrid forward osmosis membrane bioreactor (FOMBR) processes in achieving high throughput treatment of municipal wastewater with enhanced phosphorus recovery. Water Res 105, 370–382. https://doi.org/10.1016/j.watres.2016.09.017.
Qiu, M., He, C., 2019. Efficient removal of heavy metal ions by forward osmosis membrane with a polydopamine modified zeolitic imidazolate framework incorporated selective layer. J. Hazard. Mater. 367, 339–347. https://doi.org/10.1016/j.jhazmat.2018.12.096.
Quist-Jensen, C.A., Ali, A., Drioli, E., Macedonio, F., 2018b. Perspectives on mining from sea and other alternative strategies for minerals and water recovery - The development of novel membrane operations. J. Taiwan Inst. Chem. Eng. https://doi.org/10.1016/j.jtice.2018.02.002.
Quist-Jensen, C.A., Ali, A., Drioli, E., Macedonio, F., 2019. Perspectives on mining from sea and other alternative strategies for minerals and water recovery – The development of novel membrane operations. J. Taiwan Inst. Chem. Eng. 94, 129–134. https://doi.org/10.1016/j.jtice.2018.02.002.
Quist-Jensen, C.A., Ali, A., Mondal, S., Macedonio, F., Drioli, E., 2016b. A study of membrane distillation and crystallization for lithium recovery from high-concentrated aqueous solutions, J. Memb. Sci. 505 https://doi.org/10.1016/j.memsci.2016.01.033.
Quist-Jensen, C.A., Macedonio, F., Drioli, E., 2016c. Integrated membrane desalination systems with membrane crystallization units for resource recovery: a new approach for mining from the sea. Crystals 6. https://doi.org/10.3390/cryst6040036.
Quist-Jensen, C.A., Macedonio, F., Drioli, E., 2016a. Membrane crystallization for salts recovery from brine—An experimental and theoretical analysis. Desalin. Water Treat. 57 https://doi.org/10.1080/19443994.2015.1030110.
Quist-Jensen, C.A., Macedonio, F., Horbez, D., Drioli, E., 2017b. Reclamation of sodium sulfate from industrial wastewater by using membrane distillation and membrane crystallization. Desalination 401. https://doi.org/10.1016/j.desal.2016.05.007.
Quist-Jensen, C.A.A., Sørensen, J.M.M., Svenstrup, A., Scarpa, L., Carlsen, T.S.S., Jensen, H.C.C., Wybrandt, L., Christensen, M.L.L., 2018a. Membrane crystallization for phosphorus recovery and ammonia stripping from reject water from sludge dewatering process. Desalination 440, 156–160. https://doi.org/10.1016/j.desal.2017.11.034.
Quist-jensen, C.A.C.A., Ali, A., Mondal, S., Macedonio, F., Drioli, E., 2016a. A study of membrane distillation and crystallization for lithium recovery from high-concentrated aqueous solutions. J. Memb. Sci. 505, 167–173. https://doi.org/10.1016/j.memsci.2016.01.033.
Quist-jensen, C.A.C.A., Macedonio, F., Drioli, E., 2016b. Integrated membrane desalination systems with membrane crystallization units for resource recovery : a new approach for mining from the sea. Crystals 6, 1–13. https://doi.org/10.3390/cryst6040036.
Quist-Jensen, C.A.C.A., Macedonio, F., Horbez, D., Drioli, E., 2017a. Reclamation of sodium sulfate from industrial wastewater by using membrane distillation and membrane crystallization. Desalination 401, 112–119. https://doi.org/10.1016/j.desal.2016.05.007.
Ratajczak, P., Suss, M.E., Kaasik, F., Béguin, F., 2019. Carbon electrodes for capacitive technologies. Energy Storage Mater 16, 126–145. https://doi.org/10.1016/J.ENSM.2018.04.031.
Remillard, E.M., Shocron, A.N., Rahill, J., Suss, M.E., Vecitis, C.D., 2018. A direct comparison of flow-by and flow-through capacitive deionization. Desalination 444, 169–177. https://doi.org/10.1016/J.DESAL.2018.01.018.
Ren, J., McCutcheon, J.R., 2018. A new commercial biomimetic hollow fiber membrane for forward osmosis. Desalination 442, 44–50.
Saeedi-Jurkuyeh, A., Jafari, A.J., Kalantary, R.R., Esrafili, A., 2020. A novel synthetic thin-film nanocomposite forward osmosis membrane modified by graphene oxide and polyethylene glycol for heavy metals removal from aqueous solutions. React. Funct. Polym. 146 https://doi.org/10.1016/j.reactfunctpolym.2019.104397.
Sakar, H., Celik, I., Balcik Canbolat, C., Keskinler, B., Karagunduz, A., 2017. Electro-sorption of ammonium by a modified membrane capacitive deionization unit. Sep. Sci. Technol. 52, 2591–2599. https://doi.org/10.1080/01496395.2017.1336556.
Sakar, H., Celik, I., Balcik-Canbolat, C., Keskinler, B., Karagunduz, A., 2019. Ammonium removal and recovery from real digestate wastewater by a modified operational method of membrane capacitive deionization unit. J. Clean. Prod. 215, 1415–1423. https://doi.org/10.1016/J.JCLEPRO.2019.01.165.
Schneider, C., Sathyadev, R., Zarebska, A., Tsapekos, P., Hélix-nielsen, C., 2019. Treating anaerobic effluents using forward osmosis for combined water purification and biogas production. Sci. Total Environ. 647, 1021–1030. https://doi.org/10.1016/j.scitotenv.2018.08.036.
Schwantes, R., Cipollina, A., Gross, F., Koschikowski, J., Pfeifle, D., Rolletschek, M., Subiela, V., 2013. Membrane distillation : solar and waste heat driven demonstration plants for desalination. Desalination 323, 1–25. https://doi.org/10.1016/j.desal.2013.04.011.
Shaffer, D.L., Werber, J.R., Jaramillo, H., Lin, S., Elimelech, M., 2015. Forward osmosis: where are we now? Desalination 356, 271–284. https://doi.org/10.1016/j.desal.2014.10.031.

Shahmansouri, A., Min, J., Jin, L., Bellona, C., 2015. Feasibility of extracting valuable minerals from desalination concentrate: a comprehensive literature review. J. Clean. Prod. 100, 4–16. https://doi.org/10.1016/j.jclepro.2015.03.031.

Shan, J., Phillip, W.A., Elimelech, M., 2012. Coupled reverse draw solute permeation and water flux in forward osmosis with neutral draw solutes. J. Memb. Sci. 392–393, 9–17. https://doi.org/10.1016/j.memsci.2011.11.020.

Shi, S.-J., Pan, Y.-H., Wang, S.-F., Dai, Z.-W., Gu, L., Wu, Q.-Y., 2019. Aluminosilicate nanotubes embedded polyamide thin film nanocomposite forward osmosis membranes with simultaneous enhancement of water permeability and selectivity. Polymers (Basel) 11, 879. https://doi.org/10.3390/polym11050879.

Shibuya, M., Masahiro Yasukawa, T., Miyoshi, T., Higa, M., Matsuyam, H., 2015. Effect of operating conditions on osmotic-driven membrane performances of cellulose triacetate forward osmosis hollow fiber membrane.pdf. Desalination 362, 34–42.

Shirazi, M.M.A., Kargari, A., 2015. A review on applications of Membrane Distillation (MD) process for wastewater treatment. J. Membr. Sci. Res. 1, 101–112.

Siddiqui, F.A., She, Q., Fane, A.G., Field, R.W., 2018. Exploring the differences between forward osmosis and reverse osmosis fouling. J. Memb. Sci. 565, 241–253. https://doi.org/10.1016/j.memsci.2018.08.034.

Siekierka, A., 2019. Preparation of electrodes for hybrid capacitive deionization and its influence on the adsorption behaviour. Sep. Sci. Technol. 1–12. https://doi.org/10.1080/01496395.2019.1609032.

Siekierka, A., Bryjak, M., 2017. Hybrid capacitive deionization with anion-exchange membranes for lithium extraction. E3S Web Conf 22, 00157. https://doi.org/10.1051/e3sconf/20172200157.

Siekierka, A., Bryjak, M., 2019. Novel anion exchange membrane for concentration of lithium salt in hybrid capacitive deionization. Desalination 279–289. https://doi.org/10.1016/j.desal.2018.10.009.

Siekierka, A., Bryjak, M., Wolska, J., 2017a. The use of activated carbon modified with polypyrrole as a supporting electrode for lithium ions adsorption in capacitive deionization. Desalin. WATER Treat. 64, 251–254. https://doi.org/10.5004/dwt.2017.11387.

Siekierka, A., Kmiecik, E., Tomaszewska, B., Wator, K., Bryjak, M., 2018a. The evaluation of the effectiveness of lithium separation by hybrid capacitive deionization from geothermal water with the uncertainty measurement application. Desalin. WATER Treat. 128, 259–264. https://doi.org/10.5004/dwt.2018.22870.

Siekierka, A., Kujawa, J., Kujawski, W., Bryjak, M., 2018c. Lithium dedicated adsorbent for the preparation of electrodes useful in the ion pumping method. Sep. Purif. Technol 194, 231–238. https://doi.org/10.1016/j.seppur.2017.11.045.

Siekierka, A., Tomaszewska, B., Bryjak, M., 2020. Lithium capturing from geothermal water by hybrid capacitive deionization graphical abstract. Desalination 436, 8–14. https://doi.org/10.1016/j.desal.2018.02.003.

Siekierka, A., Wolska, J., Bryjak, M., Kujawski, W., 2017b. Anion exchange membranes in lithium extraction by means of capacitive deionization system. Desalin. WATER Treat. 75, 331–341. https://doi.org/10.5004/dwt.2017.20431.

Siekierka, A., Wolska, J., Kujawski, W., Bryjak, M., 2018b. Modification of poly(vinyl chloride) films by aliphatic amines to prepare anion-exchange membranes for Cr (VI) removal. Sep. Sci. Technol. 53, 1191–1197. https://doi.org/10.1080/01496395.2017.1358746.

Simone, E., Othman, R., Vladisavljević, G.T., Nagy, Z.K., 2018. Preventing crystal agglomeration of pharmaceutical crystals using temperature cycling and a novel membrane crystallization procedure for seed crystal generation. Pharmaceutics 10. https://doi.org/10.3390/pharmaceutics10010017.

Singh, D., Sirkar, K.K., 2012. Desalination by air gap membrane distillation using a two hollow-fiber-set membrane module. J. Memb. Sci. 421–422, 172–179. https://doi.org/10.1016/j.memsci.2012.07.007.

Singh, K., Bouwmeester, H.J.M., De Smet, L.C.P.M., Bazant, M.Z., Biesheuvel, P.M., 2018. Theory of water desalination with intercalation materials. Phys. Rev. Appl. 9 https://doi.org/10.1103/PhysRevApplied.9.064036.

Singh, N., Dhiman, S., Basu, S., Balakrishnan, M., Petrinic, I., Helix-Nielsen, C., 2019. Dewatering of sewage for nutrients and water recovery by Forward Osmosis (FO) using divalent draw solution. J. Water Process Eng 31, 100853. https://doi.org/10.1016/j.jwpe.2019.100853.

Sluys, J.T.M., Verdoes, D., Hanemaaijer, J.H., 1996. Water treatment in a Membrane-Assisted Crystallizer (MAC). Desalination 104, 135–139. https://doi.org/10.1016/0011-9164(96)00036-7.

Smith, K.C., 2017. Theoretical evaluation of electrochemical cell architectures using cation intercalation electrodes for desalination. Electrochim. Acta. 230, 333–341. https://doi.org/10.1016/j.electacta.2017.02.006.

Sohn, J., Valavala, R., Han, J., Her, N., Yoon, Y., 2011. Pretreatment in reverse osmosis seawater desalination: a short review. Environ. Eng. Res. 16, 205–212. https://doi.org/10.4491/eer.2011.16.4.205.

Soler-Cabezas, J.L., Mendoza-Roca, J.A., Vincent-Vela, M.C., Luján-Facundo, M.J., Pastor-Alcañiz, L., 2018. Simultaneous concentration of nutrients from anaerobically digested sludge centrate and pre-treatment of industrial effluents by forward osmosis. Sep. Purif. Technol. 193, 289–296. https://doi.org/10.1016/J.SEPPUR.2017.10.058.

Song, X., Xie, M., Li, Y., Li, G., Luo, W., 2018. Salinity build-up in osmotic membrane bioreactors: causes, impacts, and potential cures. Bioresour. Technol. https://doi.org/10.1016/j.biortech.2018.02.101.

Sparenberg, M.C., Ruiz Salmón, I., Luis, P., 2020. Economic evaluation of salt recovery from wastewater via membrane distillation-crystallization. Sep. Purif. Technol. 235, 116075 https://doi.org/10.1016/j.seppur.2019.116075.

Srisurichan, S., Jiraratananon, R., Fane, A.G., 2005. Humic acid fouling in the membrane distillation process. Desalination 174, 63–72. https://doi.org/10.1016/j.desal.2004.09.003.

Stone, M.L., Rae, C., Stewart, F.F., Wilson, A.D., 2013. Switchable polarity solvents as draw solutes for forward osmosis. Desalination 312, 124–129. https://doi.org/10.1016/j.desal.2012.07.034.

Su, J., Chung, T., Helmer, B.J., De Wit, J.S., 2012. Enhanced double-skinned FO membranes with inner dense layer for wastewater treatment and macromolecule recycle using Sucrose as draw solute. J. Memb. Sci. 396, 92–100. https://doi.org/10.1016/j.memsci.2012.01.001.

Sun, Y., Tian, J., Zhao, Z., Shi, W., Liu, D., Cui, F., 2016. Membrane fouling of forward osmosis (FO) membrane for municipal wastewater treatment: a comparison between direct FO and OMBR. Water Res 104, 330–339. https://doi.org/10.1016/j.watres.2016.08.039.

Suss, M.E., Baumann, T.F., Bourcier, W.L., Spadaccini, C.M., Rose, K.A., Santiago, J.G., Stadermann, M., 2012. Capacitive desalination with flow-through electrodes. Energy Environ. Sci. 5, 9511. https://doi.org/10.1039/c2ee21498a.

Suss, M.E., Porada, S., Sun, X., Biesheuvel, P.M., Yoon, J., Presser, V., 2015. Water desalination via capacitive deionization: what is it and what can we expect from it? Energy Environ. Sci. 8, 2296–2319. https://doi.org/10.1039/c5ee00519a.

Tan, C., He, C., Tang, W., Kovalsky, P., Fletcher, J., Waite, T.D., 2018. Integration of photovoltaic energy supply with membrane capacitive deionization (MCDI) for salt removal from brackish waters. Water Res 147, 276–286. https://doi.org/10.1016/j.watres.2018.09.056.

Tang, C., Wang, Z., Petrini, I., Fane, A.G., Hélix-nielsen, C., 2015. Biomimetic aquaporin membranes coming of age. Desalination 368, 89–105. https://doi.org/10.1016/j.desal.2015.04.026.

Tang, K., Kim, Y., Chang, J., Mayes, R.T., Gabitto, J., Yiacoumi, S., Tsouris, C., 2019b. Seawater desalination by over-potential membrane capacitive deionization: opportunities and hurdles. Chem. Eng. J. 357, 103–111. https://doi.org/10.1016/J.CEJ.2018.09.121.

Tang, W., He, D., Zhang, C., Waite, T.D., 2017. Optimization of sulfate removal from brackish water by membrane capacitive deionization (MCDI). Water Res 121, 302–310. https://doi.org/10.1016/J.WATRES.2017.05.046.

Tang, W., Liang, J., He, D., Gong, J., Tang, L., Liu, Z., Wang, D., Zeng, G., 2019a. Various cell architectures of capacitive deionization: recent advances and future trends. Water Res 150, 225–251. https://doi.org/10.1016/J.WATRES.2018.11.064.

Te Lin, J.C., Lee, D.J., Huang, C., 2010. Membrane fouling mitigation: membrane cleaning. Sep. Sci. Technol. 45, 858–872. https://doi.org/10.1080/01496391003666940.

Thomas, N., Mavukkandy, M.O., Loutatidou, S., Arafat, H.A., 2017. Membrane distillation research & implementation: lessons from the past five decades. Sep. Purif. Technol. 189, 108–127. https://doi.org/10.1016/j.seppur.2017.07.069.

Tow, E.W., Lienhard V, J.H., 2017. Unpacking compaction: effect of Hydraulic pressure on alginate fouling. J. Memb. Sci. 544, 221–233.

Tsai, J.-H., Perrotta, M.L., Gugliuzza, A., Macedonio, F., Giorno, L., Drioli, E., Tung, K.-L., Tocci, E., 2018. Membrane-assisted crystallization: a molecular view of NaCl nucleation and growth. Appl. Sci. 8, 2145. https://doi.org/10.3390/app8112145.

Tsai, J.H., Macedonio, F., Drioli, E., Giorno, L., Chou, C.Y., Hu, F.C., Li, C.L., Chuang, C. J., Tung, K.L., 2017. Membrane-based zero liquid discharge: myth or reality? J. Taiwan Inst. Chem. Eng. 80, 192–202. https://doi.org/10.1016/j.jtice.2017.06.050.

Tun, C.M., Fane, A.G., Matheickal, J.T., Sheikholeslami, R., 2005. Membrane distillation crystallization of concentrated salts—Flux and crystal formation. J. Memb. Sci. 257, 144–155. https://doi.org/10.1016/j.memsci.2004.09.051.

Tuo, L., Ruan, X., Xiao, W., Li, X., He, G., Jiang, X., 2019. A novel hollow fiber membrane-assisted antisolvent crystallization for enhanced mass transfer process control. AIChE J 65, 734–744. https://doi.org/10.1002/aic.16438.

ul Haq, O., Choi, J.-H., Lee, Y.-S., 2018. Anion-exchange membrane for membrane capacitive deionization prepared via pore-filling polymerization in a porous polyethylene supporting membrane. React. Funct. Polym. 132, 36–42. https://doi.org/10.1016/J.REACTFUNCTPOLYM.2018.09.010.

Uzun, H.I., Debik, E., 2019. Economical approach to nitrate removal via membrane capacitive deionization. Sep. Purif. Technol. 209, 776–781. https://doi.org/10.1016/J.SEPPUR.2018.09.037.

Van De Staey, G., Smits, K., Smets, I., 2015. An experimental study on the impact of bioflocculation on activated sludge separation techniques. Sep. Purif. Technol. 141, 94–104. https://doi.org/10.1016/j.seppur.2014.11.022.

Velioğlu, S., Han, L., Chew, J.W., 2018. Understanding membrane pore-wetting in the membrane distillation of oil emulsions via molecular dynamics simulations. J. Memb. Sci. 551, 76–84. https://doi.org/10.1016/j.memsci.2018.01.027.

Visvanathan, C., Ben Aim, R., Parameshwaran, K., 2000. Membrane separation bioreactors for wastewater treatment. Crit. Rev. Environ. Sci. Technol. 30, 1–48. https://doi.org/10.1080/10643380091184165.

Vital, B., Bartacek, J., Ortega-Bravo, J.C., Jeison, D., 2018. Treatment of acid mine drainage by forward osmosis: heavy metal rejection and reverse flux of draw solution constituents. Chem. Eng. J. 332, 85–91. https://doi.org/10.1016/j.cej.2017.09.034.

Volfkovich, Y.M., Rychagov, A.Y., Mikhalin, A.A., Kardash, M.M., Kononenko, N.A., Ainetdinov, D.V., Shkirskaya, S.A., Sosenkin, V.E., 2018. Capacitive deionization of water using mosaic membrane. Desalination 426, 1–10. https://doi.org/10.1016/J.DESAL.2017.10.035.

Volpin, F., Chekli, L., Phuntsho, S., Cho, J., Ghaffour, N., Vrouwenvelder, J.S., Shon, H. K., 2018b. Simultaneous phosphorous and nitrogen recovery from source- separated urine : a novel application for fertiliser drawn forward osmosis. Chemosphere 203, 482–489. https://doi.org/10.1016/j.chemosphere.2018.03.193.

Volpin, F., Chekli, L., Phuntsho, S., Ghaffour, N., Vrouwenvelder, J.S., Shon, H.K., 2019b. Optimisation of a forward osmosis and membrane distillation hybrid system for the treatment of source-separated urine. Sep. Purif. Technol. 212, 368–375. https://doi.org/10.1016/J.SEPPUR.2018.11.003.

Volpin, F., Fons, E., Chekli, L., Kim, J.E., Jang, A., Shon, H.K., 2018a. Hybrid forward osmosis-reverse osmosis for wastewater reuse and seawater desalination: understanding the optimal feed solution to minimise fouling. Process Saf. Environ. Prot. 117, 523–532. https://doi.org/10.1016/j.psep.2018.05.006.

Volpin, F., Heo, H., Johir, M.A.H., Cho, J., Phuntsho, S., Shon, H.K., 2019a. Techno-economic feasibility of recovering phosphorus, nitrogen and water from dilute human urine via forward osmosis. Water Res 150, 47–55. https://doi.org/10.1016/j.watres.2018.11.056.

Vu, M.T., Ansari, A.J., Hai, F.I., Nghiem, L.D., 2018. Performance of a seawater-driven forward osmosis process for pre-concentrating digested sludge centrate: organic enrichment and membrane fouling. Environ. Sci. Water Res. Technol. 4, 1047–1056. https://doi.org/10.1039/c8ew00132d.

Vu, M.T., Price, W.E., He, T., Zhang, X., Nghiem, L.D., 2019. Seawater-driven forward osmosis for pre-concentrating nutrients in digested sludge centrate. J. Environ. Manage. 247, 135–139. https://doi.org/10.1016/j.jenvman.2019.06.082.

Wang, C., Chen, L., Liu, S., 2019a. Activated carbon fiber for adsorption/electrodeposition of Cu (II) and the recovery of Cu (0) by controlling the applied voltage during membrane capacitive deionization. J. Colloid Interface Sci 548, 160–169. https://doi.org/10.1016/j.jcis.2019.04.030.

Wang, C., Chen, L., Zhu, L., 2019b. Effect of combined fouling on desalination performance of membrane capacitive deionization (MCDI) during long-term operation. J. Dispers. Sci. Technol. 0, 1–10. https://doi.org/10.1080/01932691.2019.1579654.

Wang, L., Biesheuvel, P.M., Lin, S., 2018b. Reversible thermodynamic cycle analysis for capacitive deionization with modified Donnan model. J. Colloid Interface Sci 512, 522–528. https://doi.org/10.1016/J.JCIS.2017.10.060.

Wang, L., Dykstra, J.E., Lin, S., 2019c. Energy efficiency of capacitive deionization. Environ. Sci. Technol. 53, 3366–3378. https://doi.org/10.1021/acs.est.8b04858.

Wang, L., He, G., Ruan, X., Zhang, D., Xiao, W., Li, X., Wu, X., Jiang, X., 2018a. Tailored robust hydrogel composite membranes for continuous protein crystallization with ultrahigh morphology selectivity. ACS Appl. Mater. Interfaces. 10, 26653–26661. https://doi.org/10.1021/acsami.8b08381.

Wang, L., Lin, S., 2019. Mechanism of selective Ion removal in membrane capacitive deionization for water softening. Environ. Sci. Technol. 53, 5797–5804. https://doi.org/10.1021/acs.est.9b00655.

Wang, X., Chang, V.W.C., Tang, C.Y., 2016. Osmotic membrane bioreactor (OMBR) technology for wastewater treatment and reclamation : advances, challenges, and prospects for the future. J. Memb. Sci. 504, 113–132. https://doi.org/10.1016/j.memsci.2016.01.010.

Wang, Y., Ou, R., Ge, Q., Wang, H., Xu, T., 2013. Preparation of polyethersulfone/carbon nanotube substrate for high-performance forward osmosis membrane. Desalination 330, 70–78. https://doi.org/10.1016/j.desal.2013.09.028.

Warsinger, D.M., Servi, A., Connors, G.B., Mavukkandy, M.O., Arafat, H.A., Gleason, K. K., Lienhard, J.H., 2017. Reversing membrane wetting in membrane distillation: comparing dryout to backwashing with pressurized air. Environ. Sci. Water Res. Technol. 3, 930–939. https://doi.org/10.1039/c7ew00085e.

Warsinger, D.M., Swaminathan, J., Guillen-Burrieza, E., Arafat, H.A., Lienhard V, J.H., 2015. Scaling and fouling in membrane distillation for desalination applications: a review. Desalination 356, 294–313. https://doi.org/10.1016/j.desal.2014.06.031.

Westerhoff, P., Lee, S., Yang, Y., Gordon, G.W., Hristovski, K., Halden, R.U., Herckes, P., 2015. Characterization, recovery opportunities, and valuation of metals in municipal sludges from U.S. wastewater treatment plants nationwide. Environ. Sci. Technol. 49, 9479–9488. https://doi.org/10.1021/es505329q.

Wu, C.-.Y., Mouri, H., Chen, S.-.S., Zhang, D.-.Z., Koga, M., Kobayashi, J., 2016. Removal of trace-amount mercury from wastewater by forward osmosis. J. Water Process Eng 14, 108–116. https://doi.org/10.1016/j.jwpe.2016.10.010.

Wu, S., Zou, S., Liang, G., Qian, G., He, Z., 2018a. Enhancing recovery of magnesium as struvite from land fi ll leachate by pretreatment of calcium with simultaneous reduction of liquid volume via forward osmosis. Sci. Total Environ. 610–611, 137–146. https://doi.org/10.1016/j.scitotenv.2017.08.038.

Wu, Y., Kong, Y., Liu, J., Zhang, J., Xu, J., 1991. An experimental study on membrane distillation-crystallization for treating waste water in taurine production. Desalination 80, 235–242.

Wu, Z., Zou, S., Zhang, B., Wang, L., He, Z., 2018b. Forward osmosis promoted in-situ formation of struvite with simultaneous water recovery from digested swine wastewater. Chem. Eng. J. 342, 274–280. https://doi.org/10.1016/j.cej.2018.02.082.

Xie, M., Zheng, M., Cooper, P., Price, W.E., Nghiem, L.D., 2015. Osmotic dilution for sustainable greenwall irrigation by liquid fertilizer : performance and implications. J. Memb. Sci. 494, 32–38. https://doi.org/10.1016/j.memsci.2015.07.026.

Xue, W., Tobino, T., Nakajima, F., Yamamoto, K., 2015. Seawater-driven forward osmosis for enriching nitrogen and phosphorous in treated municipal wastewater : effect of membrane properties and feed solution chemistry. Water Res 69, 120–130. https://doi.org/10.1016/j.watres.2014.11.007.

Xue, W., Yamamoto, K., Tobino, T., 2016. Membrane fouling and long-term performance of seawater-driven forward osmosis for enrichment of nutrients in treated municipal wastewater. J. Memb. Sci. 499, 555–562. https://doi.org/10.1016/j.memsci.2015.11.009.

Yang, F., Ma, J., Zhang, X., Huang, X., Liang, P., 2019. Decreased charge transport distance by titanium mesh-membrane assembly for flow-electrode capacitive deionization with high desalination performance. Water Res 164. https://doi.org/10.1016/j.watres.2019.114904.

Yang, X., Yu, H., Wang, R., Fane, A.G., 2012. Optimization of microstructured hollow fiber design for membrane distillation applications using CFD modeling. J. Memb. Sci. 421–422, 258–270. https://doi.org/10.1016/j.memsci.2012.07.022.

Yangali-Quintanilla, V., Li, Z., Valladares, R., Li, Q., Amy, G., 2011. Indirect desalination of Red Sea water with forward osmosis and low pressure reverse osmosis for water reuse. Desalination 280, 160–166. https://doi.org/10.1016/j.desal.2011.06.066.

Ye, W.; Lin, J.; Shen, J.; Luis, P.; Bruggen and Van Der B., Membrane Crystallization of Sodium Carbonate for Carbon Dioxide Recovery : Effect of Impurities on the Crystal Morphology, Crystal Growth and Design 2013, 13, 2362–2372.

Ye, W., Lin, J., Tækker, H., Gydesen, E., Hélix-Nielsen, C., Luis, P., Van Der Bruggen, B., 2016. Enhanced performance of a biomimetic membrane for Na2 CO3 crystallization in the scenario of CO2 capture. J. Memb. Sci. 498, 75–85. https://doi.org/10.1016/j.memsci.2015.09.010.

Yoon, H., Jo, K., Kim, K.J., Yoon, J., 2019. Effects of characteristics of cation exchange membrane on desalination performance of membrane capacitive deionization. Desalination 458, 116–121. https://doi.org/10.1016/j.desal.2019.02.009.

Yu, F., Wang, L., Wang, Y., Shen, X., Cheng, Y., Ma, J., 2019. Faradaic reactions in capacitive deionization for desalination and ion separation. J. Mater. Chem. A. 7, 15999–16027. https://doi.org/10.1039/c9ta01264h.

Yu, J., Jo, K., Kim, T., Lee, J., Yoon, J., 2018. Temporal and spatial distribution of pH in flow-mode capacitive deionization and membrane capacitive deionization. Desalination 439, 188–195. https://doi.org/10.1016/J.DESAL.2018.04.011.

Yuan, W.E.I., Zydney, A.L., 2000. Humic Acid fouling during. J. Memb. Sci. 34, 5043–5050. https://doi.org/10.1021/es0012366.

Zarebska, A., Nieto, D.R., Christensen, K.V., Norddahl, B., 2014. Ammonia recovery from agricultural wastes by membrane distillation: fouling characterization and mechanism. Water Res 56, 1–10. https://doi.org/10.1016/j.watres.2014.02.037.

Zarkadas, D.M., Sirkar, K.K., 2006. Antisolvent crystallization in porous hollow fiber devices. Chem. Eng. Sci. 61, 5030–5048. https://doi.org/10.1016/j.ces.2006.03.036.

Zhang, H., Jiang, W., Cui, H., 2017. Performance of anaerobic forward osmosis membrane bioreactor coupled with microbial electrolysis cell (AnOMEBR) for energy recovery and membrane fouling alleviation. Chem. Eng. J. 321, 375–383. https://doi.org/10.1016/j.cej.2017.03.134.

Zhang, J., Loong, W.L.C., Chou, S., Tang, C., Wang, R., Fane, A.G., 2012. Membrane biofouling and scaling in forward osmosis membrane bioreactor. J. Memb. Sci. 403–404, 8–14. https://doi.org/10.1016/j.memsci.2012.01.032.

Zhang, S., Wang, P., Fu, X., Chung, T.-.S., 2014b. Sustainable water recovery from oily wastewater via forward osmosis-membrane distillation (FO-MD). Water Res 52, 112–121. https://doi.org/10.1016/j.watres.2013.12.044.

Zhang, Y., Huang, W., Bao, S., 2014a. Treatment of industrial wastewater containing high levels of ammonia. Appl. Mech. Mater. 539, 805–810 doi:10.4028/www.scientific.net/AMM.539.805.

Zhao, R., Biesheuvel, P.M., Van Der Wal, A., 2012a. Energy consumption and constant current operation in membrane capacitive deionization. Energy Environ. Sci. 5, 9520–9527. https://doi.org/10.1039/c2ee21737f.

Zhao, R., Porada, S., Biesheuvel, P.M., van der Wal, A., 2013. Energy consumption in membrane capacitive deionization for different water recoveries and flow rates, and comparison with reverse osmosis. Desalination 330, 35–41. https://doi.org/10.1016/J.DESAL.2013.08.017.

Zhao, X., Liu, C., 2018. Efficient removal of heavy metal ions based on the optimized dissolution-diffusion-flow forward osmosis process. Chem. Eng. J. 334, 1128–1134. https://doi.org/10.1016/j.cej.2017.11.063.

Zhao, Y., Qiu, C., Li, X., Vararattanavech, A., Shen, W., Torres, J., Hélix-Nielsen, C., Wang, R., Hu, X., Fane, A.G., Tang, C.Y., 2012b. Synthesis of robust and high-performance aquaporin-based biomimetic membranes by interfacial polymerization-membrane preparation and RO performance characterization. J. Memb. Sci. 423–424, 422–428. https://doi.org/10.1016/J.MEMSCI.2012.08.039.

Zhu, Z., Zhong, L., Chen, X., Zheng, W., Zuo, J., Zeng, G., Wang, W., 2020a. Monolithic and self-roughened Janus fibrous membrane with superhydrophilic / omniphobic surface for robust antifouling and antiwetting membrane distillation. J. Memb. Sci. 615, 118499 https://doi.org/10.1016/j.memsci.2020.118499.

Zhu, Z., Zhong, L., Horseman, T., Liu, Z., Zeng, G., Li, Z., Lin, S., Wang, W., 2020b. Superhydrophobic-omniphobic membrane with anti-deformable pores for membrane distillation with excellent wetting resistance. J. Memb. Sci. 118768 https://doi.org/10.1016/j.memsci.2020.118768.

Zou, S., Qin, M., He, Z., 2019b. Tackle reverse solute flux in forward osmosis towards sustainable water recovery: reduction and perspectives. Water Res 149, 362–374. https://doi.org/10.1016/j.watres.2018.11.015.

Zou, S., Qin, M., Moreau, Y., He, Z., 2017. Nutrient-energy-water recovery from synthetic sidestream centrate using a microbial electrolysis cell - forward osmosis hybrid system. J. Clean. Prod. 154, 16–25. https://doi.org/10.1016/J.JCLEPRO.2017.03.199.

Zou, T., Kang, G., Zhou, M., Li, M., Cao, Y., 2019a. Submerged vacuum membrane distillation crystallization (S-VMDC) with turbulent intensification for the concentration of NaCl solution. Sep. Purif. Technol. 211, 151–161. https://doi.org/10.1016/j.seppur.2018.09.072.

Zuo, K., Kim, J., Jain, A., Wang, T., Verduzco, R., Long, M., Li, Q., 2018. Novel composite electrodes for selective removal of sulfate by the capacitive deionization process. Environ. Sci. Technol. 52, 9486–9494. https://doi.org/10.1021/acs.est.8b01868.